Renewable Energy Systems for the Australian Antarctic Stations

by
Christopher Brown B.Sc.(Hons.)

Submitted in fulfilment of the
requirements
for the degree of
Master of Science

Institute of Antarctic and Southern Ocean Studies
University of Tasmania
August, 1998

Declaration

This Thesis contains no material which has been accepted for a degree or diploma by the University or any other institution, except by way of background information and duly acknowledged in the Thesis, and to the best of the Candidate's knowledge and belief no material previously published or written by another person except where due acknowledgment is made in the text of the Thesis.

Christopher Brown

28 August, 1998

Acknowledgments

The author would like to thank the Australian Antarctic Foundation for their support of the project, including funds for the 'Australian Antarctic Foundation Alternative Energy Scholarship'; and additional funds to allow presentation of work conducted in the thesis at the 18th British Wind Energy Conference, Exeter, UK; and 12th Canadian Wind Energy Association Exhibition and Conference, Kananakis, Alberta, Canada.

Thanks must also be given to the Antarctic Science Advisory Committee (ASAC), and the Australian Antarctic Division (AAD) for project resources and for providing the opportunity to spend time at Casey station over the 1994/5 and 1995/6 seasons; and to all station personnel at Casey, without whose help the project would not have succeeded. Thanks also to the Australian Bureau of Meteorology and the Engineering section of the Australian Antarctic Division for providing access to data files, and for the many discussions which made this research possible.

Special thanks must go to people from whom I have also received help, both during my time at Casey and at the University of Tasmania. These include my fellow room mates in 30 Earl Street and my supervisors, Mr. David Lyons and Dr. Antoine Guichard, without whom this experience would not have been the same.

Abstract

Large quantities of fossil fuels are imported each year to meet the electrical and thermal energy needs of Australia's scientific research stations in Antarctica. A significant part of this fuel, used by diesel generator sets, could be offset through the introduction of renewable energy systems. Reduced fuel usage would lead to savings in transportation time and costs, lower atmospheric emissions and reduce the risk of fuel spills.

Research has been conducted to estimate the renewable energy resources of the four Australian Antarctic stations: Casey, Davis and Mawson and Macquarie Island. To achieve this goal, the following procedures were employed:

1. analysis of local meteorological records to identify the wind and solar energy resources;
2. identification and breakdown of station energy demands; and
3. modelling of renewable energy generation and storage systems to estimate potential fuel savings.

Analysis of the wind energy potential indicated high resources for Mawson and Macquarie Island, while low resources for Casey and Davis. The solar energy potential was identified as being promising for the continental stations, with high exploitable levels estimated for the summer months. Field work to validate these results was initiated at Casey, including the installation of a 10 kW wind-turbine and a small photovoltaic panel linked with a pyranometer measuring solar insolation levels.

Three renewable energy system configurations, envisaged to operate in conjunction with the current diesel generator system, were sized using estimates of each station's electrical energy demand. Configurations investigated include:

1. diesel displacement systems with renewable penetration limited to 40%;
2. renewables in conjunction with power conditioning equipment allowing full penetration;
3. battery storage systems; and
4. hydrogen storage systems.

Mawson and Macquarie Island have been identified as the most promising sites. Electrical fuel consumption reductions of 24% and 30% are predicted at these stations for diesel displacement systems with wind turbines rated at 100 kW and 50 kW respectively. Higher fuel consumption reductions of 48% and 75% are predicted in full renewable penetration systems with wind turbines rated at 200 kW and 100 kW. Battery storage systems, beyond a role for power regulation, indicate minimal returns for large investments. A similar result was obtained for a fully integrated renewable energy system involving hydrogen storage.

These results demonstrate that renewable energy systems would allow for substantial fuel savings if introduced to the Australian Antarctic Stations.

Contents

List of Figures

Chapter 5 - Field trials and validation exercises

Chapter 6 - Modelling

List of Tables

Chapter 5 - Field trials and validation exercises

Chapter 6 - Modelling

Chapter 7 - Modelling

Chapter 1

Introduction

1.1 Background

Antarctica is a continent rich in geological history and abundant in biological resources along its extensive coastline and surrounding waters. Antarctica also plays a critical and important role in the functioning of the Earth's climate systems, influencing both the ocean and atmosphere. As a result of these and other factors, many countries are active in the region conducting a multitude of scientific programs. These include:

- climate related studies of the atmosphere, oceans, ice and glacier fields;
- biological studies of the ecosystems;
- cosmic ray studies relating to the dynamics of the upper and outer atmosphere, ionosphere and magnetosphere; and
- geological studies including plate tectonics and paleontology.

In order to support these programs, permanent and semi-permanent stations have been established throughout the continent and surrounding oceans. Conditions at these stations can be difficult. Expeditioners must contend with potentially life threatening low temperatures, often compounded by strong winds, as well as isolation and separation from family and friends. To provide protection from the elements and create a warm friendly living and working environment to off-set the impact of remoteness, stations have been designed with a reliance on a ready and plentiful supply of electrical and thermal energy.

Until recently, the only practical method to provide this energy on a regular and dependable basis has been the use of large quantities of imported fossil fuel in diesel generator and boiler sets. Recent advancements in technology, however, have changed this situation. Methods now exist enabling sizable quantities of energy to be produced locally at the stations from renewable energy sources. Advantages associated with a move towards renewable energy systems include reduced atmospheric emissions from the burning of fossil fuels; reduced shipping times; reduced costs associated with fuel purchasing, handling and storage; and reduced risk for oil spills. Issues of major environmental and logistical concern to all Antarctic operators.

Evidence of this concern is apparent from the outcome of the XIth Antarctic Treaty Special Consultative Meeting (ATSCM). At the ATSCM the Protocol on Environmental Protection to the Antarctic Treaty (the Madrid Protocol) was agreed to and adopted - a major legal and policy document 'reaffirming the commitment by Antarctic Treaty nations to protect the Antarctic environment and dependent ecosystems' [ATCPs, 1991a]. The ATSCM also saw the establishment of a working group to review the use of alternative energies and energy saving methods in order to reduce environmental pollution in Antarctica. During discussions of this working group it was suggested that efforts be initiated into 'the use of alternative energies, such as solar and wind power in the Antarctic Treaty Area, and the study of a systematic way of implementing energy saving methods with the aim of reducing the use of fuels to the maximum extent possible' [ATCPs, 1991b].

The working group also recommended further study to be undertaken by the Scientific Committee on Antarctic Research (SCAR) and the Council of Managers of National Antarctic Programs (COMNAP). The Standing Committee on Antarctic Logistics and Operations (SCALOP) of COMNAP, convened a sub-group on Alternative Energy [SCAR, 1995]. In a 1993 report from this sub-group, alternative energies deemed applicable for use in Antarctica were categorised as:

'**Wind and solar energy:** Practical, state-of-the art technology, ready for near term application;
Hydro-power, Fuel Cells, Methane generation from wastes: Potentially practical, but needs further development and research; and
Geothermal, Atmospheric/Oceanic thermal gradients: Exotic, somewhat theoretical or impractical' [SCALOP, 1993].

As a follow up to this report, a session on 'The use of alternative energy sources in Antarctica' was conducted at the Sixth Symposium on Antarctic Logistics and Operations was held in conjunction with the XXIII SCAR meeting in Rome in 1994. Presentations to this symposium included:

- performance figures from the United States Antarctic Program (USAP) on a wind/solar/battery system operated at Black Island near McMurdo [Chiang, 1994];
- results from the Spanish Antarctic station Juan Carlos I and their efforts to establish a wind powered battery system [Castellvi, 1994];
- an outline of a solar array system for the upgraded South Pole station [Peeran, 1994];
- concepts for new energy efficient stations using passive solar heating combined with wind and solar energy systems [Sheinstein, 1994];
- an outline for an energy system using the atmospheric/ocean thermal gradient [LeGoff, 1994]; and
- a proposal for a wind and solar system including mass storage using either batteries or a hydrogen loop for the Australian and French Antarctic stations [Guichard, 1994a].

The last of these presentations (by Guichard) reported on a project investigating renewable energy systems for the French and Australian Antarctic stations. This project was initiated by the Australian Antarctic Division (AAD), operators of the Australian Antarctic stations; the Institute of Antarctic and Southern Ocean Studies (IASOS), based at the University of Tasmania; and the *Institut Français pour la Recherche et la Technologie Polaires* (IFRTP), operators of the French Antarctic Program.

Additional publications also associated with this project include: an honours thesis titled 'Alternative Energy Options for Antarctic Stations' [Steel, 1993]; and a status report on 'The Potential for the Application of Alternative Energy Systems at Antarctic Stations' [Guichard, 1994b]. Research reported in this thesis has expanded the knowledge base established in this previous work, allowing for estimates on the performance of potential renewable energy systems at the Australian Antarctic Stations.

1.2 Australian Antarctic stations

The Australian Antarctic stations are the focus of this study. Australia currently operates four permanent stations: Casey, Davis and Mawson along the remote coastline of Eastern Antarctica, and Macquarie Island in the sub-Antarctic, just north of the Antarctic convergence zone. The location of these stations can be seen in Figure 1.1.

1.2.1 History and location

Australia has a long history of involvement in the Antarctic region, with the ports of Melbourne and Hobart serving as the starting point for many early journeys of exploration and discovery. In addition, the Australian Sir Douglas Mawson, lead a number of major international expeditions in the early part of this century. These included the Australasian Antarctic Expedition of 1911-13, the first to reach the south magnetic pole; and the British, Australian and New Zealand Antarctic Research Expedition of 1929-31, exploring large areas of Eastern Antarctica for the first time. These expeditions led in due course to Australia's formal declaration in 1936 of the Australian Antarctic Territory (AAT) [Swan, 1961].

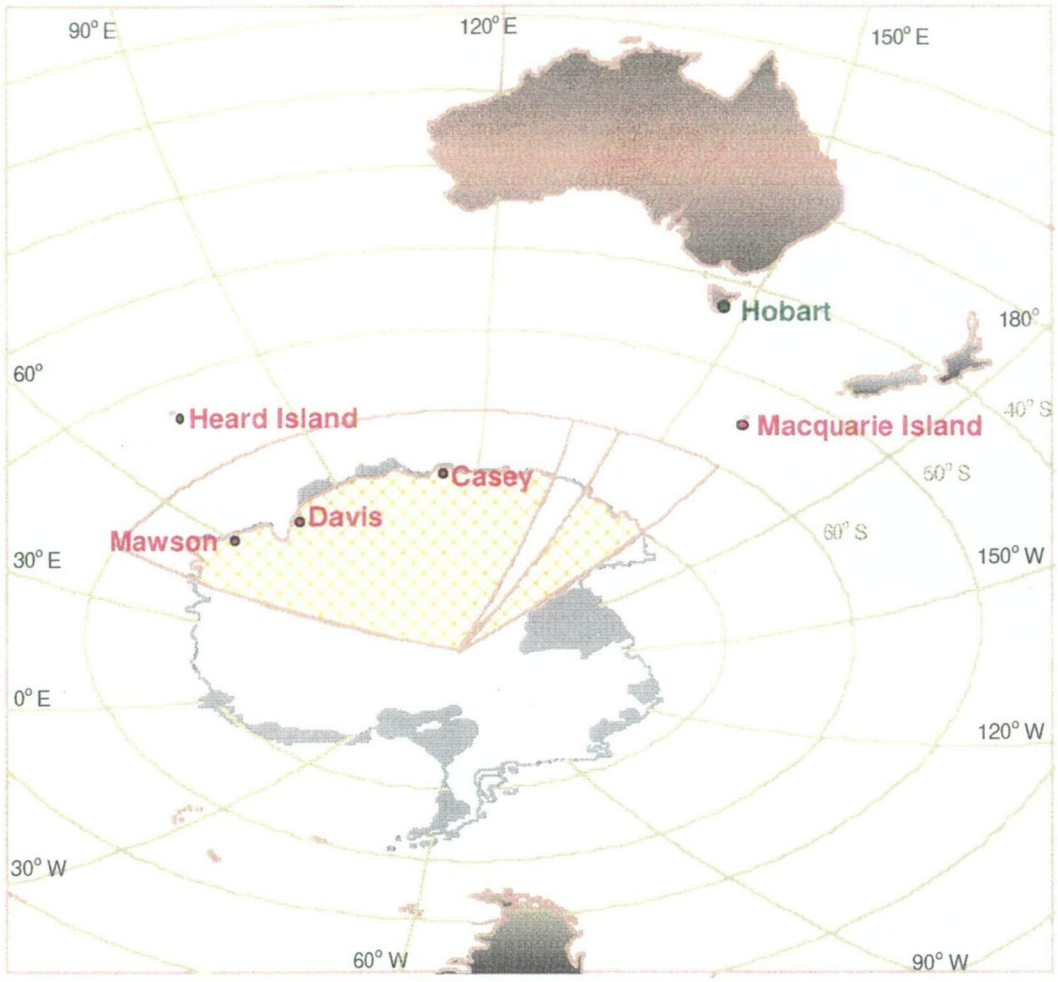

Figure 1.1: Location of Australian Antarctic Stations [source AAD Engineering]
(the crosshatched region indicates the extent of the Australian Antarctic Territory).

The modern era of Australia's Antarctic presence began in 1947 with the establishment of the Australian National Antarctic Research Expeditions (ANARE). Expeditions by ANARE were made initially into the sub-antarctic, with scientific outposts established on Heard Island in 1947 and soon after on Macquarie Island in 1948. Heard Island served as a research station until its closure in 1955, while Macquarie Island is part of the current permanent presence by Australia in the region [Haywood, 1995].

The first Australian station on the Antarctic continent was established in 1954 and named in honour of Sir Douglas Mawson. Located in Mac Robertson Land, Mawson is Australia's most westerly station. Australia's second station on the continent was Davis, founded in 1957 in preparation for the International Geophysical Year (IGY). Located in the Vestfold Hills, Davis is the most southern of the Australian permanent stations [Haywood, 1995].

Wilkes, established in 1957 by the United States as part of the IGY, became the third Australian station on the continent after administration was handed over to Australia in 1959. Encroaching ice proved a major problem at Wilkes, resulting in its eventual abandonment. A replacement station, designated Casey, was built between 1965 and 1969 on a peninsular overlooking Newcombe Bay adjacent to the old Wilkes [Haywood, 1995].

Operations and logistics for the stations are provided by the Australian Antarctic Division (AAD), with Hobart serving at the base for shipping operations. The AAD is responsible for coordinating all activities at the stations. These included recruitment, science support, station maintenance and protection of the environment. The latitude and longitude of the current permanent Australian Antarctic stations is presented in Table 1.1, together with their respective shipping distances to Hobart.

Station	Latitude	Longitude	Distance to Hobart
Casey	66°17' S	110°32' E	3,427 km
Davis	68°35' S	77°58' E	4,816 km
Mawson	67°36' S	62°52' E	5,447 km
Macquarie Island	54°30' S	158°56' E	1,495 km

Table 1.1: Australian Antarctic station geographical co-ordinates and shipping distances to Hobart [Haywood, 1995].

1.2.2 Design and layout

In the late 1970s, the Australian government made the decision to upgrade facilities at the stations. This involved complete station rebuilds, including the replacement of all buildings and services. To satisfy scientific program requirements, and provide suitable support services, the following facilities were incorporated in the new station designs:

1. Domestic and Medical complex containing all bedrooms, laundries, medical suite, dark room and hobby areas;
2. Living quarters consisting of kitchens, dining and recreational areas;
3. Power-houses, two per station, each capable of providing full station load and able to be run independently in case of emergency;
4. Workshop containing maintenance facilities for vehicles and plant and building trade areas;
5. Store capable of containing provisions to supply station for a two year period;
6. Operations building containing administration, communications and meteorological offices with room for associated support workshops;
7. Service buildings containing:
   - storage facilities for potable and fire service water,
   - waste treatment plant,
   - high temperature incinerator,
   - electrical power distribution equipment;
8. Emergency shelter containing garaging and storage for fire fighting rescue vehicle and equipment;
9. Remote building housing satellite communications equipment;
10. Science building comprising discipline specific laboratories and research equipment [Hall, 1992].

In order to complete this task, Australian Construction Services (ACS) - builders of the new stations - developed a design concept called the Australian Antarctic Building System (AANBUS). Under AANBUS, the engineering services of all facilities within the new stations were required to meet the following criteria:

1. Mechanical services to include built-in redundancy, ensuring adequate back-up;
2. All external pipe work to be protected from freezing by heat-trace and polyurethane insulated piping;

3. All structures to be designed for minimum outdoor temperatures of -40°C, maximum wind-speeds of 280 km/h, and an indoor temperature of 20°C;
4. The use of standardised items (if possible);
5. Building efficiency to be optimised through the use of large volume to surface area ratios (to reduce thermal losses through heat transfer through walls, floors and ceilings);
6. Use of braced steel partial framed structures with isolated external cladding;
7. Designs to include moisture barriers on outside and vapour barriers on the inside of buildings, with provisions also made for the prevention of cold paths; and
8. Location and orientation of buildings and services to minimise snow drift accumulation and provide interaction between Expeditioners and the environment [Hall, 1992].

The new Casey station opened in 1990. This was the first of the stations to be completed under the rebuilding program. A schematic layout of Casey station is presented in Figure 1.2, indicating the general design layout with buildings aligned parallel to the prevailing winds. Davis and Mawson are of a similar layout and design, while Macquarie Island consists of more conventional buildings.

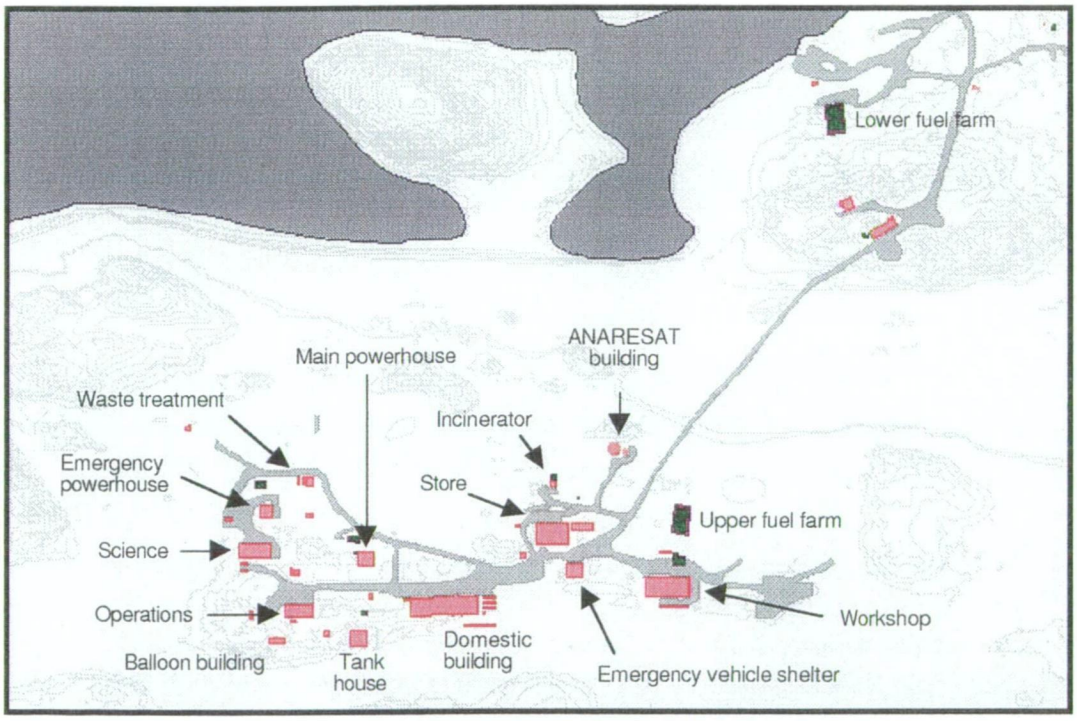

Figure 1.2: Schematic layout of Casey station [source AAD GIS].

1.2.3 Operations

Scientific research at the stations is directed towards the fulfillment of three objectives: understanding global climate change, promoting environmental protection and obtaining practical information. Research is conducted in six core disciplines: Atmospheric science, Biological science, Geoscience, Glaciology, Human Impacts and Oceanography. A program of Medical research investigating the physiological effects of the Antarctic environment on expeditioners is also supported, both on station and at the AAD headquarters in Kingston, near Hobart [Haywood, 1995].

Support services complimentary to the core disciplines are also provided through the AAD headquarters. Building materials, electronic equipment, as well as food and medical supplies, are needed at the stations in order to maintain facilities and ensure the success of scientific programs. To replenish station supplies, comprehensive logistics - including air and shipping operations - are conducted each year.

These operations are currently restricted to the brief Antarctic summer, during which sea ice conditions allow access to the stations by ship for cargo transfer and refuelling. Shipping schedules to each station in each season typically involve one major resupply, together with a number of other visits. Transportation of personnel to and from the stations is completed during these visits. Currently, the research/resupply vessel *Aurora Australis* is chartered by the AAD for these activities, with a dedicated cargo ship envisaged to operate every third year for bulk cargo operations. Time and space aboard voyages south is at a premium. Marine Science programs also require extensive use of the *Aurora Australis* - one of only a handful of vessels currently devoted to research on a regular basis in the waters surrounding Antarctica.

Transfer of fuel to the stations is a vital but time consuming aspect of each station's resupply. Special Antarctic Blend (SAB) diesel, prepared for the cold temperatures of Antarctica with a low wax content and used to meet the electrical and thermal energy demands of the stations, forms the bulk of this fuel [Steel, 1993]. Any reductions in the amount of fuel used at the stations will have positive benefits on the time required for resupply operations.

1.2.4 Station energy systems

The amount of fuel used each year by the stations is a function of their size, design and energy system. The energy systems of the new stations were designed to provide a safe, efficient and above all, reliable supply of electrical and thermal energy. Safety is of the highest priority due to the isolation of the stations, necessitating self-sufficiency over the long cold dark winter months. The current energy system of each station involves combined heat and power generation systems comprising diesel generator sets and oil-fired boilers.

Two power houses are located at each station. The main powerhouse (MPH) supplies demand during normal periods, with an emergency powerhouse (EPH) maintained as a backup. The MPH at each continental station consists of four, six-cylinder Caterpillar 3306 engines matched with 125 kVA (or the newly installed 165 kVA) alternator sets, while the EPH consists of two larger Caterpillar 3412 engines coupled with an alternator capable of an output of 350 kVA. Each power house can be operated independently and is sized to take the entire station electrical load [Archibald, 1992].

In addition to electrical energy, thermal energy is also distributed to most station buildings. Heat, in the form of hot water, is recovered from the engine cooling water and exhaust systems using water jacket heat exchange units. This is supplemented, if necessary, with additional heating from boilers located in the powerhouse and then distributed through a continuously running water circuit using insulated heat-traced piping.

Both the MPH and the EPH are controlled automatically by a programmable logic control (PLC) unit located in the control room of each power house. The PLC unit maintains the number of generator sets and boilers on-line, automatically coordinating the synchronisation of additional units or phasing out of units as required. From an operational viewpoint, the energy systems at the stations are quite effective. Electrical and thermal efficiencies for the generator and boiler sets are given in Table 1.2, based on a lower heating value (LHV) of SAB diesel fuel of 9.81 kW/l [Steel, 1993]. Further details of the fuel consumption and electrical load totals are presented in Chapters 4.

System	Efficiency	
	electrical	thermal
Generators	32%	35%
Boilers	-	80%

Table 1.2: Electrical and thermal efficiencies of the stations [source Steel 1993]

Although the energy system has high combined efficiencies, the energy-per-capita consumption rates at the Australian Antarctic stations are very high. A consequence of this under the current energy system, is that pollution levels on a per-capita basis are also disproportionately high. In 1992 the annual CO_2 production rate at the Australian stations was estimated at 78 tonnes-per-person [Guichard, 1993], 22 times the average annual world CO_2 production rate of 3.6 tonnes-per-person (or 5.6 times the Australian per capita rate at 14 tonnes-per-person [Gilchrist, 1994]). These high emission levels are an unavoidable consequence of using the current energy system to meet current station energy requirements.

1.3 Options to reduce fossil fuel use

Two main strategies have been considered in order to reduce the fossil fuel use at the stations. The first involves reducing the amount of energy required, while the second involves replacing current energy generation methods with more environmentally benign methods.

1.3.1 Load management

Load management programs reduce station energy use through either supply-side-management (SSM), or demand-side-management (DSM) techniques. SSM techniques maximise energy production efficiency. This could involve the use of multiple generating plants, of the same or different size, to preventing light loading and allow the most efficient mix to meet demand [Bass, 1987]. These ideas have been incorporated into the revised continental station designs through the use of multiple generator sets.

DSM techniques focus on demand rather than production, increasing efficiency by reducing or shifting loads. High demand peaks require a large spinning reserve, necessitating plant kept on stand-by, ready to meet sudden increases in demand. This results in large over-sized energy systems, with expensive plant often left idle. Shifting non-essential loads away from high demand peaks offers methods to increase load factors (a measure of the mean to the maximum load), allowing for systems to be sized closer to the expected mean. Typical DSM techniques used by electricity utility companies, as outlined by Bass (1987), include:

1. **Energy conservation programs:** increasing appliance efficiency to induce a general decrease in load;
2. **Direct load control:** where non-essential items are shut down as load increases, deferring their effect away from load peak periods; and
3. **Indirect or voluntary load control:** relying on consumers to consider the effect of the timing of their actions.

Load management techniques have been introduced by the AAD since 1992 as part of official policy [Steel, 1993]. These programs rely heavily on the goodwill and support of station personnel, and although they have led to positive and promising results, further improvements can be expected through additional DSM techniques.

Typical DSM techniques have yielded energy reductions of the order of 20% to 30% for utility companies in the USA [Gilchrist, 1994], savings which should, in part, be possible at the stations. Areas where DSM techniques could be extended would be best identified from a full and detailed energy audit. Key areas that could be investigated include:

1. **Distribution losses:** where do they occur and when are they highest?
2. **Under-utilised lighting:** is it possible to move towards more efficient globes and would proximity switches help reduce unnecessary lighting without compromising safety concerns?
3. **Down sizing of mechanical plant:** is it possible for a gradual move to more efficient plant as replacement becomes necessary?
4. **Heating losses:** can current air exchange practices, which involve the practice of pumping air continuously around near empty buildings throughout the year including winter, be reduced?
5. **Load shifting:** can non-critical loads be moved to low demand times?

Requiring no new generating infrastructure, load management programs represent the easiest way to reduce fuel use at the stations. However the location, climate and isolation of the stations will always result in high electrical and thermal energy requirements, restricting possible applications. Methods to reduce fuel use further must concentrate on the way energy is produced.

1.3.2 Gas turbines

Gas turbines offer a very attractive alternative to diesel generator sets for electrical power generation. Lower emission levels combined with higher efficiencies have seen gas turbines rapidly grow in the power generation market, with forecasts for over 400,000 MW of gas turbine plant to be built by 2005 [Farlin, 1994].

A gas turbine basically consists of a commercial jet engine mounted on the ground and attached to a generator. Simple aero-derivative gas turbines are already achieving electrical efficiencies of 39%, although expected to rise to 60% within ten years; while state of the art combined cycle gas turbines are reaching 53% electrical efficiency [Farlin, 1994]. These compare well to diesel generator electrical efficiencies of 32 to 36% calculated for the stations (see Section 4.2.3). Furthermore, by using sulfur reduced liquid fuels such as SFJP8 - a kerosene type fuel identified for potential Antarctic use - extremely low emission characteristics are possible.

Gas turbines have not been dealt with in this study, which is principally about renewable energy options, but they do remain an attractive option for inclusion in back-up systems.

1.3.3 Fuel cells

For the future, replacement of diesel generators with fuel cells offers perhaps the ultimate method to reduce emission levels. Typical fuel cell designs consist of an electrolyte in contact with two electrodes. Fuel is brought into contact with one electrode (the anode), with air or oxygen brought into contact with the other (the cathode). Reactions at the anode oxidise the fuel, releasing electrons ready for work. These electrons flow through an external load to the cathode where they reduce oxygen and are balanced by an ionic flow within the electrolyte [Badwal, 1992]. The by-product of a fuel cell in addition to DC current is essentially water and heat.

A number of fuel cell types are currently under development. Each design operates at different temperatures, using different electrolytes and electrodes to induce different chemical reactions. With fuel cells not restricted by Carnot cycle efficiencies (using electrochemical rather than thermochemical reactions to generate power) high electrical conversion efficiencies are expected. Designs currently under development have electrical efficiency levels ranging from 35% to 60% [Badwal, 1992]. Utilisation of waste heat from fuel cells allow for even higher combined electrical and thermal efficiencies.

Although fuel-cell power generation has been used successfully in space vehicles since the Gemini and Apollo programs, it is still in its infancy and plagued by technical problems, high costs and reliability concerns. Current problems include the use of non-standard fuels often requiring reformation before use (representing as much as 60% of total costs) combined with expensive maintenance costs associated with regular electrolyte and electrode replacement. It has been suggested, however, that these problems will be overcome in the near future [Appleby, 1994]. The emergence of a highly reliable, low maintenance product - at a competitive price - would make fuel cells potentially ideal for use at the Australian Antarctic stations.

The introduction of a fuel cell - operating on hydrogen produced locally from electrolysis of water using electricity from renewable energies - has the potential to offer an ideal method for energy storage. An energy system comprising renewables, fuel cells, electrolysers, hydrogen storage, rectifiers and inverters has been hailed as the ultimate self-sustainable, self-sufficient energy system for the future at the stations [Steel, 1993; Guichard 1993, 1994a, 1994b]. This concept has been investigated in Chapter 6.

1.3.4 Renewable energy

Power generation from renewable energy sources offers an alternative to fossil fuel based systems. The Antarctic environment provides an almost unlimited source of renewable energy, in the form of strong winds and high summer solar energy levels, potentially ideal for exploitation using wind-turbines and/or photovoltaic (PV) arrays. Such systems offer a logical method to supplement or replace fossil fuel based systems.

While providing these resources, the Antarctic environment also imposes restrictions on the design of renewable energy generation devices. In order to operate at the ANARE stations, wind-turbines and PV arrays must be capable of surviving low temperatures and strong wind gusts. These requirements reduce the choice of renewable energy generation devices. Climatic conditions also provide other problems. Production periods for renewable energy generation devices are extremely variable, being dependent on meteorological conditions rather than station demand. A natural limit on the amount of energy that can be provided using renewables will exist, requiring some form of energy storage medium - or back up system - for continuous supply.

Identifying the potential for renewable energy systems to provide a significant proportion of the Australian Antarctic stations energy needs is addressed in the remaining chapters.

1.4 Antarctic renewable energy use

Power generation by renewables is already well established in Antarctica, although usually limited to small scale applications. Wind turbines and PV panels are used to power communication devices, meteorological equipment and other scientific projects, especially in remote locations. These applications are particularly suited to renewables, where the requirement is for unattended, low maintenance, automated power: conditions for which conventional diesel power plants are unsuited.

1.4.1 Australia

Application of renewable energies in Antarctica by Australia has been primarily restricted to communications and science support. Small (under 1 kW) PV arrays in conjunction with battery packs provide power to radio receivers and boosters for VHF radio networks at each station. For over 10 years PV panels have also been used in numerous automatic weather stations maintained by the Bureau of Meteorology (BoM). Similarly, many other science projects use PV panels to power recording devices or for lighting and computers in the field. The application of PV panels for small scale power generation is widely accepted and utilised by Australia in the Antarctic.

Small wind turbines have been used along side PV systems in similar situations, but with limited success. Designs used in the past typically did not include adequate mechanisms to prevent over-speeding. This proved fatal with strong winds almost always resulting in destruction of the generator, gearbox or blades. PV systems have proved more successful than the previous generation of small wind turbines because they are more robust. Their design enables them to withstand strong winds and low temperatures. With no moving parts, snow and ice penetration problems are less of a concern. Problems that have occurred with PV systems tend to result from either snow drift due to poor positioning - or more often - from battery failure in sub-zero temperatures. However, as battery technology advances this problem should become less of an issue.

The application of sizable renewable energy systems by Australia began at Heard Island during 1992/93 when a five-member wintering scientific expedition tested three wind turbines. Two 600 W Rutland Furlmatic 1800's and one larger 7.0 m diameter twin bladed 10 kW Aerowatt UM-70X were erected near field stations on the island. The Furlmatic design proved inadequate to the task of withstanding the turbulent wind conditions, with both units being destroyed. Failure was attributed to a flaw in their furling mechanisms, designed to provide speed regulation. Without speed control over-speeding caused runaway conditions, shattering the rotating permanent magnets of both units' generators.

The Aerowatt UM-70X (specifications presented in Table 1.3) proved better designed for the conditions and was successfully operated over a three month period. During this period, when sufficient winds were present, it provided almost 90% of the expeditions electrical and heating loads, allowing diesel generator runs to be minimised [Vrana, 1995]. Problems arose near the end of the Heard Island expedition with the UM-70X. A break in the blade-root, a design problem since identified by Vergnet, resulted in the unit becoming inoperable. After repair in Australia, the unit was prepared for further testing on the Antarctic continent. Further details of the performance of the UM-70X at Heard Island and its installation at Casey are given in Chapter 5.

Type	Up-wind horizontal axis
Support tower	18 m
Turbine diameter	7 m
Number of blades	2
Rated power	10 kW
Rated wind speed	11.5 m/s
Cut-in wind speed	3 m/s
Survival wind speed	90 m/s
Speed control system	Stall regulated using variable pitch blades
Yaw control	Vane
Generator type	AC induction generator

Table 1.3: UM-70X wind-turbine design specifications[Aerowatt, 1983]

1.4.2 Japan

The Japanese have an active program involving wind turbines. Overall 16 different units, specifically designed and built for use in Antarctica, have been tested at Syowa and Asuka stations to the west of Mawson in Queen Maud Land. Climatic conditions at these station are particularly extreme, resulting in the failure of all but their latest design due to low temperature and snow penetration problems [Kimura, 1991]. The design specification for their latest generation wind turbine erected in 1991, is presented in Table 1.4. Results from this unit were promising with an estimated annual output of 1400 kWh calculated from the recorded wind distribution [Kimura, 1993].

Type	Up-wind horizontal axis
Support tower	6m
Turbine diameter	2m
Number of blades	2
Blade pitch	Fixed - 30°
Rated power	5 kW
Rated wind speed	20m/s
Cut-in wind speed	10m/s
Survival wind speed	60m/s
Speed control	load regulation
Yaw control	Fixed - manually adjustable
Generator type	AC permanent magnet

Table 1.4: Asuka wind-turbine design specifications [Kimura, 1993]

The Japanese remain committed to the introduction of renewables at their stations in order to reduce the quantity of fossil fuel they currently import, estimated to represent 60% (by volume) of the total material sent to Antarctica in each season [Kimura, 1993].

1.4.3 Germany

Germany has also been experimenting with wind turbines at their winter station Neumayer. Like the Japanese, they have chosen to develop a wind turbine specifically for the conditions they anticipate. A vertical-axis HM-rotor was selected for use rather than the more common horizontal axis turbines. The specifications of the HMW-56 installed during 1991 at Neumayer are presented in Table 1.5 [Heidelberg, 1990].

Type	Vertical-axis HM-rotor
Support tower	10m
Rotor diameter	10m
Number of blades	3
Rated power	20 kW
Rated wind speed	9m/s
Survival wind speed	68m/s
Speed control	Electronically controlled
Generator type	Travelling field permanent magnet

Table 1.5: HMW-56 wind turbine design characteristics [Heidelberg, 1990]

This choice was made due to the added simplicity associated with the design: not requiring pitch control or yawing systems. By integrating the permanent magnet field generator into the steel support structure, the need for a mechanical drive train and transmission was also eliminated. Speed control is obtained electronically using eddy currents, with braking commencing at 30 m/s.

1.4.4 Spain

Experiments with wind turbines and battery storage have also been conducted at the Spanish station Juan Carlos I. This station, manned only during the summer, required an energy system to operate meteorological equipment and a seismology station automatically over the winter. To provide power, two 500 W Eolian wind turbines were installed in 1992, with a third 1.5 kW unit added during the 1993/4 season. The specifications of these turbines are presented in Table 1.6.

Type	Up wind - horizontal axis
Support tower	6 m
Turbine diameter	2.10 m
Number of blades	3
Rated power	1 x 1.5 kW, 2 x 500 W
Rated wind speed	25 m/s
Survival wind speed	36 m/s
Speed control	Variable - load regulation
Yaw control	Vane
Generator type	48 VAC - permanent magnet

Table 1.6: Eolian wind turbine design characteristics [Castellvi, 1994]

Power from the original two 500 W turbines was used to charge a 2000 Ah battery bank, which unfortunately failed during the 1993 winter season. A rather modest load of 67 W was sustained over the period of its operation, stated as being 'most unrepresentative' of the potential of the system. The two 500 W wind turbines survived undamaged over the winter, allowing for further testing to be implemented. A third turbine, rated at 1.5 kW, together with additional battery storage was added in 1994 to increase performance [Castellvi, 1994].

1.4.5 United States

The United States Antarctic Program (USAP), operates many projects using renewables. These include remote communication repeaters and solar powered AWSs (similar to Australia), a passive solar collector at South Pole station, and a renewable power system for the Black Island Telecommunication Facility (BITF). The BITF is an unmanned satellite communications ground station serving the nearby station of McMurdo, located 22 km away near Cape Hodgson in McMurdo Sound. Wind speeds of up to 80 m/s and minimum temperatures of -55°C have been recorded at Black Island.

During construction, the USAP made the decision to power the BITF using renewables in place of a diesel power system which would have required frequent maintenance and refuelling. In 1985, the original BITF renewable power system opened with one HR3 Northern Power Systems horizontal axis wind-turbine, specifications of which are presented in Table 1.7. This unit was used to charge a lead-acid battery bank, which provided the 1.2 kW of power necessary to run the facility. If insufficient winds resulted in the battery charge level dropping below 40%, an Ormat closed-cycle vapour turbine (CCVT) was engaged to charge the battery to 80% [Coleman, 1992].

Type	Up-wind horizontal axis
Turbine diameter	5m
Number of blades	3
Rated power	3 kW
Rated wind speed	12m/s
Speed control	Variable axis rotor control system - tilts the rotor assembly backwards
Yaw control	Vane
Generator type	AC permanent magnet

Table 1.7: HR3 wind-turbine design specifications [Coleman, 1992]

The facilities at BITF were enlarged in 1994 due to increasing power loads. Three more HR3 wind-turbines were installed, together with three arrays of Solarex MSX-60 PV panels, each array with an output of 4 kW and covering an area of approximately $93m^2$. An enlarged 31,680 Ah battery bank was linked to the wind turbines and PV panels via a 24 VDC bus, with three 1.2 kW Ormat CCVT used if low battery charge developed.

Power at the new upgraded BITF site is distributed using an AC and a DC network incorporating a 3.6 kW inverter, with the whole system controlled and operated using a SC400 Intelligent Autonomous System Controller via a remote link to McMurdo. The system, although proven, is still considered under development and will be used as a prototype for future USAP applications [Chiang, 1994].

1.4.6 Other operations

A Northern Power Systems HR3, as in use at BITF, was used by Greenpeace at their Antarctic World Park Base (WPB) located at Cape Evans on Ross Island. The WPB was established during the 1986/87 summer to monitor the nearby US and New Zealand stations of McMurdo and Scott. The HR3 wind turbine together with a 600 W PV array, were installed during the 1987/88 resupply season. These were used to charge a battery bank and provide additional station heating not met through a diesel co-generation system [Ballard, 1994].

The energy systems was upgraded in 1990/91. Increased battery storage and the introduction of kerosene heating in the place of electrical heating, allowed the diesel generators to be shut-down for an eight-hour period each day, with any remaining electrical loads met through the wind/solar/battery system [Ballard, 1994].

Renewables have also been in use at the French sub-Antarctic island of Amsterdam. In 1986 Amsterdam Island saw the installation of a 30 kW Darrieus rotor CEA30-AD10, a 3 bladed 10m diameter wind-turbine rated for 13.5 m/s winds. A daily energy production of up to 400 kWh was recorded early in the project although braking faults caused serious problems on many occasions. The project was discontinued after the main engineer supporting the project retired [Guichard, 1995].

1.5 Thesis structure

The current use of renewables in Antarctica, although limited, is very encouraging. Work reported in this thesis identifies the potential for large scale renewable energy systems to provide electrical power at the Australian Antarctic stations.

1.5.1 Aims

The aim of this work is to develop a method to identify the potential for using renewable energy resources to provide electrical power at the Australian Antarctic stations. To achieve this goal, research has been directed into the following areas:

1. Identification of the renewable energy resources at the Australian Antarctic stations, focusing on wind and solar power generation;
2. Identification of the energy demands at the Australian Antarctic stations;
3. Testing of components in Antarctica at Casey Station;
4. Examination of possible renewable energy systems; and
5. Development of a model to estimate the performance of different sized renewable energy system configurations.

Results from these investigations have allowed for estimates of the performance of different configurations of renewable energy systems. Costing based on these estimates will allow decisions to be made on the potential for renewable energy systems at the Australian Antarctic Stations.

1.5.2 Chapter 2-7 outlines

Chapter 2 Provides an analysis of the wind energy resources available at the stations, using wind speed data recorded at the stations by the Australian Bureau of Meteorology (BoM).

Chapter 3 Sets out procedures to identify the recoverable energy from the sun using photovoltaics, based on an empirical model using cloud cover.

Chapter 4 Presents a study of the energy usage patterns at the stations. Statistical relationships between personnel numbers, climatic conditions and electrical power loads are determined.

Chapter 5 Describes field work conducted in Antarctica, involving testing equipment including a 10 kW wind-turbine and installation of monitoring equipment.

Chapter 6 Presents results from matching the expected renewable energy reserves to the station demands. Wind-turbine, PV and storage methods, including batteries and an 'hydrogen loop', are modelled giving the results of different configurations, sizing and control strategies.

Chapter 7 Contains a final discussion and summary of the results of this study.

Chapter 2

Wind energy resources

2.1 Introduction

Wind energy was identified by the SCALOP Sub-group on Alternative Energy as one of the most practical renewable energies, 'ready for near term application in Antarctica' [SCALOP, 1993]. To determine the potential for wind power at the ANARE stations, detailed assessments of the wind resources at each site have been made.

2.2 Analysis of wind at the Antarctic stations

Statistics indicate the winds of Eastern Antarctica can be extremely strong. Coastal zones backing onto the Antarctic ice cap are continually blasted by strong, frigid winds rolling off the central plateau. These combined with winds from the many polar storms that encircle the continent along the temperate storm belt (a converging low-pressure zone at 60°S), result in periods of high winds at each of the continental stations. Macquarie Island, situated in the Southern Ocean between the roaring forties and furious fifties, likewise experiences strong winds.

2.2.1 Wind statistics

Wind speed measuements have been recorded at the Australian Antarctic Stations since their founding by the Bureau of Meteorology (BoM). The maximum strength of wind gusts recorded for each of the stations is given in Table 2.1 [Guichard, 1995].

Station	maximum wind gust (m/s)
Casey	80.8
Davis	57.1
Mawson	68.9
Macquarie Island	51.4

Table 2.1: Maximum reported wind-gusts for the ANARE stations [source Guichard, 1995]

In addition to wind gust measurements, reported only as absolute maxima, continuous readings are also taken by the BoM. These consist of a 10 minute average taken immediately before the hour, every three hours. Using these readings, over a six year period from 1990 to 1995 with less than 1% of observations missing, statistics have been calculated for each station. The mean, maximum and standard deviation of the wind speed are presented in Table 2.2, together with the coefficient of variation and the wind ratio. The coefficient of variation (standard deviation/mean) and wind ratio (mean /maximum) indicate the degree to which the mean is related to the spread of the wind speed distribution. These statistics divide the stations into two groups, with Casey and Davis having lighter more variable winds than Mawson or Macquarie Island.

Station	maximum wind speed (m/s)	mean wind speed (m/s)	standard deviation (m/s)	coefficient of variation (std/mean)	wind ratio (max/mean)
Casey	49.4	7.1	7.8	1.10	0.14
Davis	36.0	5.3	4.2	0.82	0.18
Mawson	42.2	11.3	7.1	0.62	0.29
Macquarie Island	28.8	9.5	4.1	0.44	0.33

Table 2.2: Wind-speed statistics at the ANARE stations (calculated using BoM data consisting of 10 minute averages, taken every three hours) [source BoM, 1990-95]

2.2.2 Annual and diurnal averages

Information on the timing and strength of winds is important. The annual and diurnal wind speed averages presented in Figure 2.1 indicates the expected wind speed for a given time throughout the year. To construct these figures, wind speed measurements recorded at the stations over the period 1990-95 have been separated into three hourly intervals for each month, and then averaged. A bi-directional linear interpolation routine has then been used to fill between grid points.

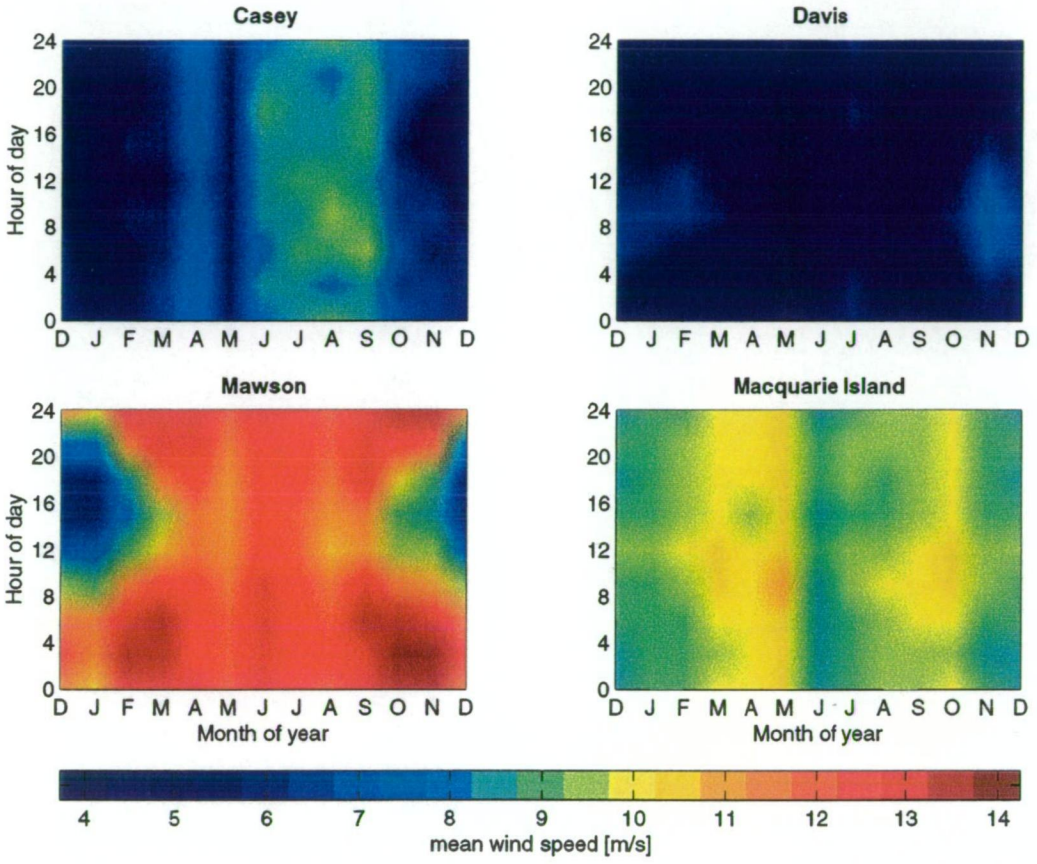

Figure 2.1: Annual and diurnal wind speed averages at the ANARE stations [using BoM data 1990-95]

The following observations of note are evident from Figure 2.1.

- **Casey:** winds average up to 9 m/s during the winter months, dropping to 6 m/s over the summer months;
- **Davis:** winds averages around 5 m/s for most of the year, except during the summer when the morning wind speed average increases to 8 m/s;
- **Mawson:** strong regular winds averaging between 12 and 14 m/s are evident for most of the year, except during a period of relative calm in summer when the afternoon wind speed average drops to 6 m/s;
- **Macquarie Island:** very regular winds, consistently averaging above 9 m/s throughout the year, increasing to just over 10 m/s during March and September.

The strong wind flow at Mawson is a result of katabatic air flow off the polar ice cap. At Macquarie Island, high wind speed averages are a result of the many storms that batter the island. These intensify during the equinoxes when gales across a broad latitude band, encompassing the island, encircling the entire Southern Hemisphere.

2.2.3 Wind direction analysis

Further information about the winds experienced at each station can be obtained by separating observations by direction. In Figure 2.2 the mean and maximum have been calculated for wind recordings separated into 16 bins, each 22.5° wide and centred on the major and minor compass directions. The frequency of winds in each of the bins has then been superimposed onto these readings, indicating the direction of the prevailing winds at each of the stations.

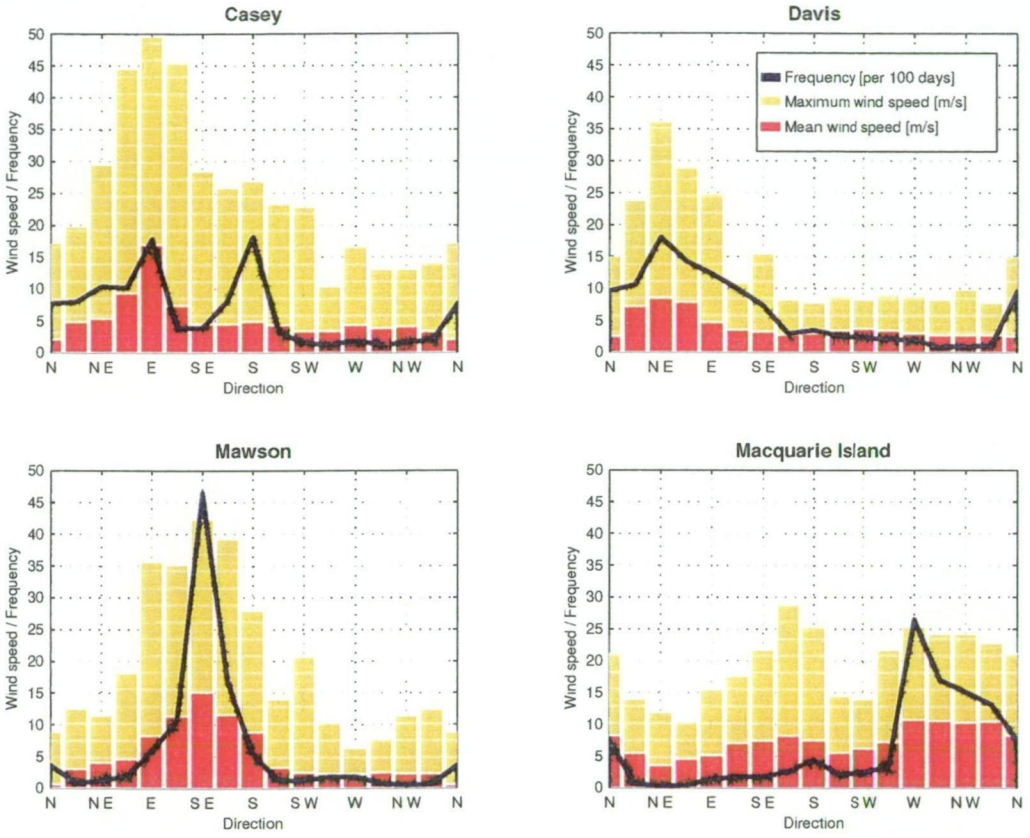

Figure 2.2: Breakdown of the wind speed record for each of the sixteen major compass directions at the ANARE stations (indicating frequency of observations, mean and maximum) [using BoM data 1990-95]

The following observations of note are evident from Figure 2.2.

- **Casey:** winds from the east and south dominate, although only winds from the east are of significant strength;
- **Davis:** easterly flow is evident, with flow from the north-east the highest, although highest directional wind speed average is low in comparison to the other stations;
- **Mawson:** extremely strong and regular winds from the south-east are evident;
- **Macquarie Island:** strong winds from the west to the north dominate.

The occurrence of high average wind speeds, in the direction of the prevailing wind, is especially high at Mawson. This would allow for simplified uni-directional wind turbine designs, an approach adopted by the Japanese at Asuka station (see Section 1.4.2). Such designs are less complicated, requiring no yaw tracking system or slip ring arrangement for power transmittance across bearings.

2.2.4 Frequency-of-occurrence distributions

The spread of the wind speed is indicated by the frequency-of-occurrence distribution. The distribution for each station, presented in Figure 2.4, has been determined by calculating the ratio of wind speeds observed within a given speed range using a 2.5 m/s bin size. Periods of calm, where the wind speeds was zero or below detectable level, have been separated and placed in a special bin at zero.

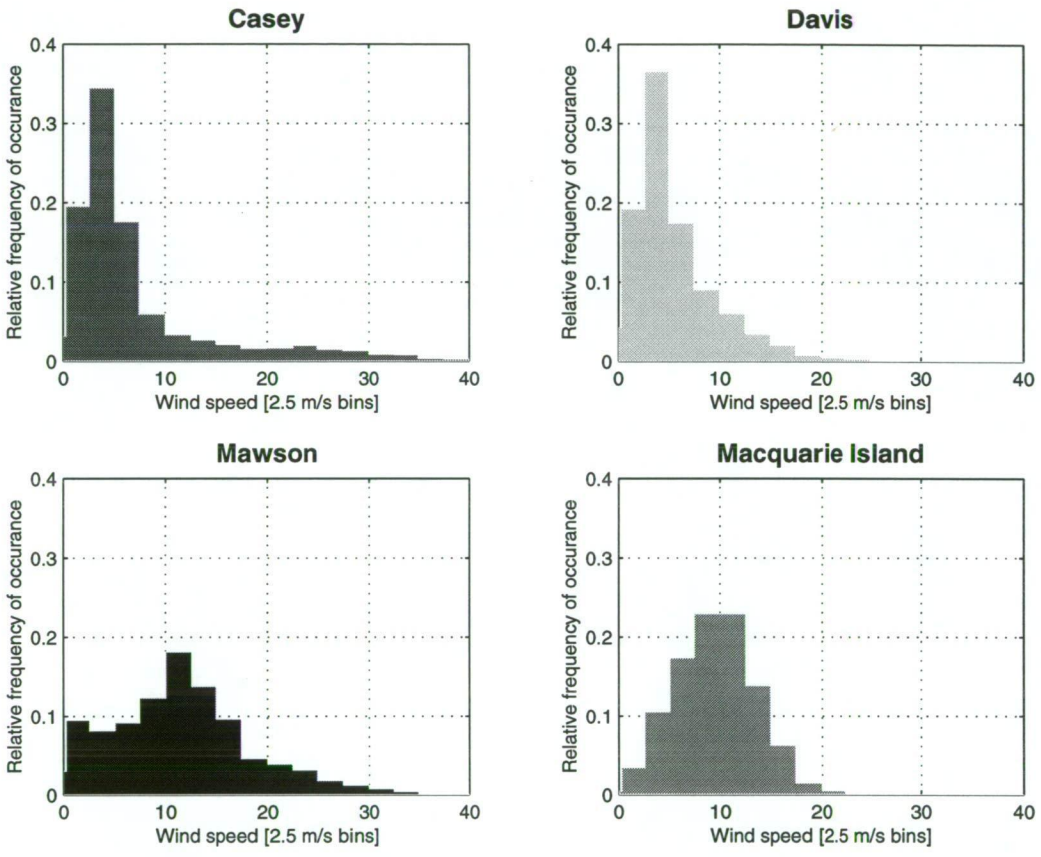

Figure 2.3: Wind speed frequency-of-occurrence distributions for the ANARE stations [using BoM data 1990-95]

Casey and Davis both have a high concentration of wind speeds under 10 m/s. Both stations record a large percentage (approximately 88% and 80% respectively), of their total winds below this level. For winds over 10 m/s, however, their distributions differ considerably. Casey has a more drawn-out distribution well up into the +40 m/s range; while for Davis the distribution ends at the 30 m/s bin. Mawson and Macquarie both experience stronger winds with their wind speed distributions shifted into higher regions. For Mawson winds peak between 10 and 12.5 m/s with a significant proportion under 2.5 m/s and greater than 20 m/s. Macquarie Island has a much more compact distribution centred around 10 m/s, with little occurrence of either very light or very strong winds.

The region of interest for power generation is for winds above 6 m/s and below 30 m/s, for which most commercial wind turbines have been designed. This is because winds below 6 m/s do not hold much energy, while wind turbines designed to operate in winds above 30 m/s, require extensive structural reinforcement, often reducing performance in low winds, and increasing costs.

A compromise is reached in most designs, maximising the total amount of power produced for a typical wind distribution against production costs. For Casey and Davis, the best period for energy production (above 10 m/s but below 30 m/s) equates to approximately 17% of observed 3 hourly readings. For Mawson and Macquarie, 55% and 45% of all observations falling into this range, three times that for Casey and Davis.

2.2.5 Weibull parameters

It is common in wind power studies to fit a known function to the wind speed distribution. This is useful for comparison between sites in wind studies and often is used by the wind power industry. The Weibull function is the most widely accepted function for this task. It has been used in many wind power reports over the last 20 years, and has become a standard to indicate the wind resources of a site (see Justus, [1976 & 1978]; Hennessey, [1977 & 1978]; & Conradsen, [1984] for example).

The Weibull function is a two parameter function that is easy to work with and has a number of useful features. This includes the ability to project a Weibull function, from an observed height to another height, allowing estimates of the wind speed field to be made for different heights. The Weibull probability function $P_{weibull}$ at a wind speed v is given by the expression [Justus, 1978]:

$$P_{weibull}(v) = \frac{k}{c}\left(\frac{v}{c}\right)^{k-1} \exp\left[-\left(\frac{v}{c}\right)^{k}\right] \qquad (2.1)$$

The scale parameter c, is closely related to the mean of the wind speed series, while k, the shape parameter is related to the skewness. For $k=1$, the Weibull probability function is exponential; while for $k = 2$, it is equal to the Rayleigh distribution, another function also often used in wind power studies; and for $k = 3.5$, it is approximately normal [Hennessey, 1977]. The probability of wind speeds below a wind speed v, is given by the Weibull cumulative function $S_{weibull}$:

$$F_{weibull}(v) = 1 - \exp\left[-\left(\frac{v}{c}\right)^{k}\right] \qquad (2.2)$$

A limitation in fitting the Weibull probability function to a wind speed distribution is that zero wind speeds are not taken into consideration. A probability of zero is always given for zero wind speeds by virtue of form of Equation 2.1. A method to correct this has been suggested by Takle (1978). This involves the introduction of an extra parameter, the frequency of zero wind-speeds F_0, resulting in the hybrid Weibull probability function given below [Takle, 1978]:

$$P_{hybrid}(v) = F_0\delta(v) + (1 - F_0)P_{weibull}(v) \qquad (2.3a)$$
$$S_{hybrid}(v) = F_0\delta(v) + (1 - F_0)S_{weibull}(v) \qquad (2.3b)$$

where $\delta(v)$ is the Dirac delta function, equal to one for $v=0$, or zero otherwise. To fit the hybrid Weibull probability function to observational data, a number of methods have been suggested (see Justus, [1978]; Conradsen, [1984]).

A simple method suggested by both these authors, involving a weighted least-squares process, has been used in this study. This method involves modifying the hybrid cumulative Weibull probability function given in Equation 2.3 using logarithms to give the linear relationship presented in Equation 2.4. This equation is easily solved for the Weibull parameters *c* and *k*, using a weighted regression fit as set out in Justus (1978).

$$\ln\left\{-\ln\left[1 - S_{hybrid}(v)\right]\right\} = k\ln c - k\ln v \qquad (2.4)$$

(Let $y = \ln\left\{-\ln\left[1 - F_{weibull}(v)\right]\right\}$ $x = \ln v$ and solving for y = k ln(c) - kx.)

Modified Weibull functions, calculated using this method, are presented in Figure 2.4 superimposed onto the frequency-of-occurrence distribution that was used to solve Equation 2.4. The Weibull functions have been scaled for a 2.5 m/s bin size to allow comparison.

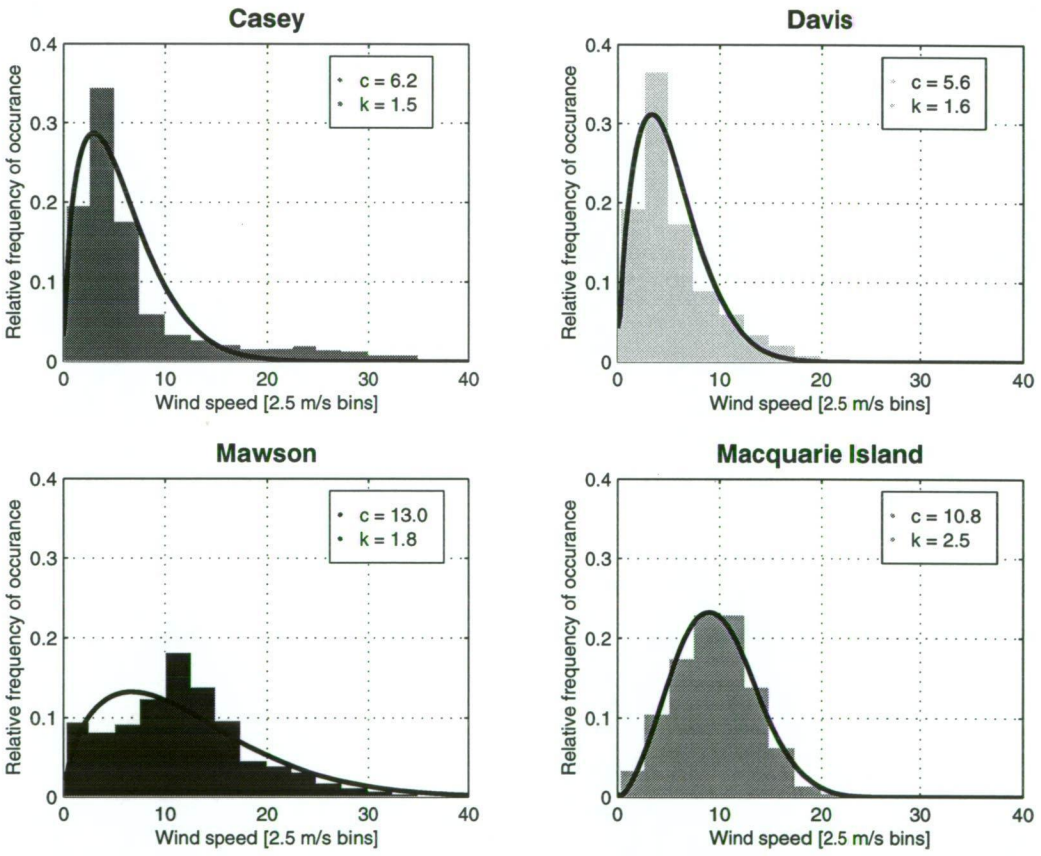

Figure 2.4: Wind speed frequency-of-occurrence distributions for the ANARE stations, with superimposed scaled Weibull functions (solid lines) and parameters.

The high occurrence of winds below 10 m/s has been captured by the Weibull function for Casey and Davis, although winds above 20 m/s are underestimated for Casey. The distribution for Mawson peaks at a lower wind speed than the frequency-of-occurrence distribution , although high winds are captured well. The Weibull function for Macquarie Island represents an excellent match with the frequency-of-occurrence distribution.

Values for the Weibull scale and shape parameters for each station are presented in Table 2.3, together with the frequency of occurrence of zero winds F_0. (Note: the frequency of zero winds and shape parameter are dimensionless).

Station	Frequency of zero wind F_0	scale parameter c [m/s]	shape parameter k
Casey	0.03	6.2	1.5
Davis	0.05	5.6	1.6
Mawson	0.03	13.0	1.8
Macquarie Island	0.004	10.8	2.5

Table 2.3: Weibull parameters for the wind speed at the ANARE stations [from BoM data 1990-95]

Mawson and Macquarie Island have higher scale parameters than either Casey or Davis, as is expected from the means reported from the stations. The continental stations also differ from Macquarie in having lower shape parameter values and a higher percentage of zero wind speeds measurements. The frequency of zero wind is ten times higher at the continental stations than at Macquarie Island. This indicates that there are more days of relative calm at the continental stations, while the winds rarely stop at Macquarie Island.

2.3 Converting wind energy into electrical power

The instantaneous power density (Wm^{-2}) available in a flow of air through a unit cross-sectional area normal to the flow is given by [Hennessey, 1977]:

$$P_{inst} = \tfrac{1}{2}\rho V^3 \qquad (2.5)$$

Where V is the instantaneous wind-speed and ρ is the density of air, equal to approximately 1.23 kg/m^3 at sea-level and assumed constant in this study. However, the proportion of this power that can be converted into electricity is much less.

2.3.1 Wind measurements

A standardised method for recording wind measurement is useful to allow comparison between sites and studies. Hourly measurements of the wind speed at a height of 10 m have been recommended, with measurements preferably from a number of years [Gjerding, 1991]. For the Antarctic stations BoM records have been used. While not hourly this data has been recorded over a number of years and captures all major synoptic wind events and conforms to the Australian Standard 2923, a 'Guide for measurement of horizontal wind for air quality applications' [SAA, 1987].

Efforts to establish a monitoring network to provide better data in future has been reported in Chapter 5, along with an estimate on the accuracy of the BoM records. Until these new readings are available from the stations, the evaluation of the power obtainable from the wind must be based on BoM wind speed measurements.

2.3.2 Wind turbine performance models

Two basic approaches exist to estimate the amount of power produced by a wind turbine based on wind speed measurements at a site. The first involves complex modelling of actual physical processes. These include mathematical descriptions of the aerodynamic interaction of the wind with the turbine blades, transmission of mechanical power through the drive train and the electro-magnetic characteristics of the generator. These models are used in design applications, employing very short time steps and are not appropriate for this investigation.

The second approach is more generalised and less concerned with the actual physical processes occurring. These models employ a 'black box' approach to power generation based on an empirical relationship between the wind speed and output power of a machine. This relationship is referred to as the power curve and is usually derived for a particular turbine from measurements taken over a period of time. This approach has been used in these investigations.

Using the power curve $w(V)$, for a given wind turbine design at a site with a known probability distribution of the wind-speeds $p(V)$ calculated over a given time period, the average recoverable power P_{rec} is given by the expression [Justus, 1976]:

$$P_{rec} = \int_0^\infty w(V).p(V).dV \qquad (2.6)$$

The accuracy of Equation 2.6 depends not only on the reliability of the power curve and its applicability under local atmospheric conditions, but also on the correctness of the wind speed probability distribution. A suitable time step over which to capture an accurate representation of the wind speed probability distribution is needed for good estimates.

Using the mean wind speed to represent the wind speed probability distribution is a simple (but very rough) method to estimate the recoverable power of the wind. If sufficient data is available at a site, the frequency-of-occurrence distribution offers a much better method. Periods of higher than average wind speed, during which power generation is maximised, are far better accounted for using this method.

The frequency-of-occurrence distributions identified for the stations, although better than the average, are still approximations for the actual wind speed probability distributions at the stations. This is due to the structure of the wind speed record at the stations (consisting of 3 hourly measurements of the 10 minute average taken, for this study, over the 6 years 1990-1995). This results in a discrete function for the frequency-of-occurrence distribution defined every 2.5 m/s. More frequent measurements over a larger period would allow for better resolution of the frequency-of-occurrence and thus better estimates for the recoverable power.

If measurements are limited, statistical properties of the observed wind speed can be used to calibrate a mathematical function to represent the wind speed probability distribution. As indicated before, the most common function associated with wind speed distributions is the Weibull function. Hennessey (1977) suggested that a continuous function such as the Weibull should always be used due to the limited resolution and discrete form of estimates based on frequency-of-occurrence measurements where cut-in, rated and furling speeds often fall between bins. A large number of measurements would, however, reduce this effect as bin sizes could be made small.

For the purpose of estimating the wind resources at the stations, direct use of frequency-of-occurrence measurements and Weibull functions have been used to estimate the wind speed probability distribution.

2.3.3 Wind power capacity factor estimates

Estimates of the power output from a particular wind turbine design, given its power curve and the wind speed probability distribution, can be used to calculate the wind power capacity at a site. The wind power capacity factor indicates the proportion of a period for which a wind turbine would have to operate at its rated power in order to produce the same amount of energy as produced over an interval due to variations in the strength of the wind speed.

The power curve given for the Aérowatt UM-70 wind-generator, rated at 10 kW, is given in Figure 2.5. This power curve will be used throughout this thesis as an example of a typical wind turbine suitable for use at the Australian Antarctic stations. A 0.85 reduction factor due to turbulence has been applied to this power curve as reported for the stations [Guichard, 1994a].

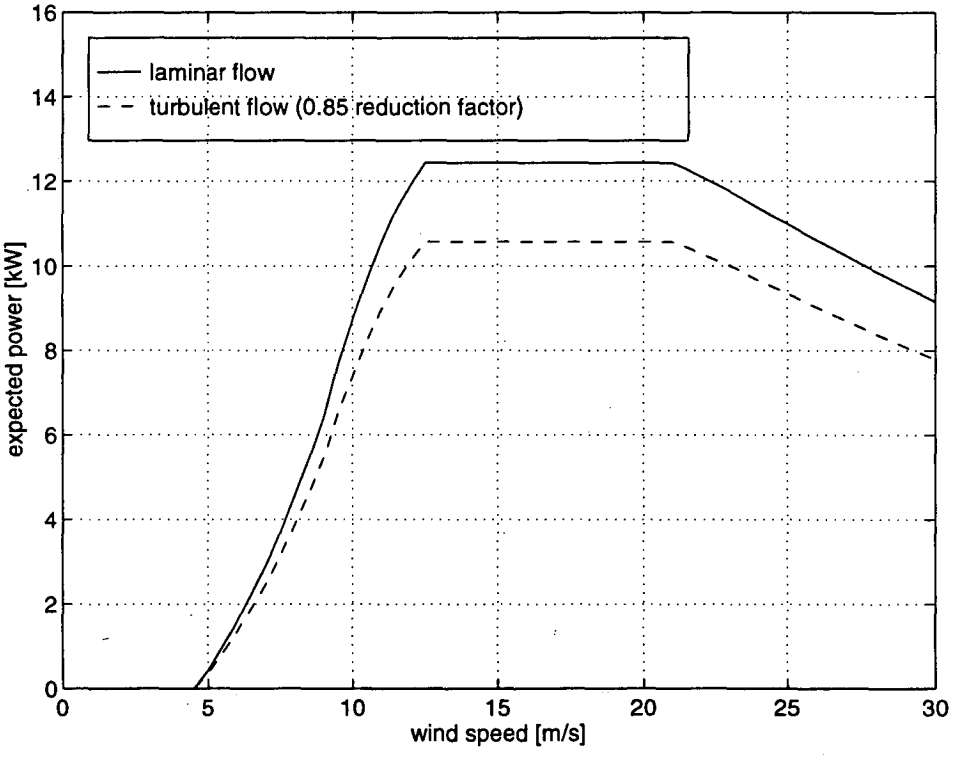

Figure 2.5: Power curve for Aerowatt UM-70X wind turbine, indicating 0.85 turbulence reduction factor for Antarctic conditions [Aerowatt, 1984].

The annual energy production and wind capacity factors for the UM-70X are presented in Table 2.4 for each of the stations. These have been calculated using both the discrete frequency of occurrence distribution and the Weibull function to approximate the probability distribution of the wind speed at each station based on 3 hourly BoM wind speed records from 1990-1995 (as reported in Sections 2.2.4 and 2.2.5). A ΔV bin size of 2.5 m/s has been used for the frequency-of-occurrence estimates while Weibull function estimates have been based on the equations calculated in Section 2.2.5.

Station	Using frequency-of-occurrence distribution		Using Weibull function	
	Energy production (MWh/y)	Wind capacity factor	Energy production (MWh/y)	Wind capacity factor
Casey	20.1	0.23	19.8	0.23
Davis	18.0	0.21	15.1	0.17
Mawson	56.7	0.65	50.3	0.57
Macquarie Island	51.9	0.59	51.1	0.58

Table 2.4: Station wind power estimates using Aerowatt UM-70X power curve, together with frequency-of-occurrence distribution and Weibull functions [using BoM data 1990-95]

Comparison of the results for the two methods indicate agreement to within 2% for Casey and Macquarie Island, and 15% for Davis and Mawson. In all cases estimates using the Weibull function were lower. Seasonal variations between the two can be seen from the monthly wind capacity factor levels given in Figure 2.6 where estimates using Weibull functions for each month have been superimposed as dashed lines onto estimates using the frequency-of-occurrence distributions.

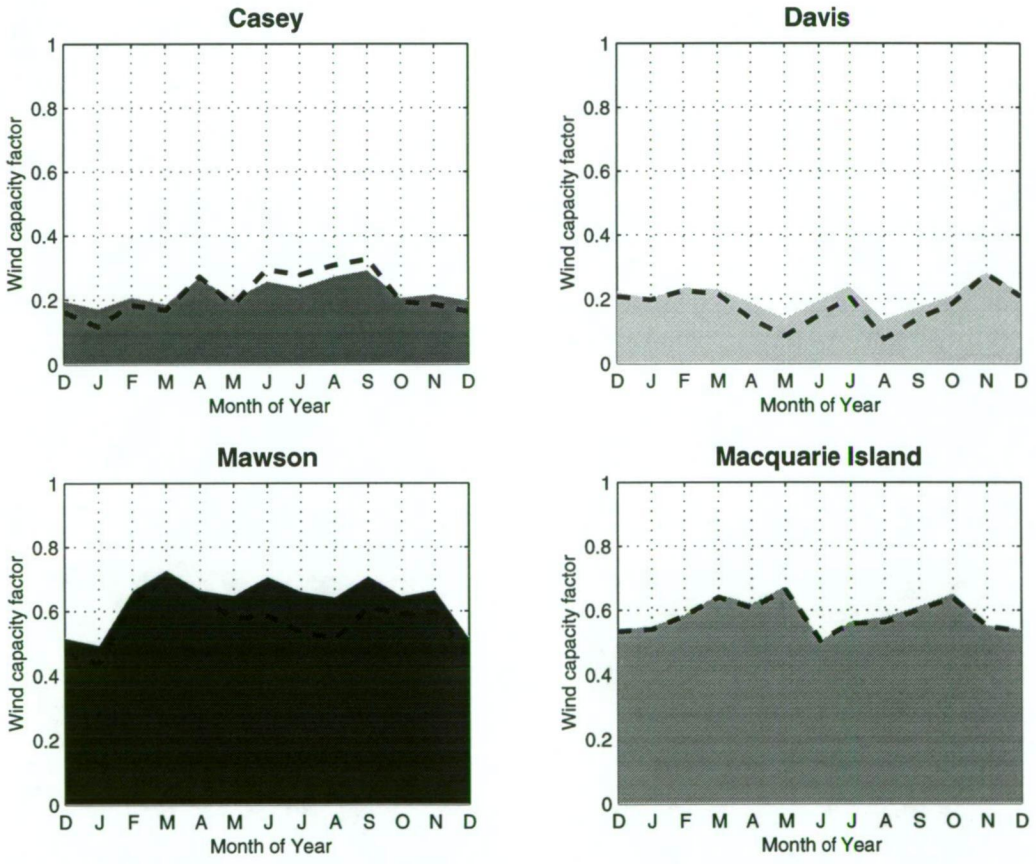

Figure 2.6: Wind power capacity estimates for the ANARE stations, for the frequency-of-occurrence (solid) and Weibull function (dashed line) [using BoM data 1990-95]

As a consequence of the different wind resources the estimated wind capacity factors for Casey and Davis are much lower than for Mawson and Macquarie Island. Periods of high wind energy production (high wind capacity factors) correspond with the high mean winter wind speeds calculated for Mawson and equinoctial peaks at Macquarie island.

There are marked differences between the stations and their respective wind resources. Mawson and Macquarie Island stand out as excellent sites for wind energy exploitation, while Casey and Davis can only expect about one-half to one-third as much energy to be produced from a similar sized unit.

2.3.4 Height projection

Boundary layer effects in the lower part of the atmosphere slow the horizontal component of the wind near the Earth's surface. This results in a vertical wind profile where the horizontal wind decreases in strength from the geostrophic wind at the top of the boundary layer to zero at the earth's surface [Barry, 1987].

To reduce these effects, wind turbines can be raised on towers to a height where stronger, more laminar flows are experienced. As a result of this, the height of wind-speed recordings (10 m for BoM data) and hub heights for wind turbines, will usually differ. Estimating the increase in wind speed with height is not straight forward. The most common methods in use assume either a logarithmic profile or a power law profile as described in Justus (1976).

An alternative to these is to use a calibration constant, defined from a simple empirical fit of data at multiple heights. A comparison of different techniques, indicates the success of different methods is highly site dependent, with no overall best method [Peterson, 1978].

One technique suggested by Justus (1976), provides for an easy estimate through projection of the Weibull parameters from a reference height to another height. This method assumes a power law profile and relationships between the Weibull parameters and height calculated empirically from experiments for a number of sites in the USA. Although this method has been criticised by Peterson (1978) and Doran (1978), particularly in their choice of constants and claim for universality between sites, it does give a simple indication of the effect of tower height on power capacity estimates. Using the expressions below, where the wind measurement height is given by z, and the turbine height by z^*, the values of c^* and k^* at height z^* can be evaluated [Justus, 1978].

$$c^*(z^*) = c(z^*/z)^n \qquad k^*(z^*) = k\left[\frac{1-0.088\ln(z/10)}{1-0.088\ln(z^*/10)}\right] \tag{2.7}$$

where the exponent n is given by:

$$n = \left[\frac{0.37-0.088\ln c}{1-0.088\ln(z/10)}\right] \tag{2.8}$$

An assumption when using this method in conjunction with the hybrid function of Takle (1978), is that the frequency of zero wind speeds does not alter with height.

Using the relevant estimates for the scale and shape parameters estimated from the BoM data taken at a standard height of 10 metres, projection of the wind capacity factors can be made for different hub heights. Table 2.5 gives the projected Weibull parameters to heights of 20 and 30 metres, and corresponding wind capacity factors with their relative increase.

Station	10 metres			20 metres (projected)				30 metres (projected)			
	c	*k*	capacity factor	*c*	*k*	capacity factor	increase (%)	*c*	*k*	capacity factor	increase (%)
Casey	6.2	1.5	0.23	7.2	1.5	0.31	35%	7.8	1.6	0.35	54%
Davis	5.6	1.6	0.17	6.5	1.7	0.24	38%	7.1	1.8	0.28	64%
Mawson	13.0	1.8	0.57	14.5	1.6	0.63	9%	15.4	1.7	0.65	14%
Macquarie I.	10.7	2.5	0.58	12.0	2.7	0.70	20%	12.8	2.8	0.75	29%

Table 2.5: Wind capacity factor and Weibull parameter estimates for different heights at the ANARE stations

Turbines with hub heights at 30 metres could expect substantial improvements over similar units at 10 metres. Even higher increases could be possible with taller towers. Structural strength and costs will be the deciding factors in tower height.

The use of tall towers does, however, offer very interesting possibilities at Casey and Davis where the wind capacity factors are estimated to increase between 54% and 64% with the use of 30 metres towers. These are impressive increases, but will need to be verified. In a study by Doran (1978), the technique used to give these estimates was found to result in overestimation of the power production level by 25% or more in 42% of 70 sites investigated.

2.4 Summary

Analysis of the wind resource at the Australian Antarctic stations indicates varied conditions. Mawson and Macquarie Island have excellent resources, with mean wind speeds of 11.3 m/s and 9.5 m/s. Casey and Davis have average to poor wind resources, with mean wind speeds of 7.1 m/s and 5.3 m/s.

Production estimates for wind turbines follow a similar pattern. Wind capacity factors, a measure of the period for which a turbine is expected to produce at its rated power, have been estimated at 0.65 for Mawson, 0.59 for Macquarie Island, 0.23 for Casey and 0.21 for Davis (based on the Aerowatt UM-70X). This indicates that output levels for a similar type of unit will be 2 to 3 times greater at Mawson and Macquarie Island than at either Casey or Davis.

Investigations on the vertical profile of the horizontal wind show substantial increases in production can be expected if wind turbines are situated on tall towers.

Chapter 3

Solar energy resources

3.1 Introduction

The SCALOP Sub-group on alternative energy for Antarctic stations identified solar power, along with wind power, as 'ready for near term application at Antarctic stations' [SCALOP, 1993]. To assess the potential for solar energy use, the incident solar radiation levels at the stations are calculated.

3.2 Definitions

Solar energy systems are dependent on the level of radiation reaching the surface of the Earth from the Sun. This is a function of the following parameters:

1. Solar output;
2. Earth-sun geometry; and
3. Interaction with the atmosphere.

A description of these parameters is presented below, using terms from elementary astronomy and physics.

3.2.1 Celestial co-ordinates

Celestial co-ordinates are used to define the position of bodies in the sky, including the sun. These are best envisaged as co-ordinates on the surface of an imaginary sphere covering the entire sky, defined as the celestial sphere. Co-ordinates are defined for objects projected onto the surface this sphere, relative to a reference point. In the horizontal systems, the centre of the celestial sphere is fixed on the centre of the Earth, and the horizon is used as a reference from which to define co-ordinates. [Sayigh, 1977].

A representation of this system is given in Figure 3.1, with the following quantities indicated:

Zenith:	Point directly above observer on celestial sphere.
Nadir:	Point directly below observer on celestial sphere (diametrically opposite zenith).
Celestial poles:	Zeniths of the terrestrial poles (ie. zenith if observer at either north or south geographical pole).
Celestial equator:	Great circle on the surface of the celestial sphere normal to the Earth's axis of rotation.
Meridian:	Great circle on the surface of the celestial sphere passing through the zenith, nadir and both celestial poles.
Hour circle:	Great circle normal to the celestial equator, passing through the sun. This is often called the declination circle as the angular distance of the sun, measured along this circle from the celestial equator, equals the solar declination (δ).
Hour angle (h):	Angular distance between the hour circle and the observer's meridian, measured either in hours or degrees. Positive values are defined for when the sun is westward of the meridian (afternoon), and negative for when it is eastward (morning). The zero

hour angle occurs when the sun is at its maximum height in the sky (mid-day).

Solar altitude (β): The angular elevation of the sun above the horizontal, measured positive towards the zenith, negative towards the nadir.

Solar azimuth (A): Angular distance from the meridian to the great circle passing through the sun and the zenith. It is measured along the horizon from North, positive to the east and negative to the west [Sayigh, 1977].

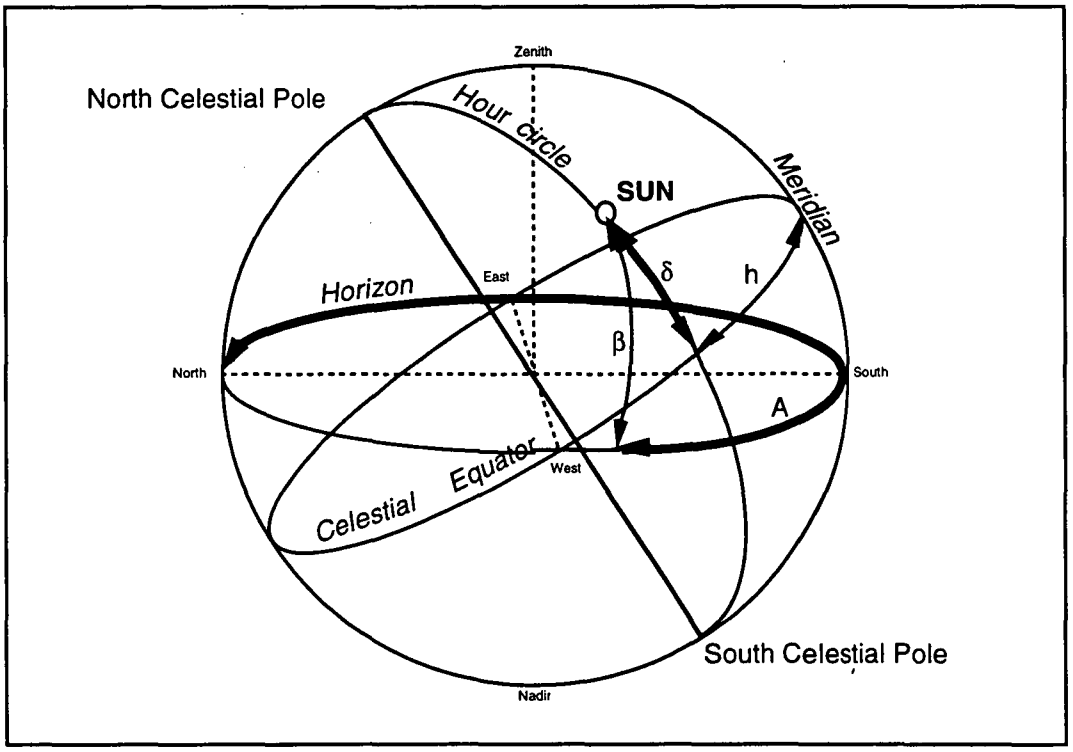

Figure 3.1: Celestial sphere indicating the solar azimuth A, solar altitude β, hour angle h, and declination δ defined for the horizontal system [adapted from Sayigh 1977]

The solar declination, δ, is a measure of the inclination of the equatorial plane, the plane normal to the Earth's axis of rotation with respect to the elliptic plane, the plane defined by the Earth's orbit around the Sun. The inclination between these planes varies by up to +/-23°27' over the course of a year as the Earth progresses along its orbit around the Sun [Sayigh, 1977].

Variations in the magnitude of the solar declination over a day are small. Taking this into account the solar declination can be approximated by the simple sinusoidal expression in Equation 3.1 [Paltridge, 1976]. In this equation the solar declination angle δ, is assumed constant over a given day, d, past the March 21 equinox. Positive angles indicate the sun is north of the celestial equator, negative angles south.

$$\delta^o = 23.45^o \times \sin\left(\frac{d}{365.25}\right) \qquad (3.1)$$

The apparent path of the Sun is along a circle parallel to the celestial equator, offset at the relevant declination angle as measured along the hour circle. Using the approximation of the solar declination angle given in Equation 3.1 for a given day of the year, we can define the position of the Sun. Equations 3.2 and 3.3 give expressions for the solar altitude, β, and solar azimuth, A, given the latitude, ϕ, and local hour angle, h, of a site [Sayigh, 1977].

$$\sin(\beta) = \sin(\delta)\sin(\phi) + \cos(\delta)\cos(\phi)\cos(h) \tag{3.2}$$

$$\cot(A) = \frac{\sin(\phi)\cos(h) - \cos(\phi)\tan(\delta)}{\sin(h)} \tag{3.3}$$

Negative latitude angles are used for southern hemisphere sites, while negative solar altitude angles indicating the sun is below the natural horizon (although local terrain must be taken into account for the actual horizon).

3.2.2 Solar radiation composition

The above definitions allow us to describe the geometry associated with radiation arriving at the surface of the Earth. The composition of the radiation is dependent on the extraterrestrial solar radiation reaching the top of the atmosphere and depletion effects from within the atmosphere.

The amount of extraterrestrial solar radiation striking the top of the atmosphere varies due to fluctuations in the energy output of the Sun and changes in the Earth-Sun distance. The magnitude of these variations are rather small at 2 to 3%, and thus can be ignored. This allows for the definition of a constant, the solar constant, representing the average extraterrestrial radiation at mean earth-sun distance. The current (NASA/ASTM) standard value for this quantity is 1354 Wm^{-2} [Sayigh, 1977].

Depletion effects from within the atmosphere lower the amount of this radiation reaching the surface of the Earth. Sayigh (1977) and Paltridge (1976), have attributed these depletion effects to the following processes:

1. **Rayleigh scattering** from air molecules smaller than the wavelength of solar radiation;
2. **Scattering by aerosols** from dust, smoke and other air particles which may be larger than the wavelength of the solar radiation; and
3. **Absorption by atmospheric gases** from O_2, N_2 and H_2O in the short wavelength region, and by O_3, CO_2 and especially H_2O in the long wavelength region.

These processes are compounded for low solar altitude angles where the effective 'air mass' of the atmosphere is increased. Cloud will also influence the amount of incoming radiation reaching the ground. Clouds reflect and absorb radiation both internally and from their lower surface to a degree dependent on their thickness, density and the size of water droplets they contain.

The radiation that does arrive at the Earth's surface consists of two components: direct radiation and diffuse radiation. Direct radiation is the proportion of the extraterrestrial solar radiation incident on the ground which has been directly transmitted through the atmosphere without reaction. It consists of short wavelength radiation concentrated in a beam.

Diffuse radiation consists of scattered radiation and is often assumed isotropic, or uniformly distributed across the sky. While this is not technically correct, with differences having been measured at up to 21% [Paltridge, 1976], it does allow for a more simple description of the radiative process.

Combined, the direct and diffuse radiation make up the global radiation incident at the earth surface. The global radiation incident on a horizontal surface is equal to the sum of vertical component of the direct radiation, together with the net diffuse radiation from the visible sky. An expression linking the global radiation G, arriving normal to a horizontal unit area on the Earth's surface, to the direct radiation I, solar altitude β, and the diffuse radiation D, is given by [Paltridge, 1976]:

$$G = I\sin(\beta) + D \tag{3.4}$$

The above relationship allows the direct radiation to be calculated, given the global and diffuse radiation levels. If available, direct measurements of the global and diffuse radiation totals offer the best method to evaluate the radiation totals at a site.

3.2.3 Solar radiation for an inclined plane

The global radiation arriving on an inclined plane, tilted at an angle γ and rotated an angle α as indicated in Figure 3.2, can be calculated using the values for global, diffuse and direct radiation on a flat horizontal plane. To calculate the global radiation on an inclined plane, reflected radiation from the ground must be considered. Assuming the ground acts as a diffuse reflector, Equation 3.5 indicates the modified expression for the global radiation G' arriving on an inclined plane; in terms of the direct, diffuse and global radiation components calculated for a flat horizontal surface:

$$G' = I\cos(\tau) + Df' + G(1 - f')\alpha_g \tag{3.5}$$

Where τ represents the angle between the normal of the inclined plane and the Sun's position vector, a_g represents the ground albedo and f' the fraction of the sky visible to the plane. Expressions for these quantities are given below in terms of the solar altitude β, solar azimuth A, tilt γ and rotation α, and surface albedo a_s when the sun is at high elevations [Paltridge, 1976]:

$$\cos(\tau) = \sin(\beta)\cos(\gamma) - \cos(\beta)\sin(\gamma)\cos(A - \alpha) \tag{3.6a}$$

$$f' = \cos^2(\gamma/2) \tag{3.6b}$$

$$\alpha_g(\beta) = \alpha_s + (1 - \alpha_s)\exp[-(90° - \beta)/10] \tag{3.6c}$$

The ground albedo alters for different surfaces as the solar altitude angle varies. The expression in Equation 3.6c accounts for this through modification of a given surface albedo for the sun at high elevations a_s by an exponential function dependent on the solar altitude β. Values of a_s vary considerably for snow, with fresh snow cover having an albedo in the order of 0.72, while for aged snow this may drop to as low as 0.38 [Paltridge, 1976].

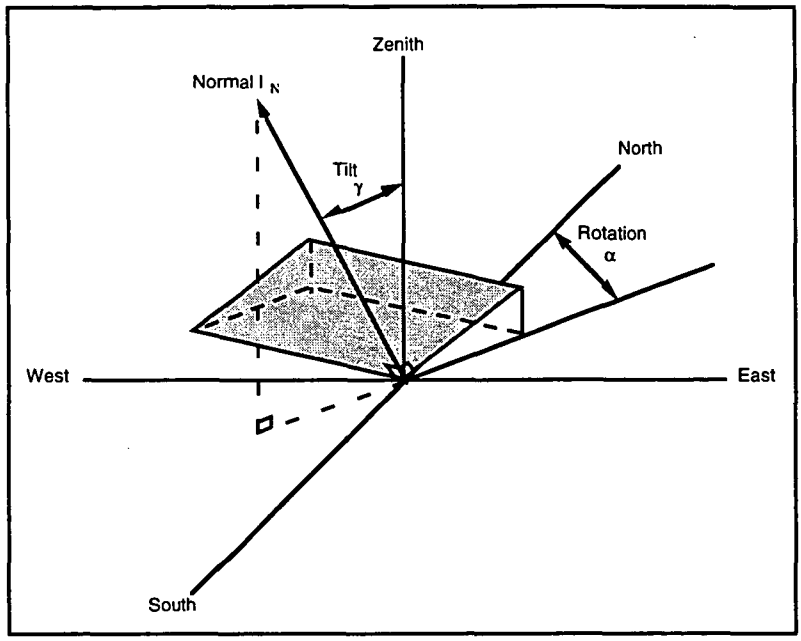

Figure 3.2: Inclined plane with normal I_N, rotated an angle a and tilted at an angle γ[source Sayigh, 1977]

Solution of equations 3.5 and 3.6 indicate that reflected radiation will always be less than the combined effect of direct and diffuse radiation. Furthermore, the magnitude of reflected radiation is heavily dependent on the tilt of the exposure surface, inclination of the Sun and to a lesser degree, the surface albedo. Given this situation and that the surface albedo is also dependent on inclination, constant ground albedoes have been assumed to exist year round at the stations to simply calculations. Albedoes of $a_s = 0.7$ have been used for the continental stations (good snow cover) and $a_s = 0.3$ for Macquarie Island (irregular/poor snow cover).

3.3 Analysis of solar radiation at the Australian stations

The solar energy resources of the stations are now presented. Actual measurements of the radiation level at the ANARE stations are limited. The records which do exist consist of monthly averages of the daily total of global and diffuse radiation totals, rather than original observations. To enable direct radiation totals to be determined, allowing for estimates on inclined surfaces, model data has been used.

3.3.1 Observed horizontal solar radiation totals

Global and diffuse radiation measurements taken at Casey, Mawson and Macquarie Island are indicated in Table 3.1. These measurements consist of monthly averages that are not continuous nor complete. This data is the sum of all observational data obtained for the stations.

Site	Global		Diffuse	
	From	To	From	To
Casey	1973	1977	1973	1977
Mawson	1961	1963	1961	1962
Macquarie Island	1968	1993	1973	1988

Table 3.1: Available global and diffuse radiation measurements for the ANARE stations [source Weller 1968; BoM 1994]

Measurements have been taken from a study at Mawson by Weller (1968), and BoM records for Casey and Macquarie Island [BoM, 1994]. Unfortunately no data was available for Davis. Totals of the yearly global and diffuse radiation for a horizontal plane are indicated in Table 3.2. (Note: direct radiation totals were not recorded).

Site	Yearly radiation totals (kWh/m^2)	
	Global	Diffuse
Casey	987	537
Mawson	1155	528
Macquarie Island	884	523

Table 3.2: Yearly global and diffuse radiation totals calculated from observations on a horizontal plane [source Weller 1968; BoM 1994]

Daily averages have been calculated for each month and are presented in Figure 3.3. Extreme seasonal variation is evident with radiation totals over the polar winter months, between March and September, virtually non-existent. This effectively restricts the solar energy season to the summer months. Mawson appears to be the most favourable site, with Macquarie Island the least, although these observations are based on rather limited data.

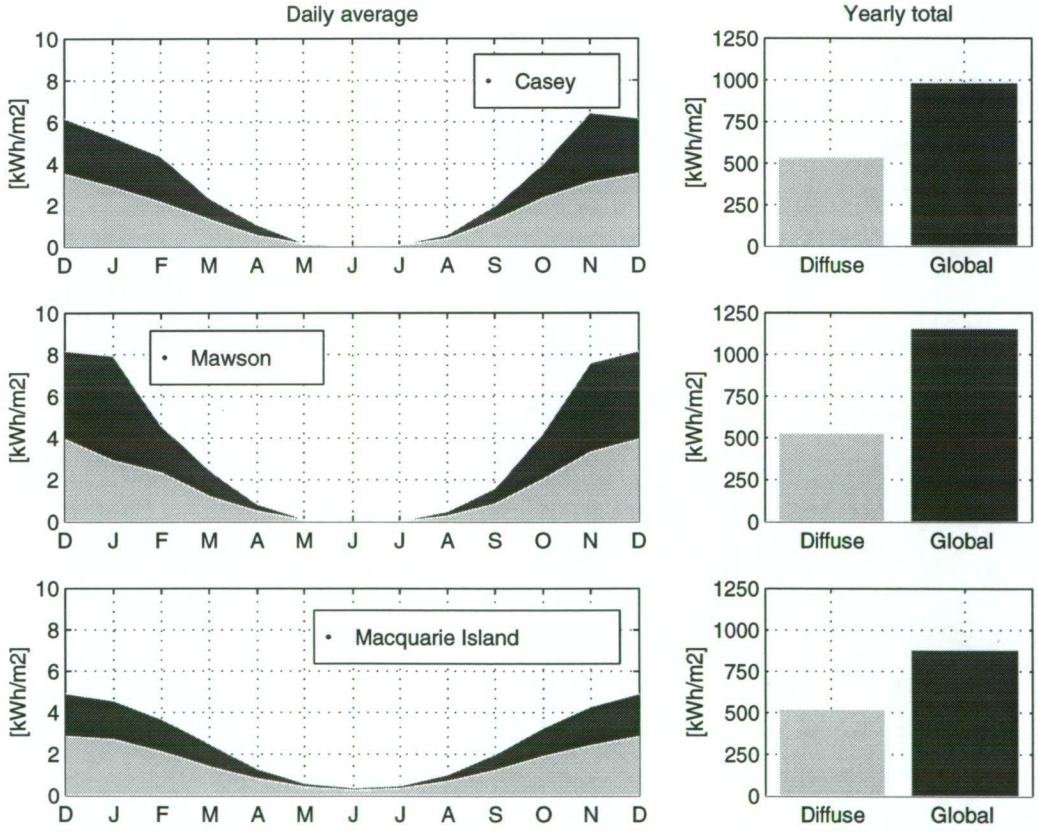

Figure 3.3: Daily average and yearly totals of global and diffuse radiation [source Weller 1968 ; BoM 1994]

To obtain more information on the radiation incident at the ANARE stations and give estimates for Davis, model data must be used.

3.3.2 Estimated horizontal solar radiation totals

When modelling solar radiation incident at the stations it is important to take into account the effect of the Antarctic environment. Weller (1968) noted that the low content of dust and water-vapour, characteristic of Antarctic air, resulted in low absorption by the atmosphere. This would account for the high summer radiation totals recorded at Mawson and Casey. Macquarie Island is situated in the middle of the Southern Ocean and does not experience these same conditions. At Macquarie increased cloudiness (see Table 3.3) would lead to higher atmospheric water-vapour resulting in greater atmospheric absorption and lower surface radiation totals.

Site	Mean cloudiness (eighths)	Percentage (%)
Casey	5.62	70.3%
Davis	5.25	65.6%
Mawson	4.60	57.5%
Macquarie Island	6.73	84.1%

Table 3.3: Mean yearly cloudiness (in eighths) for the ANARE stations [source BoM 1990-95]

To estimate solar radiation at the Australian Antarctic Stations a simple model by Paltridge (1976) based on cloud cover observations has been selected. This method was chosen in preference to other methods in order to maintain a strong dependence on recorded cloud cover, a measurement assumed to be indicative of climatic conditions in general. Other common methods used to generate radiation time series involve auto-regressive-moving average (ARMA) series or Fourier compositions (see for example: [Aguiar, 1988], [Gordon, 1988], [Graham, 1988]; or [Hay, 1979], [Hoyt, 1978], [Gardiner, 1988], [Choudhury, 1982]). These methods generate series which represent a statistically typical period rather than a series correlated to a climate indicator.

In the model used, an empirical relationship is used to express the incident direct and global radiation levels for clear skies given the solar altitude. These values are then modified using observed multi-level cloud observations with all scattering and absorption effects assumed constant. The effect of cloud cover on solar insolation levels in the temperature storms belts at 60°N and 60°S is highly significant due the experienced cloud distributions. The cloud fraction distribution indicates a high proportion of either high cloud, or no cloud [Olseth, 1984]. Since cloud variability is reported to represent the majority of the total variability in solar radiation levels [Hay, 1985], the use of this model should allow a large proportion of the variation in solar radiation to be captured.

Based on observations, an expression for the direct radiation, I, under cloud free conditions is given as a function of solar altitude, β. In the presence of clouds, this term is reduced by a factor equal to the total cloud cover ratio, T_{cc}, resulting in the expression given in Equation 3.7, calculated to agree with monthly readings from the stations:

$$I = \left[1 - T_{cc}\right]\left[1.2\left(1 - \exp[-0.06\beta]\right)\right] \ (\mathrm{kWm^{-2}}) \qquad (3.7)$$

Equation 3.7 is only valid during daylight periods, between sunrise and sunset for which solar altitude values, β, are positive. A similar expression is used to estimate the global radiation, G, is given in Equation 3.8:

$$G = I_o\left[1 - \sum_i a_c(i)F_{cc}(i)\right]\left[1 - m - a_A(1 - T_{cc})\right]\sin(\beta) \ (\mathrm{kWm^{-2}}) \qquad (3.8)$$

where β represents the solar altitude, I_0 the solar constant, m a factor representing absorption in the atmosphere due to water vapour, a_A the albedo of the atmosphere in the fraction of clear sky, $1\text{-}T_{cc}$, $a_c(i)$ the albedo of cloud plus atmosphere above them and where $F_{cc}(i)$ is the fractional amounts of cloud visible (Note: I_0 =1354 Wm^{-2}, m = 0.18 and a_A =0.10 [Paltridge, 1976]).

The cloud factors are defined for each cloud level i taking cloud overlap into account. Values for $a_c(i)$ are given as follows: 0.35 for Cirrus (level 1) cloud, 0.55 for Altocumulus-altostratus (level 2) cloud, 0.60 for low cloud 2 (level 3), and 0.5 for low cloud 1 (level 4) [Paltridge, 1976]. To calculate $F_{cc}(i)$, the recorded cloud cover observations $R_{cc}(i)$. are used in a geometric overlap summation, given in Equation 3.9, where the layer count is backwards from the top at level 4 [Paltridge, 1976]:

$$F_{cc}(i) = R_{cc}(i)\left(1 - \sum_{j=1}^{i-1} F_{cc}(j)\right) \tag{3.9}$$

Estimates for the diffuse radiation can be then calculated from the direct and global radiation using Equation 3.4. This allows the incident radiation on a flat horizontal plane to be estimated at a site where cloud measurements are available. Errors of up to 50% have been reported for individual readings when using this technique, although averages taken over a number of days fair much better with predicted monthly averages rarely in error to observations by more than 10%. [Paltridge, 1976].

Solar radiation levels estimated using this model are presented in Table 3.4. To construct these values the following technique was employed:

1. Solar altitude angles were calculated for each of the stations for the start of each hour over the period 1990-1995. Positive angles were used to define 'day-light' periods.
2. Three hourly BoM cloud cover recordings over the period 1990-95 were linearly interpolated onto a 1 hour grid for day-light periods. Where data was available (above 90% of daytime observations at all stations) cloud fractions were used on four levels: low cloud 1, low cloud 2, mid cloud and high cloud. For missing information on cloud levels, the total cloud cover (if recorded) was assumed representative of low cloud 1. If observations were not recorded values were linearly interpolated from the last and next available observations.
3. Hourly cloud totals and solar altitude angles were then used to calculate the average global, direct and diffuse radiation levels for day-light periods. A constant ground albedo value of a_s = 0.7 was used for the continental stations and a_s = 0.3 for Macquarie Island. Hourly estimates were assumed to represent the average radiation over the hour and subsequently integrated to obtain yearly totals.

Station	Average annual radiation totals (kWh/m^2)		
	Global	Diffuse	Direct
Casey	1029	640	389
Davis	1047	617	430
Mawson	1074	573	500
Macquarie Island	966	687	279

Table 3.4: Estimated yearly radiation totals for a horizontal surface using radiation model

The quality of these estimates can be obtained from a comparison of the yearly global and diffuse radiation totals calculated from the Weller and BoM observations. The difference between the yearly totals for global radiation are approximately 10% at Casey, 20% at Macquarie Island, and 2% at Mawson.

Exact agreement is not expected due to the Weller and BoM averages having been taken over different years to the cloud measurements used in the radiation model. The indicated level of agreement does however give confidence for their use. Model estimates for the horizontal radiation levels have been used in all further calculations.

3.3.3 Exposure levels for non horizontal surfaces

An inclined plane, facing north at the stations, will receive a greater proportion of direct radiation. By positioning solar panels on inclined surfaces, either fixed or in tracking systems, exposure levels can be increased. To investigate the potential increases from different orientations, radiation levels were estimated for a range of different planes. Yearly global totals on horizontal, vertical and an inclined plane at a tilt angle calculated to maximise exposure, are presented in Table 3.5.

Station	Yearly global radiation (kWh/m^2)			best angle for inclined plane
	horizontal	vertical	inclined	
Casey	1029	1127	1223	60°
Davis	1047	1177	1268	60°
Mawson	1074	1277	1374	60°
Macquarie Island	966	781	1040	40°

Table 3.5: Estimated average yearly radiation totals various inclined planes using radiation model

Significant increases in radiation levels occur for optimally orientated planes over horizontal and vertical planes. Tracking mechanisms have the potential to further increase the total radiation exposure. Two methods exist to achieve greater radiation totals. The first uses light sensor to locate the brightest position in the sky and then uses motors to steer the array to face this location. The second uses a simple algorithm to follow the sun, maximising the direct radiation component. Light sensing tracking systems are complex, and require extensive data on the sky condition to estimate their output levels, information unavailable in this study. Only algorithm controlled tracking systems will be investigated in this section. Estimates for the following systems have been calculated:

- azimuth tracking systems (at fixed tilt angles);
- tilt tracking systems (along the north/south axis); and
- dual axis tracking systems (combination tilt and azimuth tracking).

For azimuth tracking systems, the rotation angle of the tracking system is matched to the solar azimuth angle, with the tilt angle held constant. In tilt and dual tracking systems, the direct radiation exposure is maximised. For tilt only tracking systems, movement only occurs in the North-South plane. For dual tracking systems, however, movement is in all directions. The yearly totals for the different tracking systems are presented in Table 3.6; along with the best tilt angle for azimuth tracking systems (calculated to maximise radiation exposure).

Station	Yearly global radiation (kWh/m^2)			Best tilt angle for azimuth tracking systems
	tilt tracking	azimuth tracking	dual tracking	
Casey	1307	1609	1624	70°
Davis	1387	1743	1757	70°
Mawson	1486	1895	1911	70°
Macquarie Island	1076	1178	1193	50°

Table 3.6: Yearly solar radiation model estimates for tracking systems at the ANARE stations using radiation model

A comparison of estimated radiation totals on surfaces set at different tilt angles, with and with out azimuth tracking, is given in Figure 3.4. Totals for tilt and dual axis tracking systems are also presented for comparison.

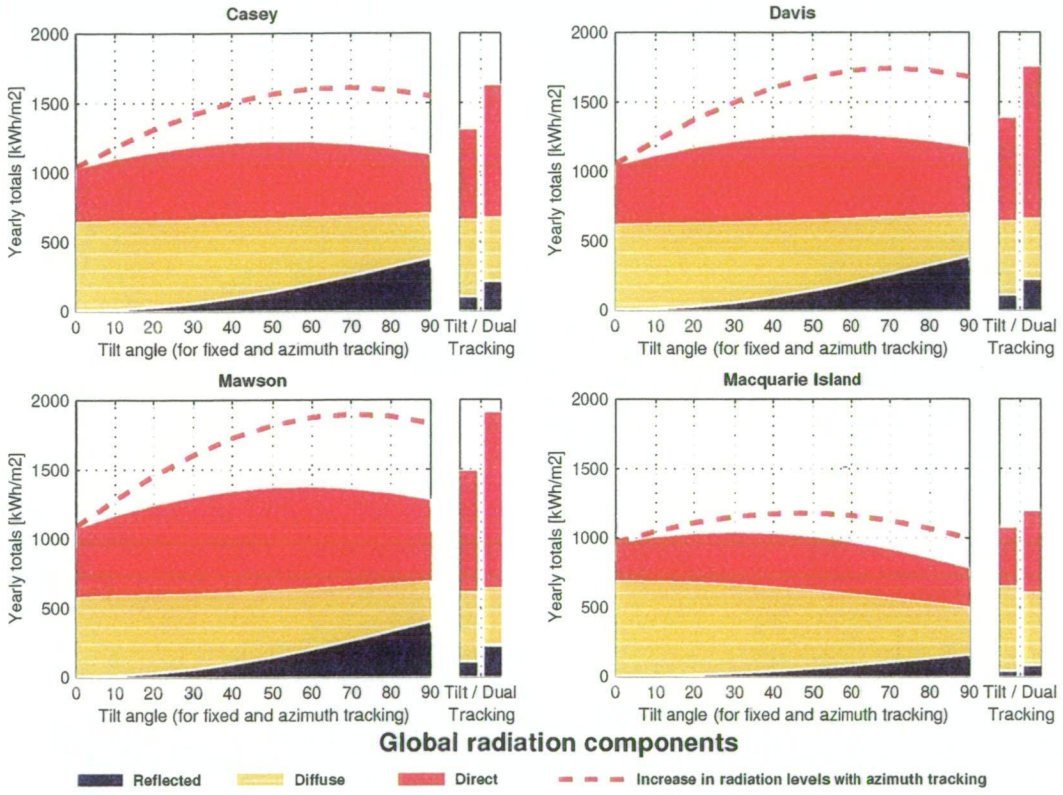

Figure 3.4: Comparison of tracking system exposures to fixed planes at the ANARE stations

Radiation estimates for the continental stations are similar, although Mawson is the best site due to higher direct radiation levels. Macquarie Island totals are well below the other stations, possibly due to limitations in the radiation model. The surface albedo assumed for Macquarie Island compounded low direct radiation estimates due to high cloud cover, resulting in the very low estimates for direct and reflected radiation levels. Observations are necessary to determine if this effect is real or an artifact of the model.

At all stations tracking systems enjoy significant increases over passive systems. Azimuth tracking systems offering the best possibilities, with yearly totals approaching those for dual axis tracking systems and with motor positioning systems only required in one plane. Unfortunately the use of tracking systems come at a price.

Tracking equipment requires extra civil work, is expensive to maintain and is more easily damaged. If costs associated with establishing and maintaining tracking systems are comparable with those for a larger fixed system able to generate the same amount of power, it would be unwise to use tracking systems.

For an installation built to survive the conditions at the Australian Antarctic stations, simplicity and durability are the key. Fixing PV panels flat on the roofs and North facing walls of buildings is extremely convenient structurally and aesthetically. In such an arrangement, an increased generating surface would be required over optimally angled or tracking systems. However, power would be produced where it is required, thus eliminating the need for extensive distribution systems. Integrating panels into the cladding of buildings, along these lines, has been proposed in the design of the upgraded US South Pole station [Peeran, 1994].

3.3.4 Diurnal and Seasonal variation

The energy totals given in the previous section indicate the amount of solar energy available. To indicate the rate at which this energy is available throughout the year, the diurnal and seasonal variation in the estimated global radiation flux density for each of the stations has been presented in Figure 3.5.

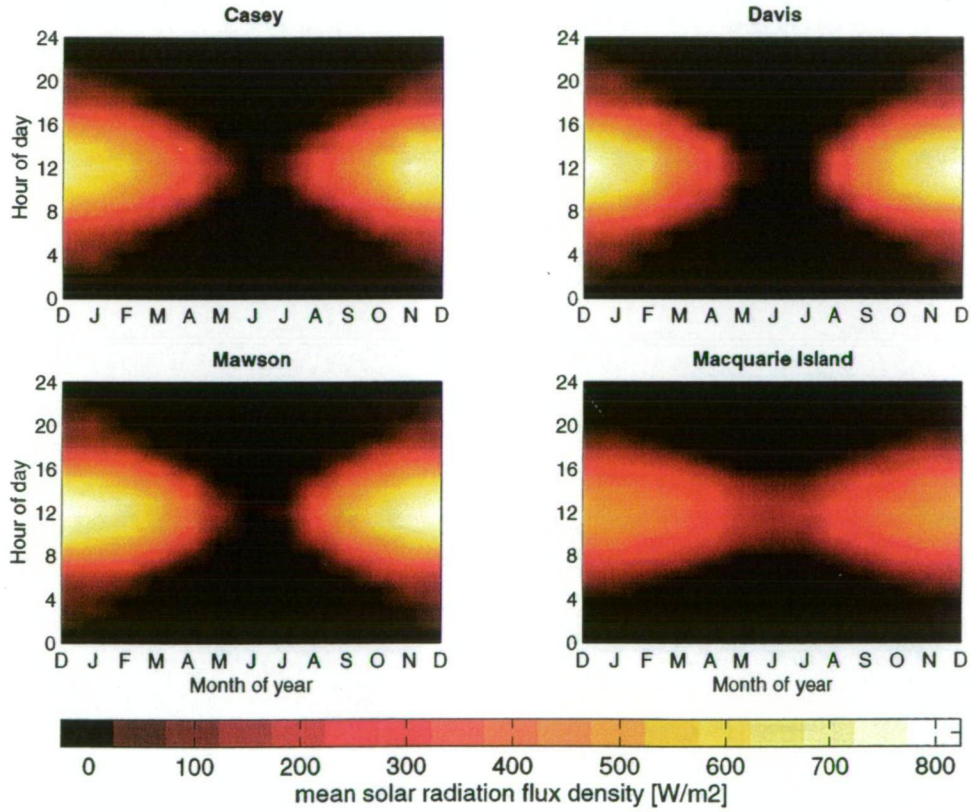

Figure 3.5: Estimated annual and diurnal solar radiation levels on an optimally inclined plane at the ANARE stations

These have been calculated using radiation estimates from the cloud model over the period 1990 to 1995. Hourly estimates of the global radiation have been averaged for each month, with a bi-linear smoothing function applied to obtain the fields given in Figure 3.5. Global radiation levels were estimated for an inclined plane at the most productive inclination identified for each station, given in Table 3.5.

This figure indicates clearly that day time summer is the only time during which sizable solar energy quantities are experienced. The average level of radiation during these periods are extremely promising, with radiation levels averaging in excess of 600 Wm^{-2} for the continental stations. These levels are extremely high, comparable to regions in central Australia where solar energy systems are already in use.

Comparison of the average wind and solar resources presented in Figures 2.2 and 3.5 indicate that periods of high wind speed and high solar radiation may not occur at the same time. This offers potential for mixed solar and wind systems which could produce power over a greater period than either wind only or solar only systems alone. This will depend on the serial structure of wind and solar production times rather than the averages, an issue that is investigated further in Chapter 6.

3.4 Converting solar energy into electrical power

Electrical power can be generated from solar radiation using solar-thermal systems or photovoltaics. Solar-thermal generation devices are based on a Rankine cycle, using a gas heated by the Sun to drive a turbine connected to a generator. Photovoltaic systems make use of the photovoltaic effect, defined as the generation of an electromotive force as a result of the absorption of ionising radiation [Sayigh, 1977].

Solar-thermal systems are still in development and have seen only limited use, while photovoltaics are emerging as one of the leading generation devices used in small scale power systems. Investigations in this section will focus on the production of electrical energy by photovoltaics, although results are general enough to be applied to solar-thermal generation systems.

3.4.1 Photovoltaics

The photovoltaic effect is observed in nature by a variety of materials, with semiconductors having the best performance in sunlight. Silicon is by far the most utilised material in the production of the standard 'solar cell'. A full description of the photovoltaic effect can be found in Sayigh (1977). Photovoltaics are typically responsive between 0.4 μm and 1.1 μm, peaking in response around 0.9 μm (although exact responses are material dependent) [Sayigh, 1977]. For the purpose of this study an efficiency independent of wavelength will be assumed.

An overall efficiency is used instead, representing the amount of incident radiation made available for use as electrical power. This efficiency η is defined as the ratio of the maximum power point P_{mp}, to the total power density available from the sun P_{sun}, as given in Equation 3.10. (The current and voltage at the maximum power point are defined at the maximum power point current I_{mp} and maximum power point voltage V_{mp}).

$$\eta = \frac{P_{mp}}{P_{sun}} = \frac{I_{mp} V_{mp}}{P_{sun}} \tag{3.10}$$

For the purpose of these investigations, it will be assumed that the maximum power point responds linearly to increases in solar radiation. This will result in the efficiency of a cell remaining constant over a range of different incident solar radiation levels. Typical efficiencies of 10% are reported for commercial solar cells, while levels up to 23% have been recorded for experimental cells.

Efficiency is, however, affected by temperature. The performance of a typical cells is increased as temperature decreases, potentially assisting systems operating at the Antarctic stations. Until the level of this effect can be quantified at the stations, temperature variations in performance will be ignored.

3.4.2 Solar power capacity factor estimates

A rated power is often used to indicate the size of a PV system. This is the theoretical response of the cell when orientated directly at the sun, exposed to cloud free sunlight of an intensity of 1 kW/m^2 at 25°C. The performance of a PV system of given rated power will vary between sites due to differences in incident solar radiation. By defining a term analogous to the wind power capacity factor the solar resources of a site can be standardised. The solar capacity factor of a PV system is defined as the actual output of the system divided by the expected output if the system had produced at full power for the entire period. This results in the solar capacity factor being equivalent to the solar radiation incident on a surface over a given period, relative to the standard rate of 1 kW/m^2.

Figure 3.6 provides a key to determining the size of a PV system, rated at 1 kW, for different efficiencies. The performance of one square metre of this array given the incident solar radiation power flux is also presented.

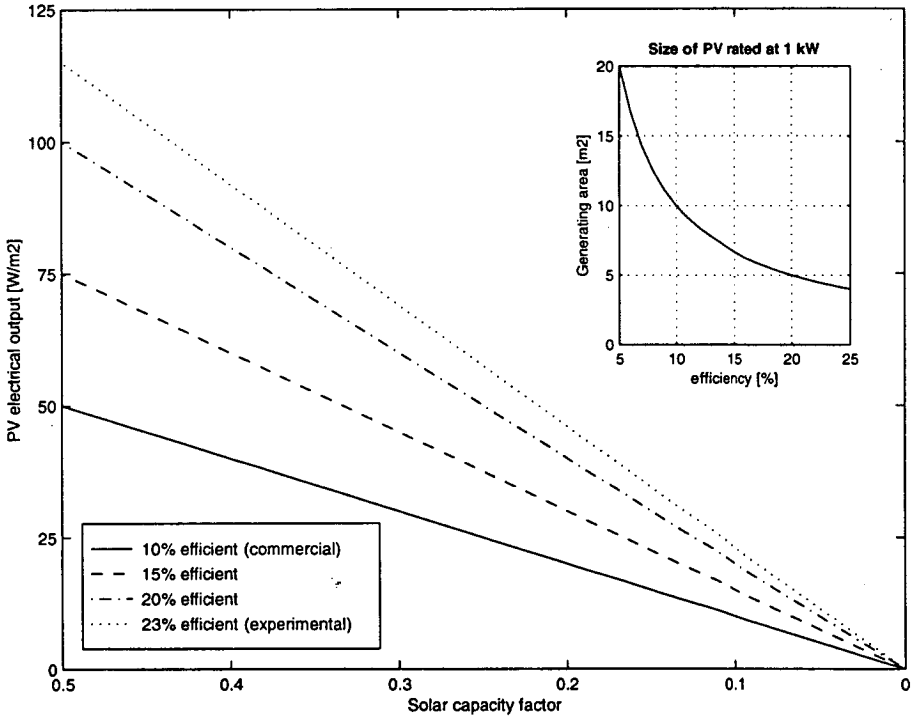

Figure 3.6: Sizing and performance of a PV array rated at 1 kW for a range of assumed efficiencies.

An increase in the efficiency of a cell has marked consequences for the sizing of systems. A PV system rated at 1 kW, would occupy 10 m^2 if comprised of cells of 10% efficiency, but only half this area if comprised of cells of 20% efficiency. Costs of PV systems are extremely dependent on efficiency, with the cheapest option usually covering a greater area. Future PV advances indicate that commercially produced cells, with efficiencies in the order of 20%, may become available in the near future allowing for smaller generating area and cheaper prices compared to similar rated systems available today.

Using the expected global radiation levels estimated for different surfaces allows for calculation of expected solar power capacity factors, given in Table 3.7, for the Australian Antarctic stations.

Site	Yearly solar power capacity factors for fixed systems			Yearly solar power capacity factors for tracking systems		
	horizontal	vertical	best inclined	tilt tracking	azimuth tracking	dual axis tracking
Casey	0.12	0.13	0.14	0.15	0.18	0.19
Davis	0.12	0.13	0.15	0.16	0.20	0.20
Mawson	0.12	0.15	0.16	0.17	0.22	0.22
Macquarie Is.	0.11	0.09	0.12	0.12	0.13	0.14

Table 3.7: Estimated solar capacity factors for fixed and tracking systems at the ANARE stations

A comparison of monthly values of the solar capacity factor for the best fixed systems, at optimal tilt angle, have been presented in Figure 3.7 with the performance of azimuth tracking systems, similarly at optimal tilt angle, superimposed to give an indication of the seasonal variation in the solar capacity factor.

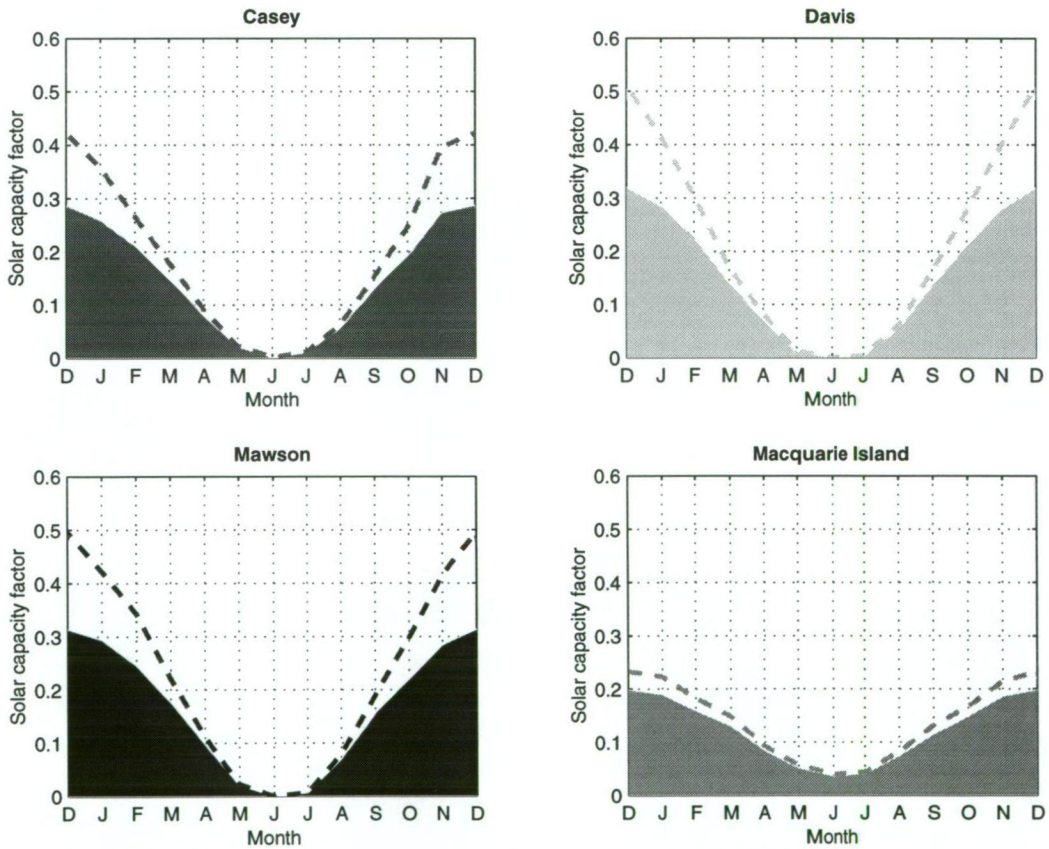

Figure 3.7: Monthly solar power capacity factors, for optimally inclined fixed PV systems (solid), and azimuth tracking systems (dashed), at the ANARE stations.

Azimuth only tracking systems enjoying significant (20%) increases over the best fixed systems. These anticipated increases are impressive but as mentioned before, the extra complexity and cost associated with tracking system designed to operate and survive the low temperatures and high winds experienced at the stations may not justify their use. For this reason further investigations into the use of solar energy at the stations, presented in Chapter 6, will concentrate on fixed PV systems.

3.5 Summary

Solar radiation levels at the stations are highly seasonally dependent. In summer, long sunshine hours and a high occurrence of clear skies result in high incident radiation levels. Summer global radiation levels on a horizontal surface have been recorded at 6 to 8 kWh/m^2 for the continental stations and between 4 to 5 kWh/m^2 for Macquarie Island. In winter, reduced sunshine hours and low solar altitudes result in very low incident radiation levels. Global radiation levels are virtually non-existent at the continental stations from April to August, while only slightly better at Macquarie Island where daily totals were recorded below 1 kWh/m^2 over the same period.

Solar generation systems at the stations would be able to generate large amounts of energy, but only during daytime in summer. Solar capacity factors, representative of the period for which an array can be expected to produce at its rated power, have been estimated for both tracking and passive systems. Exposure levels can be maximised for passive systems by facing the generating surface to the North, and then inclining it at a 60° angle at the continental stations, 40° angle at Macquarie Island. Similarly, exposure levels can be maximised for azimuth tracking systems by inclining the generating surface at a 70° angle at the continental stations, 50° angle at Macquarie Island.

For fixed systems, summer solar capacity factors have been estimated at between 0.2 and 0.3 for Casey, Davis, Mawson and just below 0.2 for Macquarie Island. For azimuth tracking systems, increases as high as 30% can be achieved during the summer months at Casey, Davis and Mawson, and 10% at Macquarie Island. However, these advantages may be off-set due to cost and reliability concerns associated with the tracking mechanisms and their ability to withstand high winds and icing.

Chapter 4

Station Energy Demands

4.1 Introduction

Australia's Antarctic stations are large, modern and extremely well equipped facilities representing an enormous investment and commitment by Australia in the region. The rebuilding programs commenced in the early 1980s have resulted in stations which are, in the words of an Australian Construction Services architect, 'a buffer against the hardship of being away from family and friends and a pleasant place in which to work' [Incoll, 1993].

The fuel use and energy consumption patterns at the stations have been investigated, allowing for the size of potential fuel savings from the use of renewable energy systems to be calculated in Chapter 6.

4.2 Diesel fuel use and energy production at the stations

Ninety percent of all fuel imported to the stations is used by diesel generator and boiler sets [Hall, 1992]. The generator sets are driven in response to the electrical energy demands of the stations, while the boiler sets are used when station thermal energy requirements exceed thermal energy production levels from the generator sets.

4.2.1 Generator and boiler fuel consumption levels: 1992-95

Information presented in this section has been obtained from internal ADD Engineering Section reports, made available for the stations over the period 1992 to 1995. Records prior to 1992 have not been used, as the upgraded facilities at the stations were still in construction, biasing fuel consumption and electrical load totals. Average daily fuel consumption levels are presented for the stations in Figures 4.1 to 4.4. These totals represent the fuel used by the generator and boilers sets, with any fuel used by station vehicles and incinerators **not** included. (Note: a blank has been inserted where monthly totals were unavailable.)

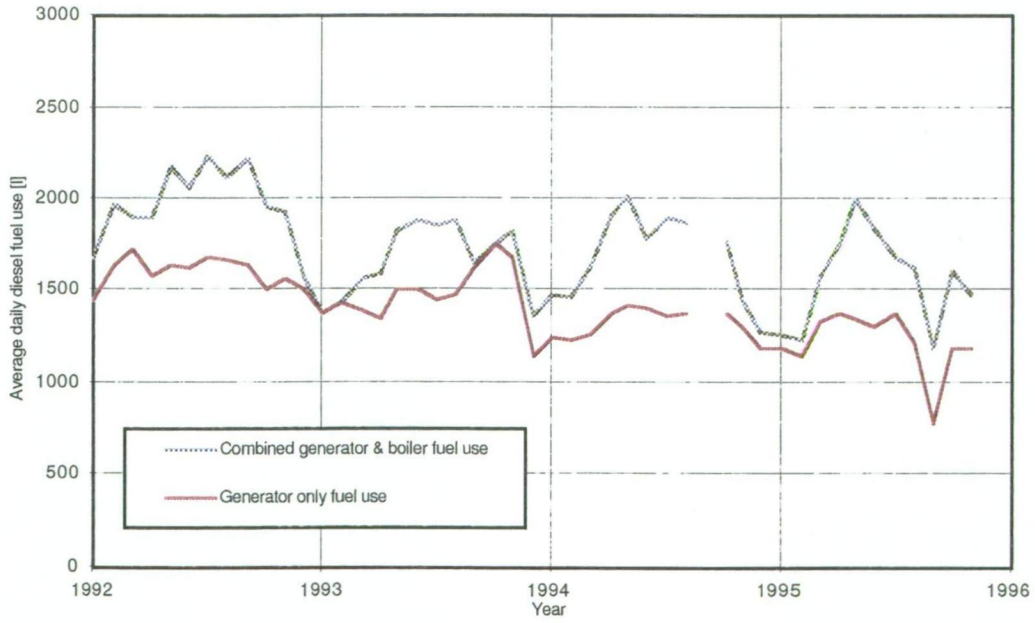

Figure 4.1: Casey - diesel usage in generator sets and boilers [source AAD Engineering 1992-95]

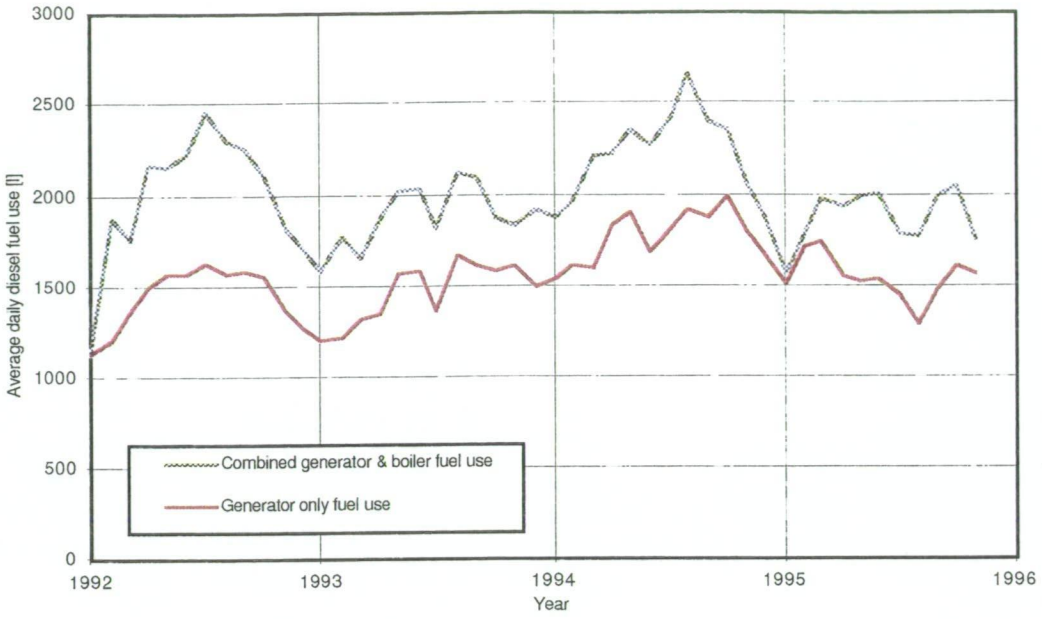

Figure 4.2: Davis - diesel usage in generator sets and boilers [source AAD Engineering 1992-95]

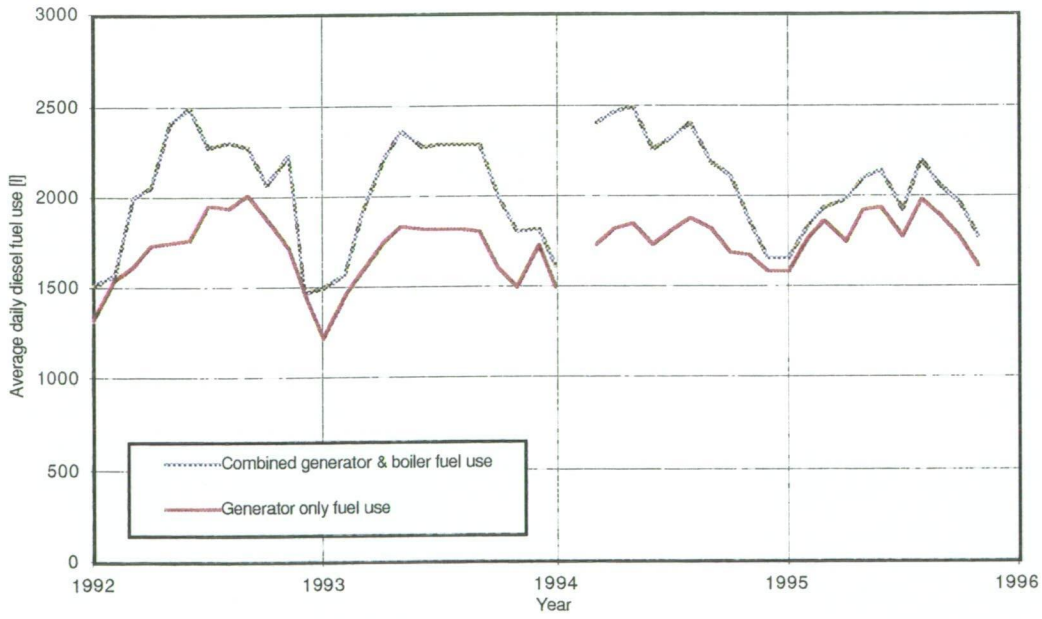

Figure 4.3: Mawson - diesel usage in generator sets and boilers [source AAD Engineering 1992-95]

Similar consumption levels and patterns are observed at the three continental stations which experience similar climatic conditions and are of similar design. The general trend at these stations is for higher winter diesel usage, from both increased generator and boiler usage. The magnitude of this seasonal variation is in the order of 30% of the base load. Exact agreement between stations is not expected due to the nature of the different scientific programs undertaken at each station.

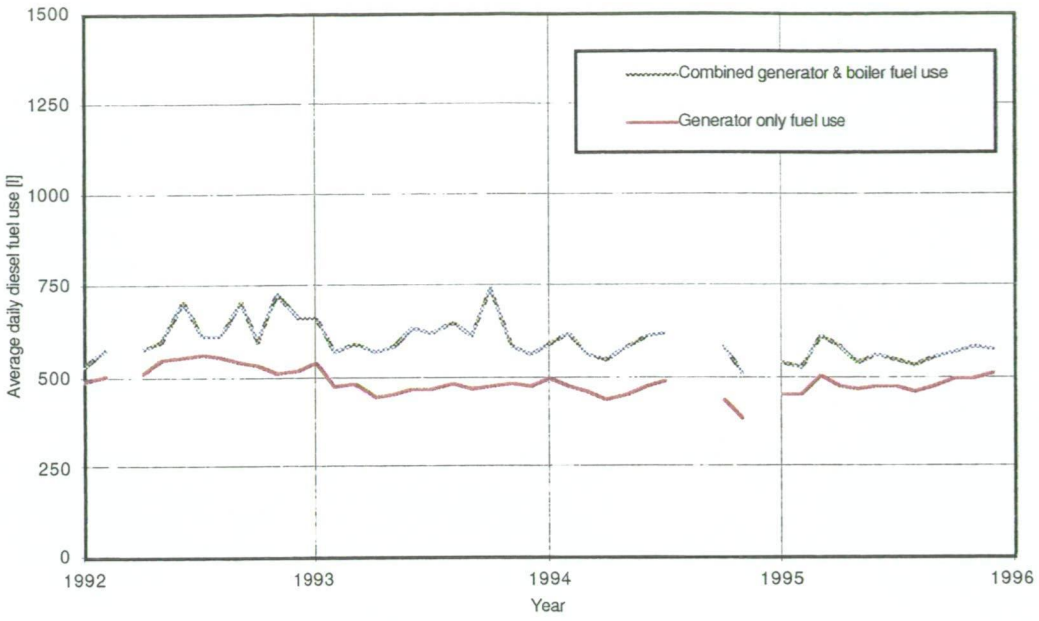

Figure 4.4: Macquarie Island - diesel usage in generator sets and boilers [source AAD Engineering 1992-95]

Fuel consumption levels at Macquarie Island are much lower, due to the different - more traditional - building designs, lower population levels and milder climate. Usage throughout the year is more stable, with summer and winter consumption levels comparable.

The yearly total of diesel used in the generator and boiler sets, for the years from 1992 to 1995, is presented in Tables 4.1 and 4.2. (Note: where monthly totals were unavailable, the average for that month from the other years has been used.)

Station	Total diesel use by generator sets (kl)				
	1992	1993	1994	1995	average
Casey	584	538	483	447	513
Davis	526	535	646	561	567
Mawson	630	608	630	653	630
Macquarie Island	202	174	168	174	180

Table 4.1: Estimated annual diesel usage in the generator sets at the ANARE stations [source AAD Engineering 1992-95]

Station	Total diesel use by boiler sets (kl)				
	1992	1993	1994	1995	average
Casey	140	90	131	121	120
Davis	324	152	166	126	192
Mawson	122	134	145	142	136
Macquarie Island	38	51	46	30	41

Table 4.2: Estimated annual diesel usage in the boiler sets at the ANARE stations [source AAD Engineering 1992-95]

The four year linear trend in fuel usage at each station is given in Table 4.3; calculated by dividing the gradient of a regression fit of monthly fuel totals for the years 1992-95, by the average monthly fuel consumption over the years 1992-95. Decreasing generator fuel use is evident for Casey and Macquarie, while increasing fuel use is apparent for Davis and Mawson. When boiler fuel usage is combined with these values, decreasing fuel use is evident for all stations, although marginal at Davis and Mawson.

Station	4-year linear trend in diesel fuel use		
	generators	boilers	combined
Casey	-8.9%	+3.6%	-6.5%
Davis	+4.1%	-16.9%	-0.5%
Mawson	+0.6%	-3.5%	-0.1%
Macquarie Island	-3.1%	-7.2%	-3.5%

Table 4.3: Four year linear trends of diesel usage in generators and boilers at the ANARE stations over 1992-95

The general trend for decrease at Casey over the last four years is due to the completion of building programs at that station in the early 1990s, allowing station operations and loads to be optimised. A similar trend should occur at Davis and Mawson, as rebuilding programs are also completed. More efficient alternators, progressively being installed at each station, combined with energy conservation programs, should see a continued trend for decreasing fuel use, unless new scientific programs result in additional fuel use from increased electrical and thermal loads.

4.2.2 Electrical energy production levels: 1992-95

Daily electrical energy production levels, calculated from monthly recorded totals from each station, over the period 1992-95, are presented in Figures 4.5 to 4.8. A linear trend, indicated by the broken line, has been fitted to this data using a least squares regression fit.

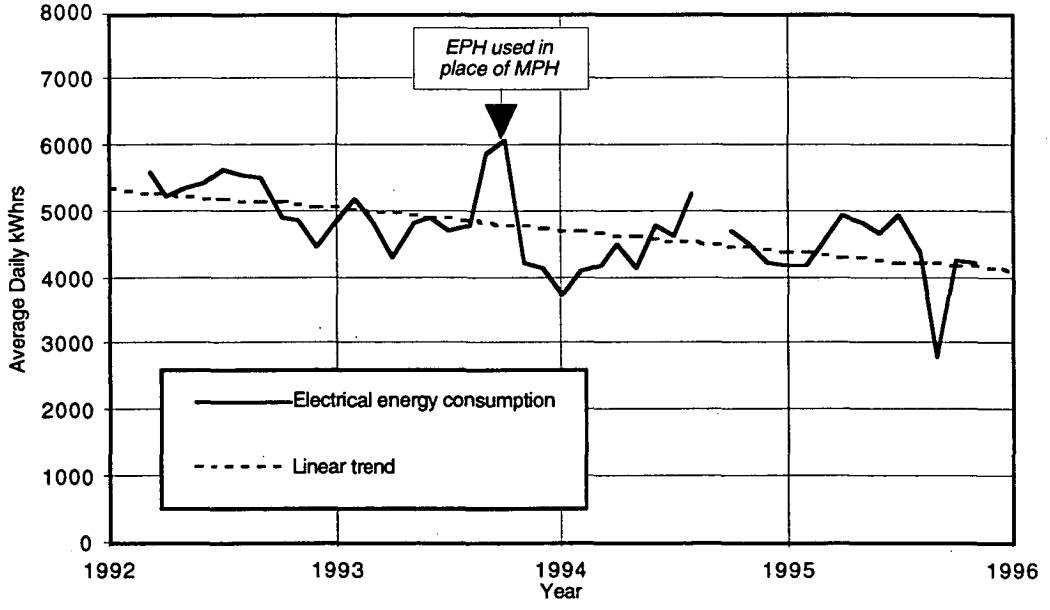

Figure 4.5: Casey - daily electrical energy production levels [source AAD Engineering 1992-95]

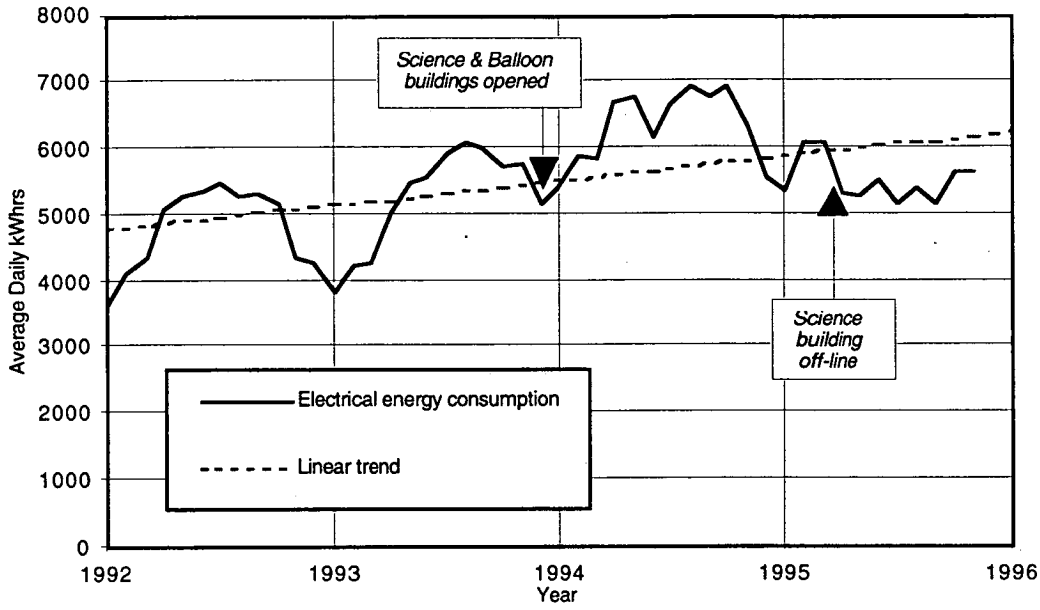

Figure 4.6: Davis - daily electrical energy production levels [source AAD Engineering 1992-95]

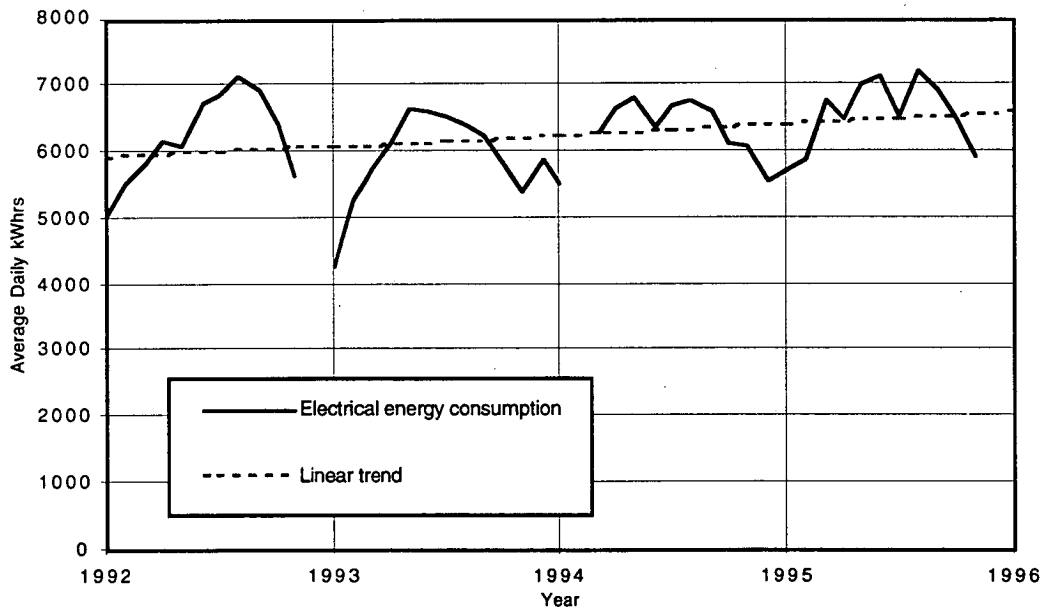

Figure 4.7: Mawson - daily electrical energy production levels [AAD Engineering, 1992-95]

Electrical energy production at the continental bases follow a summer - low / winter - high pattern, as previously identified in the fuel usage figures. Notable deviations from the general trend occur at Casey in October 1993, and at Davis for the winter of 1995. The above average electrical energy usage at Casey in 1993 coincided with use of the emergency powerhouse (EPH) in place of the main powerhouse (MPH). The reversal of the usual winter peak occurring at Davis in 1995, resulted from the combined effects of a large summer population, increasing summer demands early in the year, and the closure of the Science Building for maintenance over the winter.

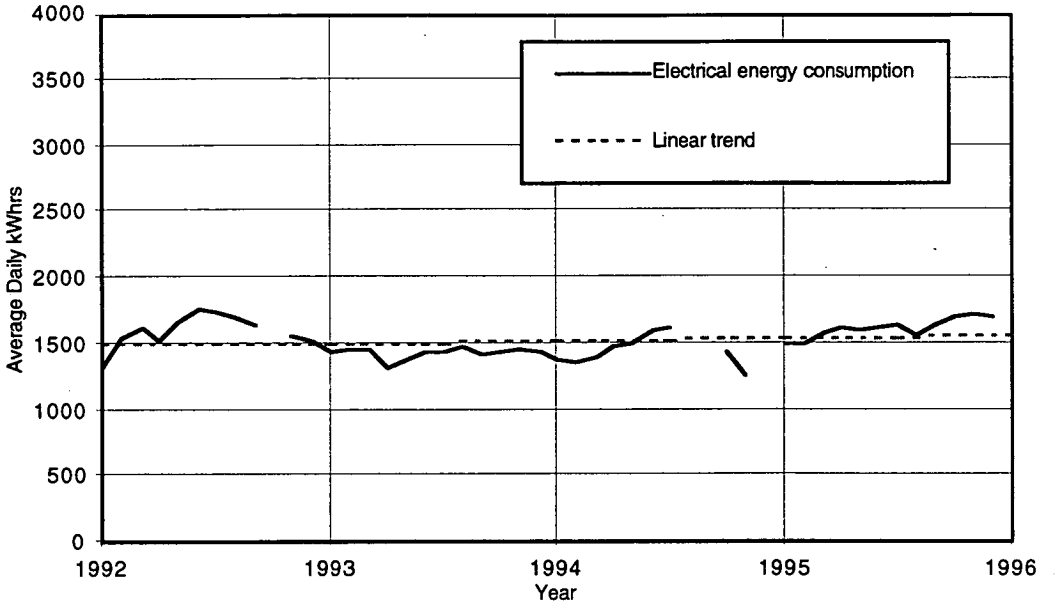

Figure 4.8: Macquarie Island - daily electrical energy production levels [source AAD Engineering, 1992-95]

Electrical consumption patterns at Macquarie Island are remarkably consistent, remaining relatively constant throughout the year and between years. The yearly electrical energy production levels at the stations are indicated in Table 4.4, calculated from station monthly reports. Where monthly totals were unavailable, the average over the other years was used.

Station	Yearly electrical energy production (MWh)				
	1992	1993	1994	1995	average
Casey	1,871	1,786	1,630	1,595	1,721
Davis	1,756	1,919	2,311	1,996	1,996
Mawson	2,255	2,163	2,284	2,368	2,267
Macquarie Island	584	521	542	594	560

Table 4.4: Estimated annual electrical energy production levels at the ANARE stations [source AAD Engineering 1992-95]

The four-year linear trends in electrical power use at the stations, calculated from a least-squares regression fit to the monthly data, are presented in Table 4.5. The trend for decreased electrical production at Casey over the last four years, is a result from the commissioning of the new station and the fine tuning of its electrical systems.

Station	4-year linear trend in electrical production
Casey	-6.6%
Davis	+6.7%
Mawson	+2.7%
Macquarie Island	+1.2%

Table 4.5: Four year linear trends in electrical energy production at the ANARE stations over 1992-95

Davis electrical energy usage peaked in 1994 after three years of increase, while a decrease was recorded for 1995, most likely due to the closure of the science building over winter. Mawson indicated a marginal increase over the last three years after a drop from 1992 to 1993, while Macquarie Island has remained relatively consistent over the last four years.

4.2.3 Electrical efficiency of the diesel generator sets

Comparison of the daily fuel totals and the electrical energy production totals is given in Figure 4.9. The line of best fit, calculated using a least squares regression fit to the data, indicates the average electrical performance of the current diesel generator systems.

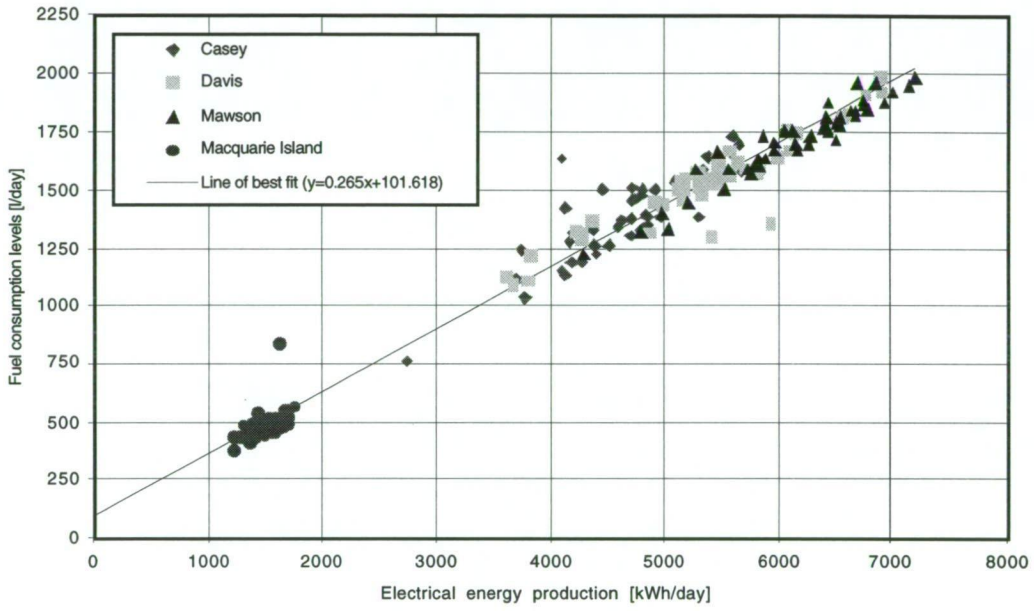

Figure 4.9: Comparison of the daily generator diesel fuel usage and electrical energy production

The electrical efficiency of the generator sets, based on this data, is presented in Table 4.6. These values have been calculated assuming a lower heating value (LHV) of 9.8 kWh/l for Special Antarctic Blend (SAB) diesel, the low wax diesel fuel prepared for use at the stations [Guichard, 1993].

Station	Electrical efficiency of generator sets	
	(kWh/l)	(%)
Casey	3.38	34.5%
Davis	3.52	35.9%
Mawson	3.60	36.7%
Macquarie Island	3.12	31.8%

Table 4.6: Electrical efficiency of generator system (based on LHV of SAB diesel of 9.8 kWh/l)

Macquarie Island stands out as having the least efficient system, with lower electrical loads resulting in less optimal diesel loading conditions. Comparison of the continental stations, indicates that Mawson has the best electrical efficiency.

4.2.4 Thermal energy production estimates

In addition to electrical energy, the stations need large quantities of thermal energy. Estimating the size of this requirement is not straight forward. A centralised co-generation system is currently used at the stations (described in Section 1.2.4), where heat from the powerhouse generators and boilers is fed into a heating hot water (HHW) 'ring-main' circuit. While raising the overall efficiencies of the generator sets through the capture of waste thermal energy, this system results in extra electrical loads from pumping plant used in the HHW circuit. Losses in thermal energy associated with the HHW circuit are difficult to judge, with very little data available from monitoring. In addition, some buildings use stand-alone systems, separate from the ring-main, operating automatically on separate fuel stocks.

The situation is further complicated by the fact that production is not always driven by requirement. Fundamental differences exist between the thermal output of the stations and the thermal needs of the stations, with periods of high thermal demand and high thermal production not always coinciding. In the case of thermal demand exceeding the thermal production from the generator sets and any losses associated with the distribution system, the boilers are engaged. Potential inefficiencies arise when thermal production exceeds thermal demand. In these situations any excess thermal energy is simply vented into the atmosphere.

In the absence of detailed recordings of either the thermal production or thermal needs of the stations, estimates based on fuel consumption levels have to be used. Assuming thermal energy conversion efficiencies of 35% for the generators and 80% for the boilers based on a LHV of SAB diesel of 9.81 kW/l [Steel, 1993], allows for the calculation of thermal energy estimates presented. These are presented in Table 4.7 for each of the stations. As this method does not take into account periods of over-production, these values represent estimates of thermal energy production at the stations, rather than the thermal needs of the stations.

Station	Yearly station thermal energy output (MWh)				
	1992	1993	1994	1995	average
Casey	2,899	2,389	2,544	2,351	2,546
Davis	4,192	2,868	3,327	2,746	3,283
Mawson	2,934	2,954	3,110	2,471	2,867
Macquarie Island	930	946	887	780	886

Table 4.7: Estimated thermal output of stations, based on heat recovery efficiencies from the generators and boilers [source AAD Engineering 1992-95]

The seasonal distribution of thermal energy production at the stations is indicated in Figure 4.10, calculated using the methods outlined above for the years 1992-95. The total energy for each month has been separated into two components: that derived from the generators, and that from the boilers. Based on these estimates, the following observations are apparent:

- During the summer months, most thermal production is obtained through the heat exchange units of the generator sets;
- During winter, thermal production is increased, with boilers the source for most of the additional heat production; and
- Thermal energy production levels are equal to or greater than electrical energy consumption levels throughout the year.

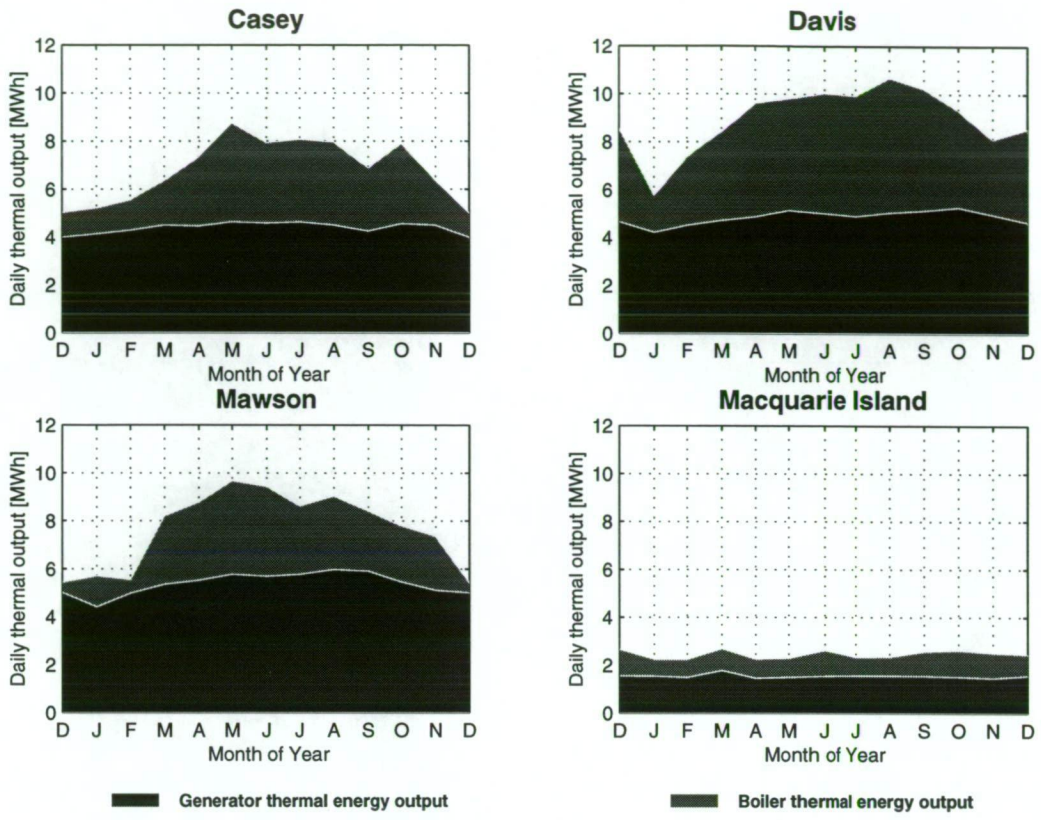

Figure 4.10: Estimated average daily station thermal energy production levels [1992-95]

The last of these points has interesting consequences. Renewable energy systems, displacing the need for electrical power generation from the diesel generator sets, would reduce the amount of thermal energy produced by these generators. In order for current levels of thermal energy to be maintained in this situation, additional heat would have to be provided by boilers. At 35% thermal efficiency each litre of diesel fuel used by the generator sets provides 3.4 kW of thermal energy. At 80% thermal efficiency it would take the boilers 0.44 litres of diesel fuel to produce the same amount of thermal energy. This results in a net fuel savings of 0.56 litres for every litre actually displaced from the generator sets for equivalent thermal energy production levels to be maintained. It is against this potential net fuel saving that costing renewable energy systems will need to be determined.

This situation represents a worst case scenario, where periods of renewable power production coincide with periods of high thermal demand. In such a situation, additional thermal energy production from the boilers is required to compensate for all thermal production lost from the generators. If periods of renewable power production are not in phase with periods of high thermal demand the lower generator thermal output may still cover station requirements. If this is the case additional boiler production will not be required resulting in higher net fuel savings.

More information is needed before the actual thermal energy needs at the stations can be determined, allowing the net fuel savings from mixed electrical and thermal energy systems to be determined. The remainder of this study has concentrated on the possibilities of electrical energy generation by renewables based on information on the electrical consumption patterns of the stations. Net fuel savings including reductions for fuel needed by the boilers to produce extra thermal energy (equivalent to that lost from the generator units due to electrical production from renewables) are given in Chapter 7.

4.3 Analysis of station electrical loads

Monthly station reports are useful to define the average energy totals, but for the purpose of load matching with renewables, more detailed information on the rate at which this energy is being produced is needed. The value of these energy rates, referred to as power levels or station load, have been analysed and their serial structure determined.

4.3.1 Electrical load statistics

In order to allow problems with the engineering services of the stations to be identified and resolved, a monitoring system was installed at each continental station as part of the rebuilding program. Referred to as the Local Monitoring and Control System (LMCS), this system consists of a network of Datataker DT200 dataloggers in each major station building of the continental stations Casey, Davis and Mawson.

A range of sensors are connected to each datalogger, monitoring the electrical, plumbing, fire and thermal systems of each building under observation. An RS485 serial network is used to link each datalogger to an operations computer. These computers are, in turn, linked via satellite to a central computer at the AAD headquarters in Kingston.

Using this system, time series have been recorded at each of the continental stations. These series consisted of ten minute averages of the electrical power output and fuel use of the diesel generator sets located in the main powerhouse (MPH), together with the flow rate and temperature (input and output) of the ring main heating hot water (HHW) system.

This study has been the first attempt to collect and record data using the LMCS, for which there were a number of problems often resulting in periods when data could not be recorded. Difficulties that occurred with the system included faults with the LMCS operating software, periodic power failures to the operations computer at the station, and frequent use of the EPH during maintenance periods of the MPH (no monitors are connected to the LMCS in the EPH). The link from the stations to Kingston also proved unreliable, resulting in periodic loss of data. Data that was able to be obtained is given in Table 4.8. (Note: no LMCS system has been installed at Macquarie Island).

Station	LMCS electrical load sequence availability			
	starting date	ending date	duration (days)	coverage (%)
Casey	28/7/94	2/11/95	462	11.6%
Davis	9/8/94	19/11/95	467	91.1%
Mawson	24/8/94	25/11/95	372	17.2%
Macquarie Island	n/a	n/a	n/a	n/a

Table 4.8: LMCS power sequences obtained for the ANARE stations

Data from Davis forms the most comprehensive set, spanning over one year at 91% coverage. For this reason, analysis has concentrated on this data, with results assumed characteristic of all stations. One hour averages of the recorded power output of the MPH, calculated from the LMCS data recorded at each of the continental stations, is displayed in Figure 4.11. The sparse coverage of the data sets at Casey and Mawson can been seen from this figure, with Davis the only station with an almost continuous coverage in excess of one year.

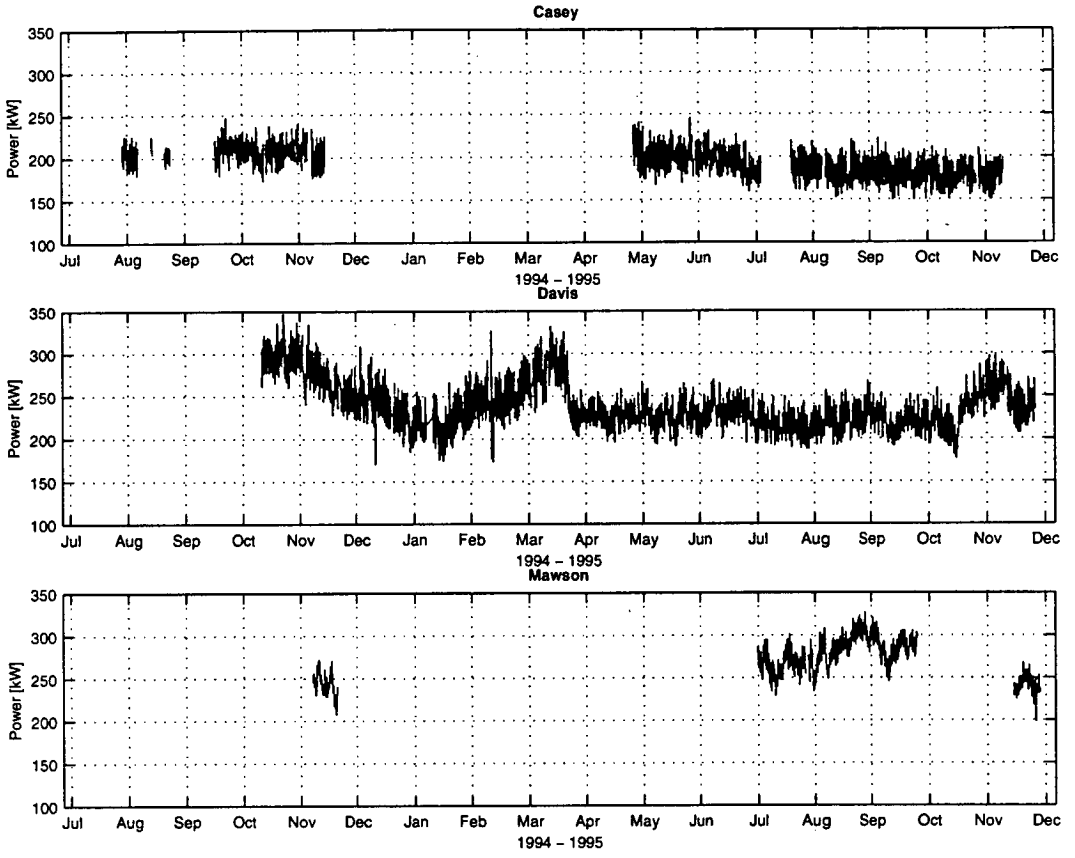

Figure 4.11: LMCS MPH power data, averaged over 1 hour, for Casey, Davis and Mawson

The statistical properties of this data are presented in Table 4.9. The coefficient of variation, as defined for wind speed, is the ratio of the standard deviation to the mean; while the load ratio is the ratio of the mean to the maximum. High load ratios indicate that the extremes to which the system must respond are close to the mean - a good result for power systems.

Station	Power sequence (kW)			coefficient of variation	load ratio
	max	mean	std		
Casey	271	193	13	0.07	0.79
Davis	367	240	22	0.09	0.78
Mawson	335	267	13	0.05	0.88
Macquarie Island	n/a	n/a	n/a	n/a	n/a

Table 4.9: LMCS power statistics for the ANARE stations

The statistics for Davis are more complete, based on data from over one year. When considering this, the range of these statistics indicate similar properties for each of the continental stations. This supports the use of properties derived from Davis as being characteristic of the other continental stations. A similar, although less justified assumption will be made for Macquarie Island in the absence of true power level data.

4.3.2 Analysis of electrical load at Davis

By subtracting the daily average from readings over a given day, separation of inter-daily variation from intra-daily variation can be achieved. The results of this procedure, using the Davis LMCS electrical power series, are presented in Figure 4.12.

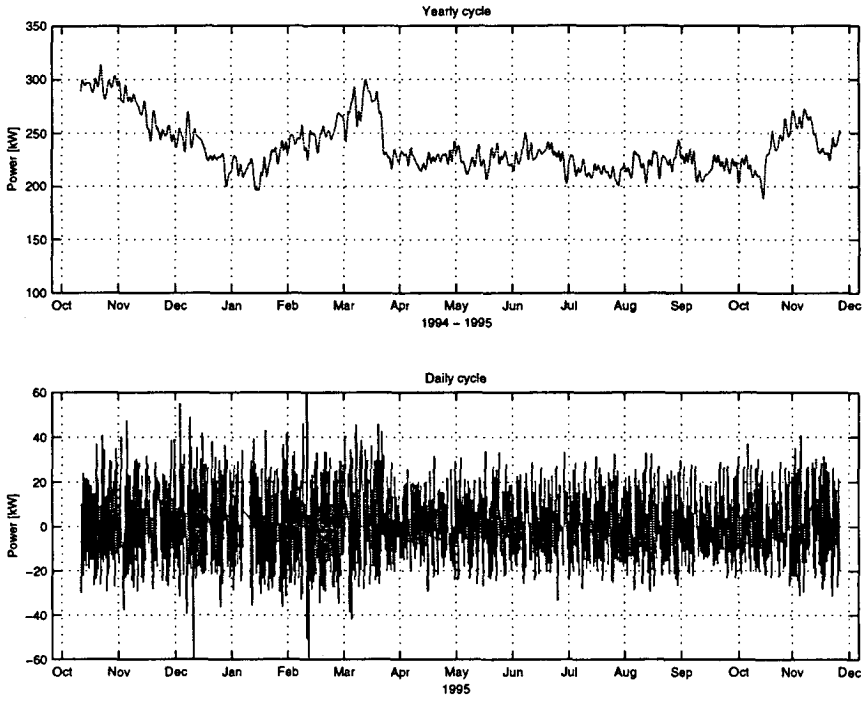

Figure 4.12: Separation of Davis power load sequence into inter and intra daily components

The daily power load pattern can be seen to vary up +/- 40 kW, with summer variation higher than winter. The cause of the major discontinuity in both the inter daily cycle and intra daily cycles is most likely due to population changes. These change dramatically around the same time, as indicated in Figure 4.13.

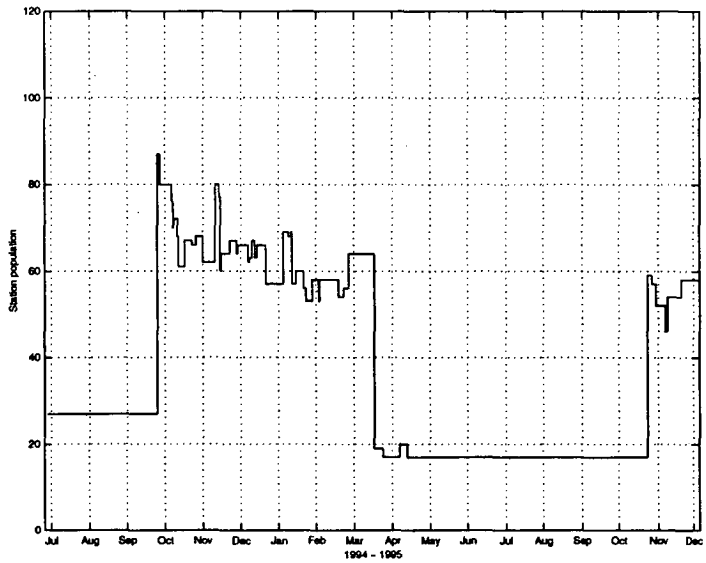

Figure 4.13: Davis population numbers [source, AAD Engineering]

The inter-daily and intra-daily breakdowns indicate the presence of cyclic patterns. The period of these cycles can be identified using spectral analysis. To achieve this, a technique described by Schickedanz (1977) has been used. This technique involves fitting non-integer (NI) sine and cosine functions to a data sequence using a series of multi-linear regression equations. This method was chosen over the more usual Fast Fourier Transform (FFT) due to the irregularity of the data, with embedded periods of missing values. When using integer sine and cosine values, the NI regression method is equivalent to the FFT.

The sine and cosine terms to be fitted to the data are [Schickedanz, 1977]:

$$XS_{ij} = \sin(2\pi ij/P), \qquad \text{j=1,2,...n} \qquad (4.1)$$

$$XC_{ij} = \cos(2\pi ij/P), \qquad \text{j=1,2,...n} \qquad (4.2)$$

Where i can assume both integer and non-integer values, j is an integer value corresponding to the data points of the original data sequence x_j (containing n points), and P represents the fundamental period under investigation. The resultant multi-linear regression equation is given by the expression:

$$\hat{x}_j = x_{ij} = a_i + b_i XS_{ij} + c_i XC_{ij} \qquad \text{j=1,2,...n} \qquad (4.3)$$

Where a_i is the intercept, b_i and c_i are the partial regression coefficients for a given value of i, for the fitted data sequence $\hat{x}_j$. The multiple correlation coefficient R_i, and partial correlation coefficients r_i between the sine and cosine, are determined for a range of i. An estimation of the normalised spectral density, representative of the fractional amount of the variance of the original data sequence explained by the regression, is then given from R_i^2, the coefficient of determination. There will be some disagreement between this value and the true spectral density, for non-integer values of i, due to a lack of orthogonality (ie. independence) between the sine and cosine terms, but for small values of r_i this can be ignored. The significance of R_i, r_i, b_i and c_i can be tested using the usual tests employed in multiple regression and correlation analysis such as the F test. For a full description of this technique see Snedecor (1980).

The nature of the NI technique results in the calculation of a continuous rather than a discrete spectrum, dependent on the values of i. For large values of i the limit of maximum resolution is approached, imposed by the length of the data sequence, giving unreliable results. The spectrum of the electrical power from LMCS data at Davis, representing R_i^2 for a range of values of i, is presented in Figure 4.14. To calculate this spectrum the fundamental period P was set to 1 year and the wavelength i varied to enable R_i^2 to be calculated for periods ranging from 3 hours to 1 year.

Distinct peaks in the spectrum occur for daily, weekly and yearly cycles and their harmonics. The position of the first four peaks correspond with the first three daily harmonics at wavelengths of 1/3 day, 1/2 day and 1 day. The next group of significant peaks are for wavelengths of 7 days and 14 days, representative of weekly cycles. Yearly harmonics, ranging from 47 days (~1/8 year), 61 days (~1/6 year), 91 days (~1/4 year), 122 (~1/3 year) and 185 (~1/2 year) complete the significant peaks present in the spectrum.

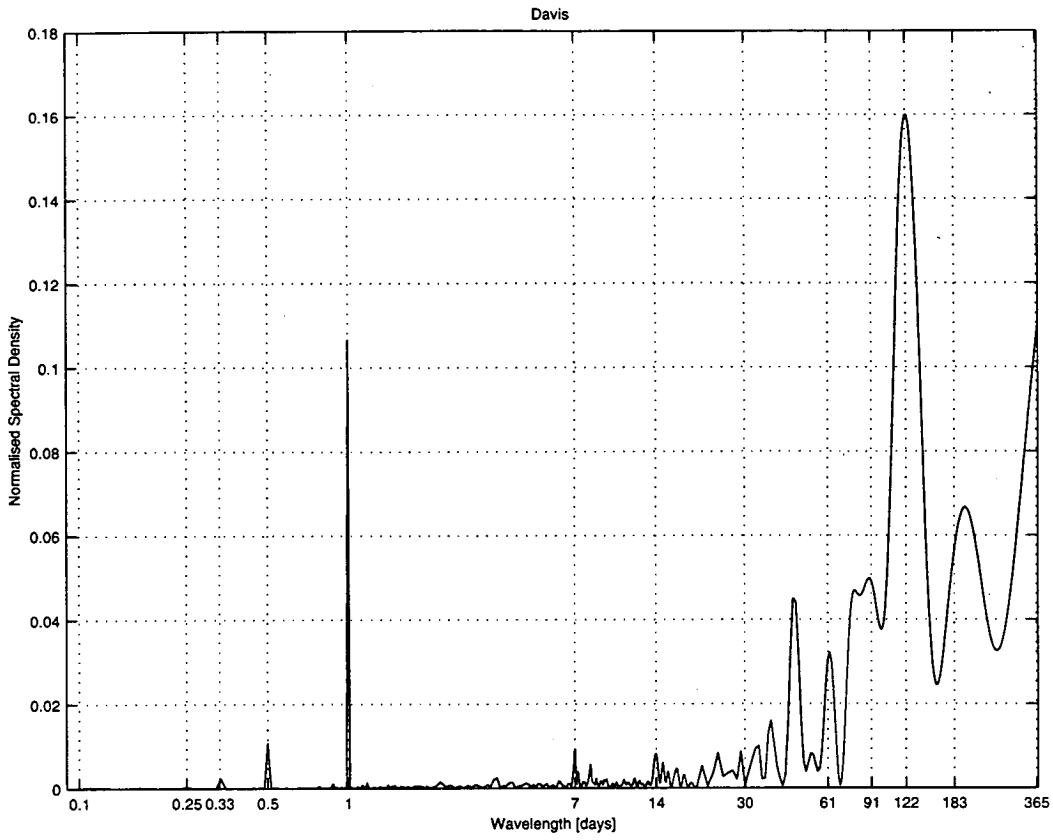

Figure 4.14: Davis electrical power spectrum, constructed from 10 minute LMCS data

The time series of the electrical power for Davis indicates daily, weekly and yearly cycles. These cycles constitute periodic loads at the stations that are dependent on regular work patterns of people and automatic plant. In addition to these are non-periodic loads; dependent on individual day-to-day work patterns, station population numbers and climatic conditions.

4.3.3 Climate and population influenced loads at Davis

Climatic conditions influence the electrical and thermal loads at the stations. The outdoor ambient temperature will affect the air exchange and circulation systems of station buildings, inducing extra loads from both convective cooling and cold air penetration. Low temperatures will also result in use of heating elements (heat trace) in the outdoor pipes of the 'ring-main'; keeping sewage, potable and fire-fighting water, liquid. Cooling effects will be enhanced during periods of strong winds, when the rate of cooling increases, often referred to as the 'wind-chill'.

Changing climatic conditions also influence station loads indirectly, altering work patterns by forcing personnel to spend more time indoors when low temperatures and strong winds occur. In a report by Hall (1993), monthly variations in the outdoor temperature were compared to electrical and thermal output of the stations. The level of relationship identified using this method was low. A better indication of climatic forcing can be obtained from comparison of the variance of the electrical power time-series and climate series over the same period.

Using this method a climate induced load of 5% of the peak was calculated for the region around St John's, Newfoundland - a region where typical winter night time temperatures have been known to drop below -25°C [Little, 1993]. In this study, Little identified temperature as having the highest influence on the weather sensitive proportion of the load, followed by wind speed. Other variables such as cloud cover, humidity and precipitation were reported as being only distantly influential on the load [Little, 1993].

An extension to this procedure has been developed for use at the Australian Antarctic stations. Load at the stations has been assumed to consist of a population sensitive proportion in addition to a climatic sensitive proportion. In the method used, a regression equation is developed to match the variance in the temperature, wind speed and population series with that of the station load. Non-weather or population dependent proportions of the load are modelled using sinusoids representing yearly, weekly and daily patterns in load.

The difference between the recorded series and regression fit is assumed to represent the contribution of random events. To represent the yearly cyclic patterns, the first three seasonal harmonics will be used, identified from the spectrum as significant. Equations for these series are as follows, where t represents the time in days from the beginning of the year, and α the phase shift:

$$a_j = \sin\left(\frac{t_j}{365 \times 2\pi} + \alpha_A\right)$$

$$b_j = \sin\left(\frac{2t_j}{365 \times 2\pi} + \alpha_B\right) \qquad \text{j=1,2,...n} \quad (4.4)$$

$$c_j = \sin\left(\frac{3t_j}{365 \times 2\pi} + \alpha_C\right)$$

To represent weekly and daily cyclic variation the first harmonic of each will be used.

$$d_j = \sin\left(\frac{t_j}{7 \times 2\pi} + \alpha_D\right) \qquad \text{j=1,2,...n} \quad (4.5)$$

$$e_j = \sin\left(\frac{t_j}{2\pi} + \alpha_E\right) \qquad \text{j=1,2,...n} \quad (4.6)$$

A 1-hour time step has been used for the series. The climate sensitive proportion of load are investigated using temperature gradient T_j and wind speed series W_j, calculated from linearly interpolated 3 hourly BoM readings of the 10 minute average. The temperature gradient series has been calculated using an inside reference temperature of 18°C.

The population sensitive proportion of the load has been assumed to consist of two components: a component dependent on the overall population level of the station, and a component that influences the size of daily fluctuations. To take into consideration these two influences; series for the population P_j, and the product of the population and daily cycles E_jP_j, have been included in the regression equation. The resultant regression equation to be fitted against LMCS power levels for Davis, averaged over 1-hour x_j for each point j, is given in Equation 4.7.

$$x_j = Aa_j + Bb_j + Cc_j + Dd_j + Ee_j + Fe_jp_j + Pp_j + Tt_j + Ww_j + Z \qquad j=1,2,...n \quad (4.7)$$

Solution of this equation using the LMCS power readings from Davis, results in the regression coefficients presented in Table 4.10:

Series	phase shift (days)	regression coefficient	correlation to power R^2
yearly	105.9	-13.1	0.38
1/2 yearly	41.7	-11.8	-0.29
1/3 yearly	26.2	9.9	0.48
weekly	-0.8	2.5	0.08
daily	0.1	-11.2	-0.28
daily population	-0.2	0.2	-0.24
population		1.3	0.59
temperature gradient		1.3	-0.05
wind speed		0.7	-0.09
constant		150.8	
Resultant regression fit R^2			0.89

Table 4.10: Regression results

The daily, weekly and yearly phase shifts were solved using a regression equation with separate sine and cosine terms. These were then combined into a single sinusoid with a phase angle α, after solution of the partial regression coefficients indicated they were sufficiently orthogonal in all cases as outlined by Schickedanz (1977). The value of these phase angles are given in Table 4.10.

The coefficient of determination, indicating the level of similarity in variance between two series, is used to indicate the level of the regression fit. A perfect match is represented by 1, indicating 100% of the variance has been explained [Snedecor, 1980]. The value of the coefficient of determination, for each of the series used in the regression fit against the power series, is also given in Table 4.10, together with the overall coefficient of determination for the series combined.

The fit of this regression is high, with 89% of the variance matched. The proportion of load influenced by the temperature gradient, wind speed and population level at the station is presented in Figure 4.15, together with regression fit and recorded load. The load proportions attributed to temperature, wind and population represent both direct and indirect influences such as lighting during winter. The correlation values presented in Table 4.10 should be considered as giving an indication of all loads coinciding with changes in population, temperature gradient and wind speed, rather than loads directly dependent on them.

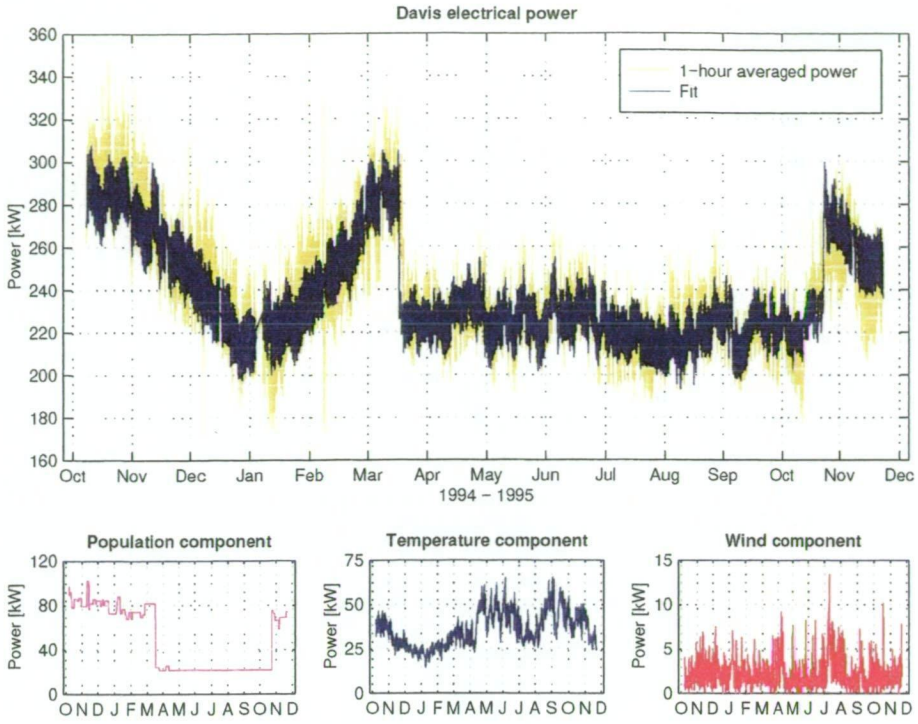

Figure 4.15: Regression fit to Davis LMCS electrical power series

Integrating the sequence population, temperature and wind speed loads presented in Figure 4.15 results in the following energy influence break-downs:

Load sensitive variable	Proportion of electrical energy production	Regression fit coefficient (and dependency)
Population	20%	1.27 kW (per person)
Temperature gradient	15%	1.31 kW (per °C)
Wind speed	1%	0.70 kW (per m/s)
Base load	64%	150.8 kW (independent)

Table 4.11: Correlation of population numbers, temperature and wind speed to the Davis station electrical energy total

These values indicate that changes in population and temperature gradient have greater influence on station load than changes in wind speed. The consequence of high base loads and low wind dependence on the ability of wind based energy systems will be investigated in Chapter 6. In order for this to be achieved a model has been developed to generate a time series for each station.

4.4 Electrical load time-series

In order to further investigate load matching of wind and solar resources to station demands, it is desirable to have power load series, not just for Davis during 1994/5, but for all stations over a number of years. To achieve this it will be assumed that the daily, weekly and climate related loads at all stations are statistically similar to those at Davis. The base yearly and monthly power loads however will be considered site dependent and matched to local records.

4.4.1 Model for climate and population influenced loads

Load patterns at the station will be assumed to be influenced by climatic conditions and population levels, in addition to an indeterminate proportion, affected by work programs and the personal preference of people at the stations. To ensure there is strong agreement with typical loads experienced at the stations, yearly influences will be deduced from the average monthly station load reported at the station under investigation, presented earlier for each of the stations in Figure 4.5 to 4.8, rather than sinusoids.

Yearly sequences of daily average power consumption levels have been calculated from the monthly reported station average, by assuming that they represent the daily power level at mid-month. Cubic splines have then been used to interpolate between these values to obtain a full sequence, referred to as the 'mean daily power levels' (MDPL).

Correlation of the mean daily power level time series $MDPL_j$ with the LMCS power load series x_j, population numbers p_j, temperature gradient t_j and wind speed w_j sequences for Davis is given in Table 4.12:

Sequence	correlation with MDPL R	coefficient of determination R^2
population	0.709	0.503
temperature gradient	-0.305	0.093
wind speed	-0.127	0.016
power	0.656	0.430

Table 4.12: Correlation of MDPL with other regression sequences

These results indicate a high level of similarity between the power sequence and the MDPL sequence. Approximately 43% of the variance of the power sequence can be explained by the MDPL alone. Most of the remaining variance in the power sequence, not correlated with the MDPL, is due to variations of less than one month. It is against this remaining variance that the daily, weekly, population, and climate sequences will be matched.

The MDPL sequence has been then introduced to a regression equation similar to that described in the previous section, with the yearly cyclic patterns omitted. Solving this regression equation for Davis allows for the solution of regression coefficients, assumed representative of conditions at the other stations.

The modified regression equation to be used, including the mean daily power level sequence $MDPL_j$, is given by Equation 4.8.

$$x_j = Y.MDPL_j + Dd_j + Ee_j + Fe_jp_j + Pp_j + Tt_j + Ww_j + Z \qquad j=1,2,...n \qquad (4.8)$$

Solution of this equation, using the same series as defined previously in Section 4.4.1, results in the regression coefficients presented in Table 4.13.

Series	phase shift (days)	regression coefficient	regression fit to power R^2
MDPL		0.8	0.66
weekly	1.2	2.3	0.08
daily	0.1	-11.0	-0.29
daily population	-0.2	0.2	-0.25
population		0.7	0.59
temperature gradient		1.8	-0.05
wind speed		1.9	-0.09
constant		-25.9	
		Resultant regression fit R^2	0.84

Table 4.13: Regression results including MDPL

The resultant fit of this regression to the recorded power levels is given in Figure 4.16, together with the subsequent residual.

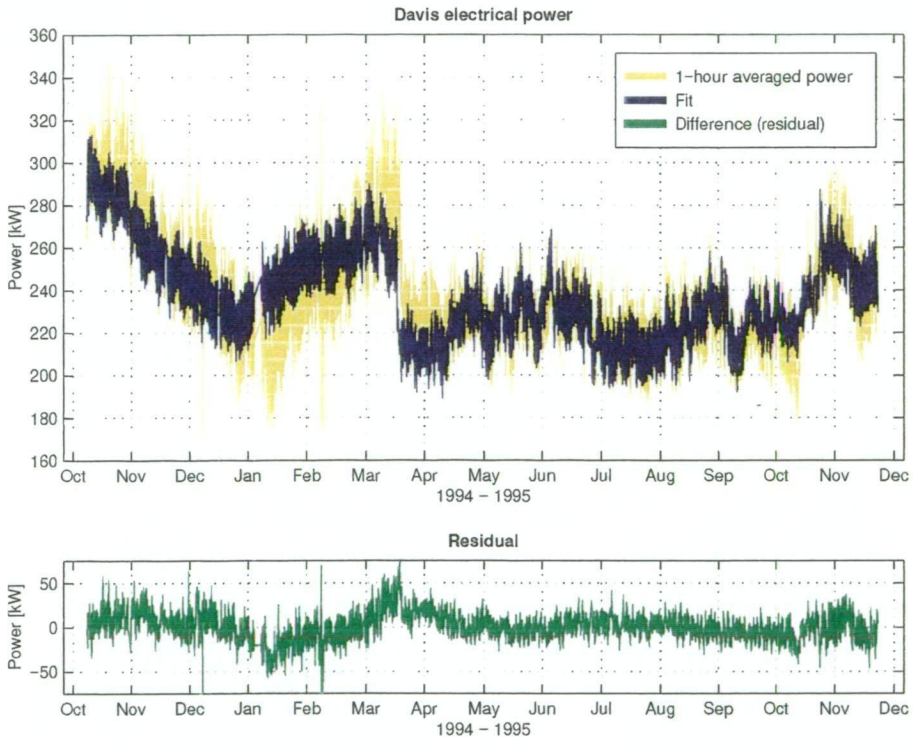

Figure 4.16: Regression fit to Davis LMCS electrical power series including monthly daily average load from station reports

The fit of this regression is very similar to that identified using yearly sinusoids, except the introduction of the MDPL has sensitised the proportion due to wind influence loads.

The regression equation given by Equation 4.8, together with the regression coefficients given in Table 4.13 define the model for determinable station load sequences. Non-determinable loads, represented by the residual in Figure 4.16, are assumed to represent load fluctuations due to work patterns. There is logical structure to work patterns, but it is not cyclic in nature. Extension of the station load model to include the structure from work patterns has been achieved through analysis of the residual.

4.4.2 ARMA model for residual

To determine the serial structure of the residual, indicating the typical length of these random unpredictable work pattern loads, standard time series analysis techniques have been employed.

These involve the use of ARMA models, as described by Box and Jenkins (1985). The simplest of these models, are autoregressive (AR) and moving average (MA) models, rather than combinations of the two. In these models white noise is modified using a pre-calibrated linear filter to create a data series with similar statistical and serial characteristic to a known series.

For an AR(p) process of order p, the value of the sequence at point j is given by:

$$x_j = \phi_1 x_{j-1} + \phi_2 x_{j-2} + \ldots + \phi_p x_{j-p} + a_j \qquad (4.9)$$

where ϕ_k are the autoregression coefficients and a_j is random noise derived from a Gaussian distribution of mean zero and variance σ_a^2. For a MA(q) process of order q, where a_k is as for a AR process and θ_k represents the moving average coefficients, a similar sequence is given as follows:

$$x_j = a_j + \theta_1 a_{j-1} + \theta_2 a_{j-2} + \ldots + \theta_q a_{j-q} \qquad (4.10)$$

Combined, these models give a ARMA(p,q) model of order p,q. To determine the type of the model best suited to represent the serial structure of the residual, the autocorrelation function (ACF) and partial autocorrelation function (PACF) have been used according to the methods outlined by Box and Jenkins. The ACF gives an indication of the degree to which a series is correlated to itself. Calculation of the ACF coefficient r_k at lag k for the original data series X_j is given by:

$$r_k = covariance(X_j, X_{j+k}) \,/\, variance(X_j) \qquad (4.11)$$

The PACF coefficient at lag k is described as the variance not explained by a AR(k-1) model. A method outlined by Box and Jenkins for calculation of the PACF involves solution of the Yule-Walker equations. This is presented in Equation 4.12, where the PACF coefficient at lag k is given by the term f_{kk}:

$$r_j = f_{k1} r_{j-1} + f_{k2} r_{j-2} + \ldots + f_{k(k-1)} r_{j-k+1} + f_{kk} r_{j-k}$$

$$(1 \le k \le n) \qquad j=1,2,\ldots n \qquad (4.12)$$

The frequency-of-occurrence distribution, ACF and PACF for the residual as calculated from Equations 4.11 and 4.12, are in given in Figure 4.17. The ACF decays exponentially while the PACF drops off after lag $k=1$, indicating an AR(1) model, also known as a Markov process.

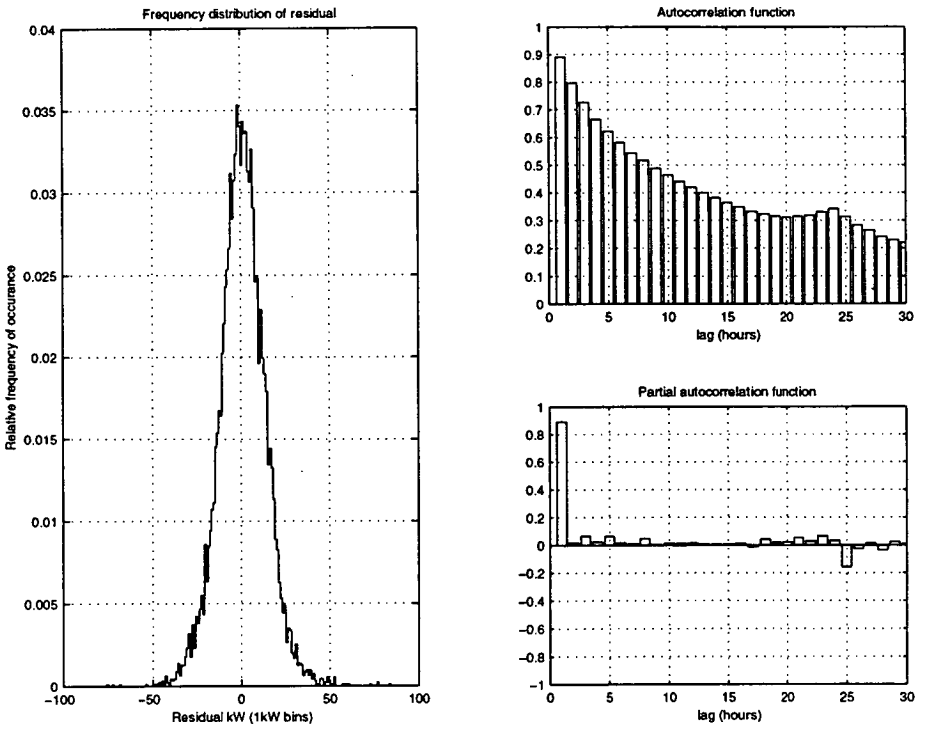

Figure 4.17: Residual frequency-of-occurrence, autocorrelation and partial autocorrelation functions

There is a residual 24 hour sub-structure to this series, but this will be assumed small for the purpose of this exercise, allowing simplifications. The equation for this model is given below, where a_i represents a random number series with variance σ_a^2[Blanchard, 1984].

$$x_j = \phi_1 x_{j-1} + a_i \tag{4.13}$$

The autocorrelation coefficient φ_1 and the variance of the random noise σ_a^2, are calculated using the first ACF coefficient r_1 and the sample variance σ_X^2:

$$\phi_1 = r_1 \qquad \sigma_a^2 = \left(1 - r_1 \phi_1^2\right)\sigma_X^2 \tag{4.14}$$

Solving for the residual power sequence at Davis gives:

$$x_j = 0.92\, x_{j-1} + a_j \tag{4.15}$$

where, σ_a=2.54

This allows for generation of a random series with a similar serial structure to the residual, and thus random work pattern loads. Combining this with the regression equation allows for generation of load series that are statistically similar to the recorded power level sequence at Davis.

4.4.3 Station electrical load time-series estimates

Extension of this model to Casey and Mawson allows the construction of a time series representative of hourly station load. Using coefficients solved for Davis gives Equation 4.16, describing the station load x_j in terms of the variables given in Table 4.14:

$$x_j = 0.8MDPLj + 2.3\sin\left(\frac{j}{14\pi} + 1.2\right) - 11.0\sin\left(\frac{j}{2\pi} + 0.1\right)$$
$$+0.2p_j \sin\left(\frac{j}{2\pi} - 0.2\right) + 0.7p_j + 1.8t_j + 1.9w_j - 25.9 \quad \text{j=1,2,...n} \qquad (4.16)$$

Variable	Description	Units
j	Hours past midnight, January 1 1992	[hrs]
$MDPL$	Mean daily power levels	[kW]
p	Station population levels	[-]
t	Temperature gradient relative to 18°C	[°C]
w	Wind speed	[m/s]

Table 4.14: Station load series variables

For the continental stations hourly temperature and wind speed series over the period 1992-1995 were constructed through linear interpolation of 3 hourly BoM records. Mean daily power levels were constructed using cubic splines to interpolate between mid-month average daily power consumption levels, calculated from station monthly totals (presented in section 4.2.2).

Population series were simplified for this exercise, with the number of people at the continental stations set to 70 over summer (September 21 - March 21) and 10 over winter (March 22 - September 20). For Macquarie Island where loads are much smaller than at the continental stations the influence of climatic effects will be assumed to be reduced by approximately 50%. Population levels were set at 45 over summer (September 21 - March 21) and 10 over winter (March 22 - September 20). These simplifications have been used only after analysis indicated that the results obtained differed minimally (~1%) when using actual figures.

In addition, to ensure that power loads estimated by these series are realistic of loads recorded at the stations, the recorded average for each station over the period 1992-1995 was compared to that given by Equation 4.16. To ensure matching of these amounts, particularly Macquarie Island, the relaxation constants given in Table 4.15 were added to each hourly value.

Station	Observed load average	Calculated load average	Relaxation constant
Casey	196.5 kW	216.4 kW	-19.9 kW
Davis	227.9 kW	238.3 kW	-10.4 kW
Mawson	258.8 kW	275.3 kW	-16.5 kW
Macquarie Island	63.9 kW	50.3 kW	+13.6 kW

Table 4.15: Relaxation constants

An ARMA series constructed from Equation 4.15 representing random work patterns was then added to each series (reduced by 50% for Macquarie Island) to complete the simulated load series. In the absence of actual measured data, these series will be assummed representative of actual station loads over the period 1992-1995 and used to assess various renewable energy systems (further details described in Chapter 6).

4.5 Summary

Fuel consumption and electrical energy production totals from monthly stations reports indicate a summer/low, winter/high consumption and production pattern. Resolution of the electrical load at Davis indicates that there is significant correlation with station population levels, temperature gradient (inside-to-outside temperature difference), and to a lesser degree wind speed.

Temperature gradient correlated loads amounted to 1.3 kW per degree, representing 15% of the total station energy consumption. Population correlated loads amounted to 1.3 kW per person, representing 20% of the total station energy consumption. Wind correlated loads amounted to 0.7 kW per m/s, representing 1% of total station energy consumption.

Based on load influences from climate and population, a model was developed to generate load sequences, statistically representative of the load demand at each station. These can then be used to assess various renewable energy system configurations.

Chapter 5

Field trials and validation exercises

5.1 Introduction

A description of the field work conducted in support of this project is presented in this chapter, providing practical insights into issues of concern for renewable energy systems at the stations. Field work in Antarctica is necessary to test equipment, confirm assumptions used in estimating the wind and solar energy reserves, as well to develop a better understanding of station energy use patterns.

5.2 Field work programs

A total of six months was spent by the author on location at Casey station over the 1994/5 and 1995/6 summer seasons as part of the 48th and 49th ANARE expeditions. Work conducted during this time was directed towards development of a reference data base on renewable energy. This involved field testing of a wind turbine, recording of meteorological conditions, and familiarisation with the current energy systems of the stations.

5.2.1 Field work goals

Issues addressed by field work included:

1. Is the strength of current wind turbine designs sufficient for Antarctic use, or will modifications be necessary?
2. Does the power curve accurately describe the performance of a wind turbine under Antarctic conditions, including effects from small period wind speed pulsing (a phenomena often reported at the stations)?
3. What is the relationship between BoM meteorological records, involving 3 hourly recordings of the 10 minute wind speed at 10 metres height (which current estimates are based on), and the actual wind speed regimes at common operational heights for wind turbines?
4. Are model estimates of the hourly solar energy totals (given in Chapter 3) accurate and to what degree can low temperatures experienced at the stations be expected to effect the performance of PV systems?
5. Which station electrical loads should be reduced or rescheduled to make the use of renewable energy systems more viable?

Preliminary information obtained during the establishment of programs to answer these issues allow for some qualitative results to be presented in this thesis, although further time is required before enough data is available for detailed conclusions.

5.2.2 Field work programs at Casey

A major component of the field work conducted at Casey involved the installation of an Aerowatt UM-70X wind turbine for testing. Exposure to sub-zero temperatures and extreme wind speeds, combined with the possibility of snow and ice infiltration (a common problem in Antarctica), may lead to reduced operational life-times for standard wind turbine designs. Field trials at the stations allow potential problems to be identified, and through feedback to the manufacturers, rectified. Operation of the UM-70X under Antarctic conditions is also important for other reasons. It provides a practical demonstration of the technology, allowing confidence and experience to be gained by the AAD.

The establishment of an environmental monitoring network also began at Casey. This system consists of a number of wind speed and wind direction monitors positioned at different heights, and a small test PV panel in conjunction with a pyranometer. It is intended to provide more detailed information on the wind and solar energy reserves at the stations, complimenting the estimates given in Chapters 2 and 3. A preliminary energy audit was also initiated, involving the monitoring of a number of buildings at Casey to enable a greater understanding of the energy consumption patterns at the station.

5.3 Wind turbine testing

The potential for the use of wind turbines at the stations has been outlined for over a decade. An interim report on 'Wind-power generation at Mawson', by Lovatt (1983), was conducted for the Antarctic rebuilding program. Four key areas potentially suitable for wind power application were identified:

1. Wind/Solar combination to charge batteries for communication systems (60 W)
2. Wind-electric boiler combination to melt ice for domestic water (10 kW)
3. Wind-electric power generation to work in conjunction with base-load diesel generator sets (up to 50 kW)
4. Wind-electric (transportable) for mounting on a tractor train for battery charging, sump heating and cabin heating (500 W - 1 kW) [Lovatt, 1983].

Of these suggestions, only the first was implemented. The second suggestion, the focus of the interim report, was considered but not acted on, while the third suggestion forms the basis for these investigations. (The fourth suggestion has also not been acted on).

The use of sizeable wind power by the AAD was to wait until the 1992/3 ANARE expedition to Heard Island where, thanks to the work of expedition leader Attila Vrana, a number of small wind turbine designs were purchased and installed. The most successful of these proved to be the Aerowatt UM-70X. A brief description of this unit and its use at Heard Island have been provided in Chapter 1, while further details, including its installment and operation at Casey, provided below.

5.3.1 Description of Aerowatt UM-70X wind turbine

The operating characteristics of the UM-70X, built by the former Aerowatt company, are presented in Table 5.1. (See also Table 1.2 and Figure 2.5 for power curve).

Type of turbine	Up-wind horizontal axis
Number of blades	2
Blade length	3.5 m
Rated power	10 kW / 12 kVA
Rated wind speed	11.5 m/s
Drive train	7:1 step up gearbox
Generator	Induction
Rated voltage	380 V (3 phase) @ 50 Hz
Cut-in wind speed	3 m/s
Production start	3.5 - 5.3 m/s
Survival wind speed	90 m/s

Table 5.1: UM-70X wind-turbine operating characteristics

The support tower for the unit consisted of three 6 m sections of 250 mm diameter galvanised steel tubing bolted together to give an overall height of 18 metres. A pivot at the base of the tower, allows for easy raising and lowering with the aid of a gin-pole arrangement. The tower is held in place by four main guy cables at right angles to each other, with four minor cables used to dampen any oscillatory modes that could have arisen in the tower structure. The modular nature of the tower, combined with the pivot arrangement, allows for erection in remote areas, an important consideration for use in Antarctica.

In addition to easy installation, an important attraction of the UM-70X is its ability to survive strong winds. A variable pitch control mechanism gives the UM-70X a survival wind speed of 90 m/s, one of the highest of any commercially available unit. A schematic of this pitch control mechanism is provided in Figure 5.1.

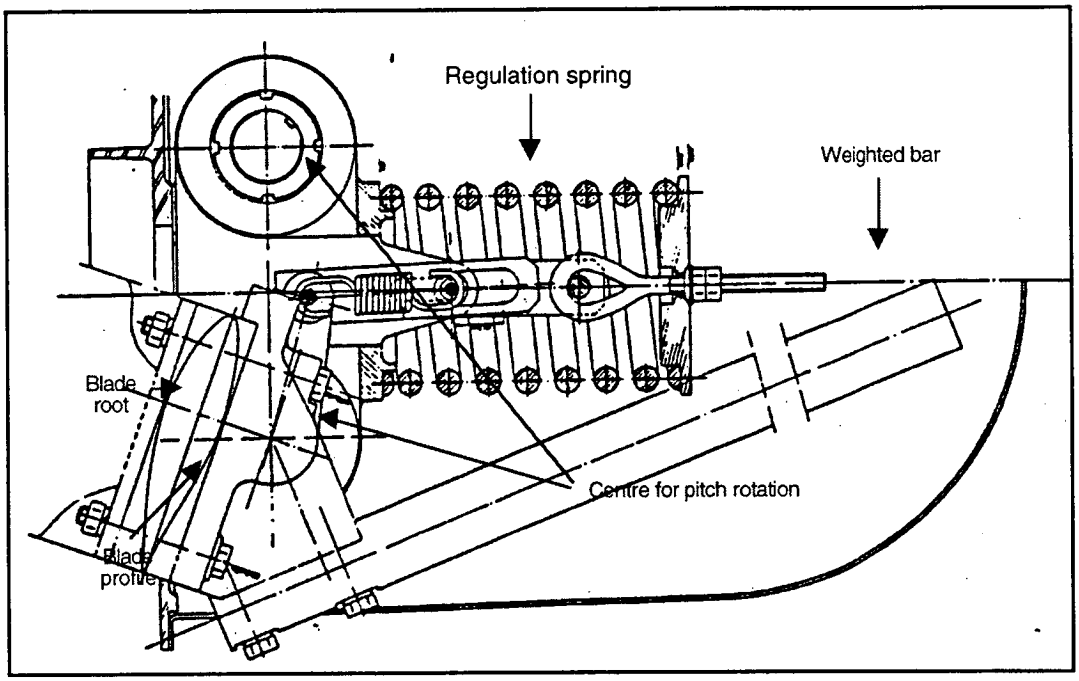

Figure 5.1: Schematic diagram of UM-70X speed-control mechanism [Aerowatt, 1983].

The variable pitch mechanism prevents over-speeding by inducing stall conditions. Air movements over the surface of the blades of the wind turbines induce lift. This in turn provides rotational torque, causing the turbine to rotate. The magnitude of the induced lift, and hence the rotational moment, is dependent on the relative wind speed over the surface of the blades, a function of the pitch of the blades. In the UM-70X, angle is controlled mechanically using a calibrated spring connected to a pair of precision-weighted bars, off set from the pitch centre of rotation of the blade root as indicated in Figure 5.1.

When in motion the weighted bars are forced outwards, changing the pitch angle of the blades, until balanced by forces from the regulation spring. Under-load conditions, torque provided by the turbine is balanced by the generator, resulting in a constant speed of revolution. If load drops out, or wind speed changes, this balance is upset. With a balance no longer in place, the rotational speed of the turbine changes. Higher turbine speeds increase the pitch angle of the blades, reducing the relative speed of the wind, until stall conditions occur, unless balanced by loading from the generator. Lower turbine speeds, however, will decrease the pitch of the blades, increasing lift and speeding up the turbine.

The UM-70X unit, purchased by the AAD, has two configurational modes: battery mode, and grid mode. In battery mode, as used at Heard Island, capacitors connected across the three-phase power output, allow self-excitation of the induction generator. Unregulated power of variable voltage and frequency, results from operation of the UM-70X in battery mode, which can be used directly for heating or rectified and fed into a battery bank.

In grid mode, as used at Casey, the inductive load needed to excite and maintain the magnetic field of the generator is obtained from the grid. This results in grid voltage and frequency being adopted by the unit. A logic circuit is used to connect and disconnect the UM-70X. The output frequency of the residual voltage of the unexcited generator is monitored. When a frequency of above 50 Hz is detected, the isolator in the grid connection box is closed, connecting the generator to the grid and power production commences. If winds drop below the speed necessary to maintain power production, the generator will start acting as a motor, attempting to drive the turbine. When this situation occurs, the logic control circuit begins to sum the total consumption power. Once a preset amount of power has been continually consumed, without production being re-established, the unit is isolated from the grid.

A revised design of UM-70X has been developed by Vergnet, the successors to Aerowatt. Designated the GEV 7.10, this design has incorporated improvements to the speed control mechanism including stronger blade roots and heftier blades, correcting design problems that frequently shortened the operational life of many early units. A version of this new pitch control mechanism, and eventually a whole GEV 7.10 unit, was provided by Vergnet for testing at Casey.

5.3.2 Heard Island testing

Heard Island is situated in the Southern Indian Ocean, south of the Antarctic circumpolar current. During 1992/1993, a small five member expedition party visited the island to conduct a number of assorted research programs. To facilitate and support their stay, a temporary field station was established on the island at Spit Bay at 53°06'S 73°43'E. This was at the other side of the island to the original 1950's outpost on the island at Atlas Cove, as indicated in Figure 5.2.

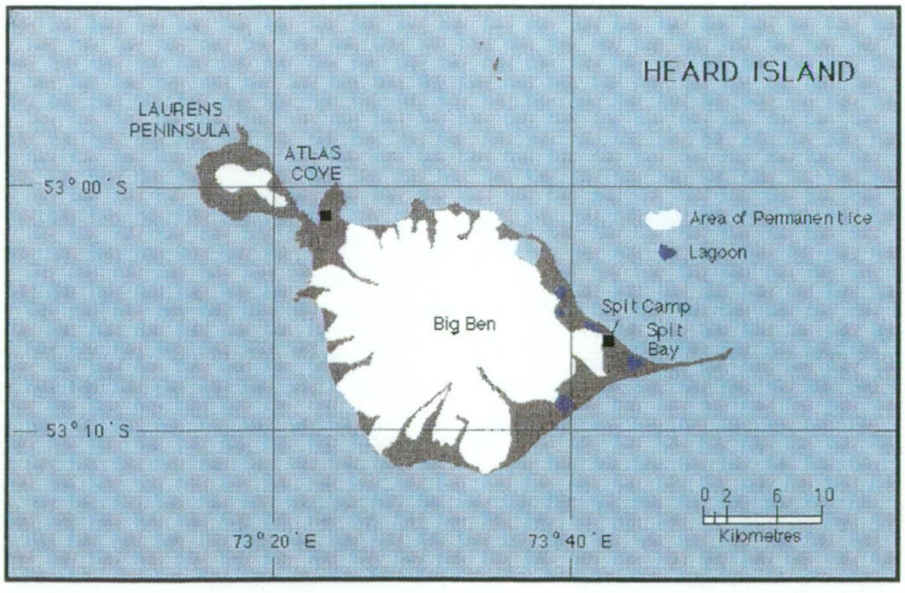

Figure 5.2: Heard Island map [source AAD]

The location of Heard Island south of the Antarctic circumpolar current, unlike Macquarie Island situated north of the Antarctic circumpolar current, results in extremely harsh conditions including the presence of permanent ice fields. Gale force winds and frigid temperatures continuously batter the island, placing high demands on any structures. Three turbines were sent to Heard Island with the Aerowatt UM-70X, the only unit able to survive the conditions. (See Section 1.4.1 for an overview).

The main base infrastructure consisted of eight prefabricated fibreglass huts and a modular store building (see Figure 5.3). Energy requirements consisted of non-interruptable loads for scientific and communication equipment and intermittent loads associated with heating and with powering freezers. The non-interruptable loads were provided for using a 24 V 1000 Ah battery bank via a DC/AC power inverter, while the intermittent loads were operated when power was available. It was found that running a 15 kW diesel generator twice a day for four hours was sufficient to provide adequate power [Vrana, 1995].

The UM-70X was installed for the 1993 summer of the expedition and operated successfully for a ninety day period. The unit was run in stand alone mode, with power for the station met exclusively by the wind turbine, or by the diesel generator. No attempt was made to synchronise and operate both the wind turbine and diesel generator in parallel.

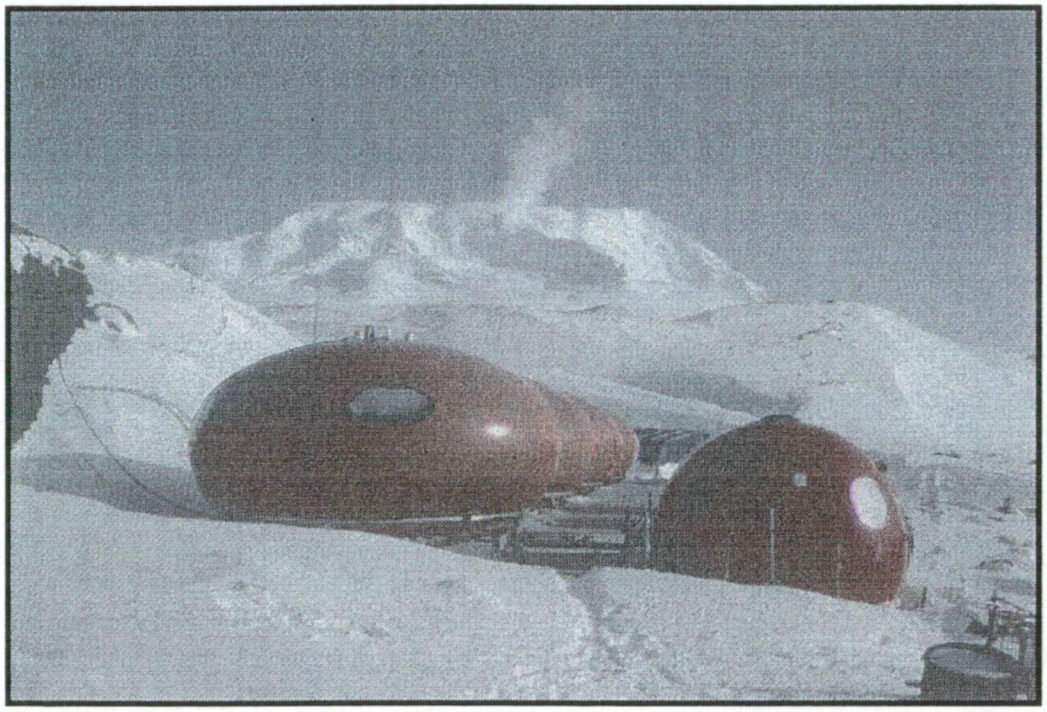

Figure 5.3: Heard Island main station with Big Ben in background 1993 [Photo A. Vrana]

During its operation, the UM-70X produced an estimated 6000 kWh of electricity at a daily average of 62.2 kWh. The amount of energy able to be used over a day was reported as being substantially limited by the size of the batteries and the huts potential for heat storage [Vrana, 1994]. Failure of the main blade root casting caused the unit to be lowered and its use discontinued. This failure demonstrates a potential problem that reduces the number of wind turbines suitable for use in Antarctica. Designs must be able to withstand continuously varying conditions including large wind gusts, fast wind-shifts and low temperatures.

Bird strikes attributed to the wind turbine were monitored at Heard Island, an area of concern if units are situated near bird colonies. Monitoring indicated less than a dozen deaths were directly attributed to the wind turbine. This represents approximately one third of all bird strikes recorded during the expedition. The majority of other bird strikes were due to birds flying into aerial masts, antenna wires and their associated guy wires. The use of free standing lattice or tubular towers, in preference to guyed towers, should reduce the likelihood of bird strikes.

The success of the UM-70X wind turbine at Heard Island prompted the proposal to deploy it at one of the continental bases. After return to Australia, the blade root casting was repaired and plans were made to conduct further trials. For logistical reasons due the 1994/5 summer shipping schedule, Casey was selected as the location for these trials. Although Casey has poor wind resources when compared to Mawson and Macquarie Island, it does have the highest recorded wind gust. In hindsight, this makes Casey a good site for testing wind turbine designs for extreme Antarctic conditions.

5.3.3 Casey installation

After consideration of ease of installation, maintenance and environmental impact, a site within the Casey station confines was selected and approved by the Antarctic Division Environmental Committee. This site is unfortunately situated between a number of buildings. Interference from these buildings, in addition to the upper fuel farm in the direction of the prevailing winds to the east, may reduce the overall performance of the unit. A picture of Casey station, taken in 1991-92 before the arrival of the UM-70X wind-turbine, is presented in Figure 5.4 with the test site indicated.

Figure 5.4: View of Casey looking towards Newcombe Bay 1991-2 [Photo G.Snow]

A population of approximately 15 people stay at the station over the winter months, while up to 70 people can be on-station during the summer months. Casey station consists of a number of buildings situated along a main thoroughfare, the general station layout of which can be seen in Figure 5.4. The largest building on station is the domestic building, known locally as the 'Red Shed'. Living, medical, cafeteria and recreation areas are housed in this building, and as such, it is the hub of most indoor activities on station. To the west of the Red shed is the tank house, main powerhouse, emergency powerhouse, operations building and science building. Buildings to the east of the Red Shed, making up the remaining structures of the station are the store, incinerator, ANARESAT and workshop (see Figure 1.2 for a schematic layout).

Preparations and installation of the UM-70X were completed by the summering personnel of the 48th ANARE expedition during the 1994/95 season. Civil work for the UM-70X involved the laying of a reinforced concrete block to provide a foundation for the tower. The tower was attached to the base plate on a pivot, facilitating raising and lowering during installation and maintenance. Cable anchor points, made from 3 m length sections of steel bar, were drilled into suitable rock, 12 metres from the base of the tower in four locations to lock the tower in position. A picture of the UM-70X when first erected at Casey can be seen in Figure 5.5.

Figure 5.5: Aerowatt UM-70X installed at Casey, March 1995 [Photo C.Brown]

Electrical cable was placed underground, from the base of the wind turbine tower to the ANARESAT building, where appropriate connection equipment was installed. To prevent overload situations thermal isolators, set to disconnect the unit for currents in excess of 32 amps, were installed in three locations. A logic circuit within the grid connection box controlled the last of these isolators.

The Aerowatt UM-70 turbine was operational on 14 April, 1995; much later than hoped due to the following problems:

1. Difficulties in locating suitable positions for the side anchor points
2. Compatibility problems with a new GEV 7.10 nacelle supplied by Vergnet especially for this project. This had to be abandoned and the original nacelle from the Heard Island Aerowatt UM-70X unit used;
3. Adjustments to the feathering mechanism.

Although the difficulties encountered during the installation of the UM-70X were satisfactorily overcome, they did high-light the potential difficulties associated with construction in Antarctica.

5.3.4 Performance breakdown over the initial 90 days

The output of the UM-70X was monitored by current and voltage transducers on each phase, together with an Elcontrol power meter. The voltage and current transducers were connected to a 486 computer via an analog to digital card. This allowed instantaneous readings of the current and voltage to be read as the unit came on line. The Elcontrol unit conducted 4 ms sweeps of the voltage and current of each phase to calculate power readings every 2 to 3 seconds. A fiber optic output relayed this information via an RS232 converter to the computer. A program was written to read these values and store them every 30 seconds.

The monitoring system performed quite well, with the recorded power output readings over the first 90 days (from April 10 to July 9 1995), presented in Figure 5.6. Unfortunately data was lost from May 1 to May 9 (day 121 to 129) when the computer failed to restart automatically after a blackout. On July 9 1995 the UM-70X developed problems and had to be lowered for repairs. A summary of the performance of the unit up until this date is given in Table 5.2. The five operational states of the turbine indicate its speed relative to that at which power production is possible:

- **Stationary:** not moving;
- **Under speed:** turning, but slowly;
- **At speed:** turning at production speed;
- **Just below speed:** turning, but just having fallen below production speed; and
- **Over speeding:** turning at the stall limited speed.

The operational states of the generator indicate whether the unit is disconnected; connected and either producing or consuming power, dependent on the speed of the turbine, or in the special case, isolated when the circuit breakers have been activated either manually or due to current overloads.

Wind turbine operational state		Average output power (kW)	Equivalent time (days)	Percentage of total time (%)
turbine	generator			
Stationary	disconnected	-	54.4 days	61.1 %
Under speed	disconnected	-	8.8 days	9.8 %
At speed	producing	7.31 kW	14.8 days	16.4 %
Just below speed	consuming	-0.43 kW	10.3 days	11.4 %
Over speeding	isolated	-	1.2 days	1.3 %
		Total	90.0 days	100.0 %

Table 5.2: UM-70X operational state at Casey from April 10 to July 9, 1995
(note internal rounding may result in totals not adding to the indicated amount)

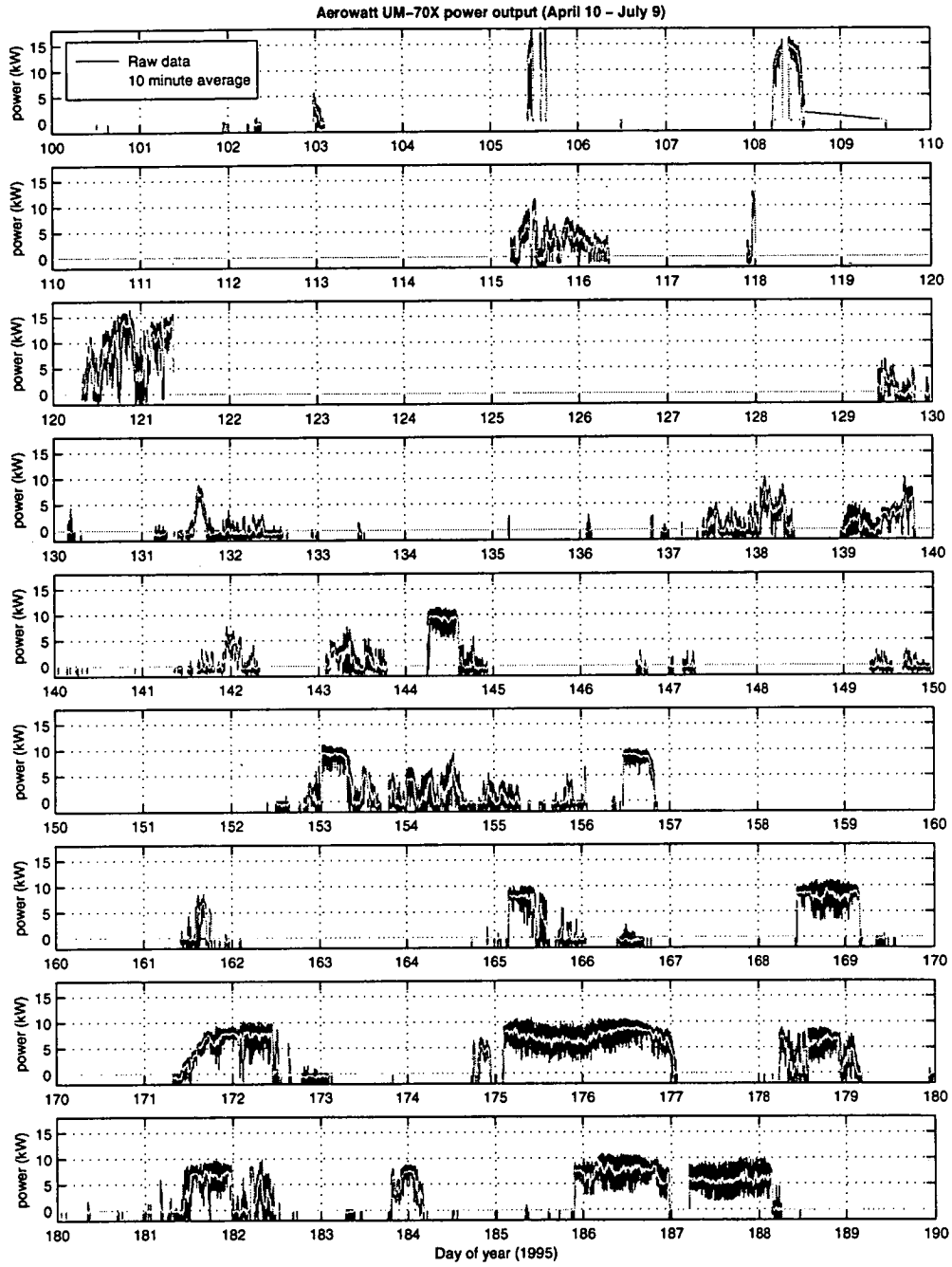

Figure 5.6: Aerowatt UM-70X power output over April 10 to July 9, 1995

Power measurements were taken over 4 seconds every 30 seconds. The variance of this data presented in Figure 5.6 is extremely large with fluctuations in the order of 6-7 kW (60-70%) common between measurements. With the UM-70X output only representing approximately 5% of station load, these variations were effectively absorbed by the grid and regulated by the inertia of the system. These results have profound implications for larger or multiple units, where this situation would no longer be the case.

Comparison with the superimposed 10 minute average indicates that most of the fluctuations are of a short period. This infers that a small amount of smoothing, provided by some form of regulation or energy storage system, should be sufficient to deal with these variations. Methods to deal with this situation are dealt with further in Chapter 6.

As well as short term fluctuations, low power factors were evident. The power factor for the turbine at Casey presented in Figure 5.7 appears to reach a maximum of 0.68. This is of concern considering the station was run at a 0.8 power factor and capacitors rated at 7 kVA were connected across the output phases. A low power factor for the turbine (a common issue associated with induction generators) will result in lower active power conversion efficiencies.

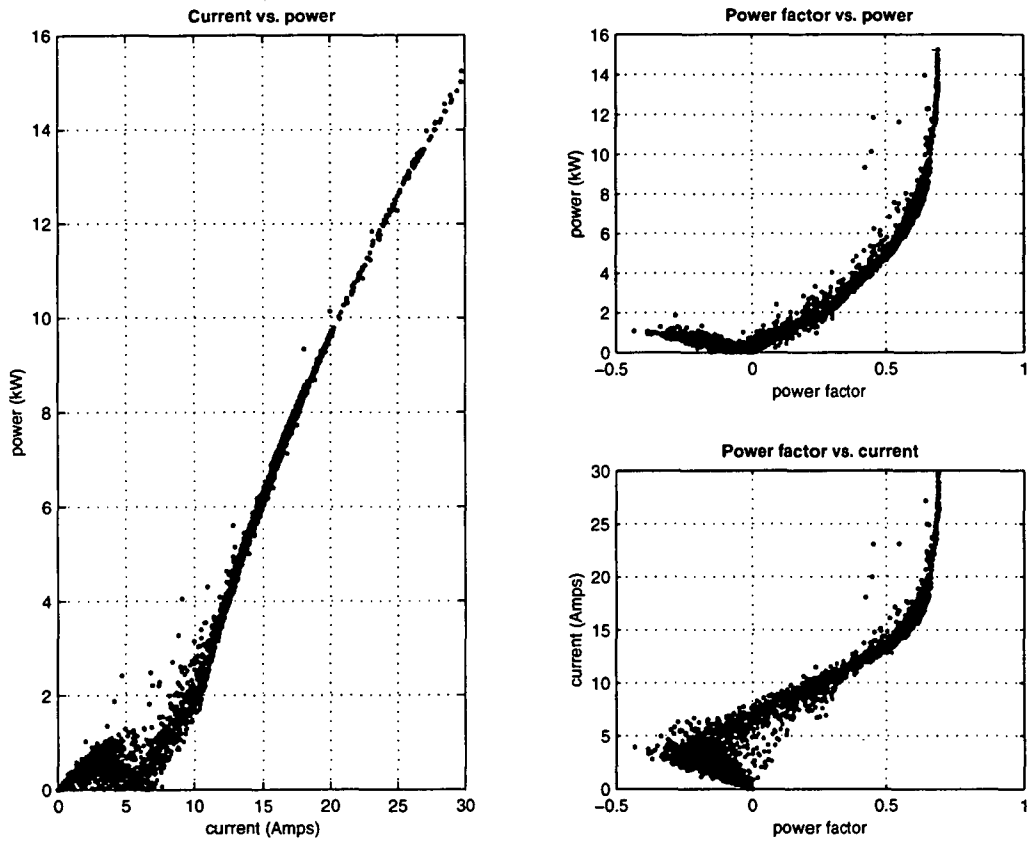

Figure 5.7: Power and current relationships with the power-factor for UM-70X at Casey

The Elcontrol unit summed total energy in KWh from both production and consumption. To gauge the total net energy produced by the wind turbine, energy measurements were averaged over a 10 minute time interval and then separated into consumption or production amounts, according to the sign of the average power factor over the interval.

Using this technique the ratio of energy consumption to production was calculated at 1:24, resulting in a net production total amounting to 92% of the total energy as recorded by the Elcontrol unit. This results in the consumption and production totals presented in Table 5.3:

UM-70X performance	Total Energy Recorded	Energy Consumed	Energy Produced	Net Energy Produced
Total energy	2699 kWh	107 kWh	2592 kWh	2485 kWh
Average daily energy	30.0 kWh	1.2 kWh	28.8 kWh	27.6 kWh
		Wind capacity factor	0.120	0.115

Table 5.3: Power production and consumption figures for the UM-70X (April 10 - July 9 1995).

The expected performance of the UM-70X over the period April 10 to July 9 can be determined using the methods outlined in Chapter 2, based on wind speed measurements and the power curve for the UM-70X. The frequency-of-occurrence of the wind speed over this period is given in Figure 5.8, constructed from 3-hourly BoM observations using a 1 m/s bin size.

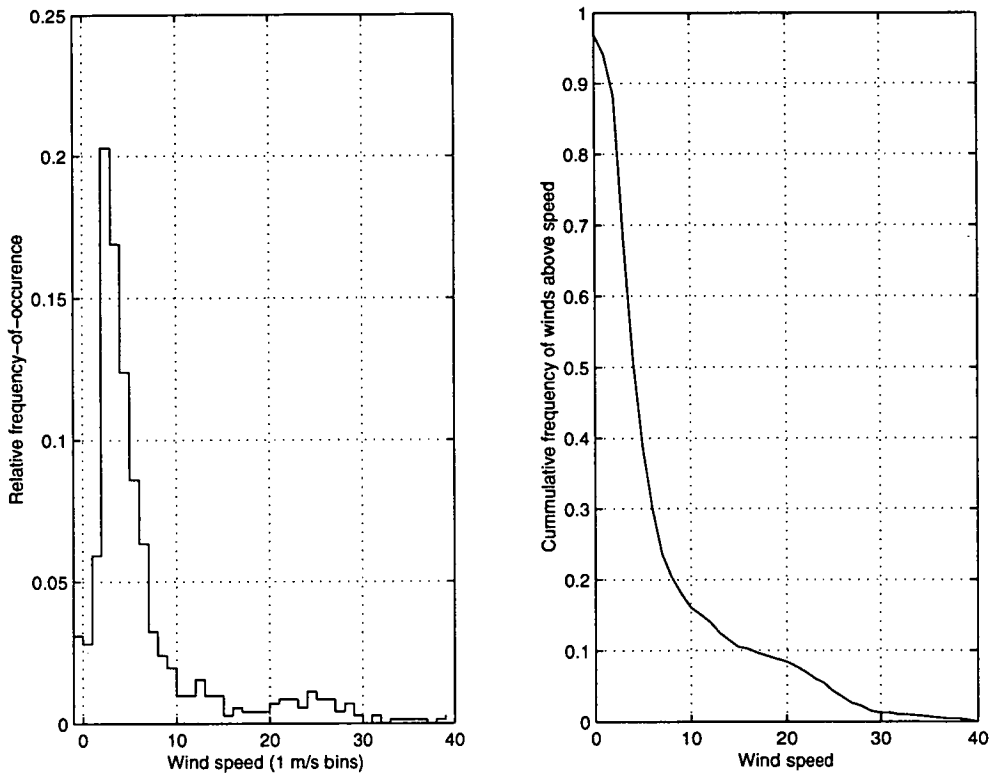

Figure 5.8: Wind speed frequency distribution for April 10 - July 9.

Meteorology over this period was typical for Casey. A maximum wind speed of 39.6 m/s was recorded on 24 June, while the mean and standard deviation were calculated at 6.47 m/s and 7.03 m/s respectively. The expected output power for the UM-70X from these winds is given in Table 5.4, together with the recorded total.

Performance indicator	Estimated	Actual
Power-hours	4,456 kWh	2,485 kWh
Load-factor	0.206	0.115

Table 5.4: Expected power production (calculated using wind speed frequency of occurrence and UM-70X power curve) vs, actual recorded power production.

Only 55.8% of the expected power was realised over this period, a rather disappointing result. Icing on the regulation bar of the pitch control mechanism combined with a perforated oil seal in the gearbox were identified as major contributing factors to this poor result after lowering and inspection of the unit in July 1995.

Strong winds, ideal for power generation, delayed re-erection until early September 1995, after which the unit continued to produced until its replacement in May 1996. A summary of the performance of the UM-70X and its replacement the GEV 7.10 is presented next.

5.3.5 Monthly generation totals March 1995 - June 1996

A summary of the performance of the Casey wind turbine from its erection in March 1995 through until June 1996 is presented in Figure 5.9. For down-time periods when the unit was not able to be connected to the grid due to problems, adjustments have been indicated for the capacity factor. This adjustments amount to restricting calculations of the capacity factor to operation periods when the unit was able to connect to the grid rather than to the entire month. The difference between this amount and the actual amount is highlighted in red in Figure 5.9. (Note: no attempt was made to incorporate different wind conditions between operational periods and down-time periods).

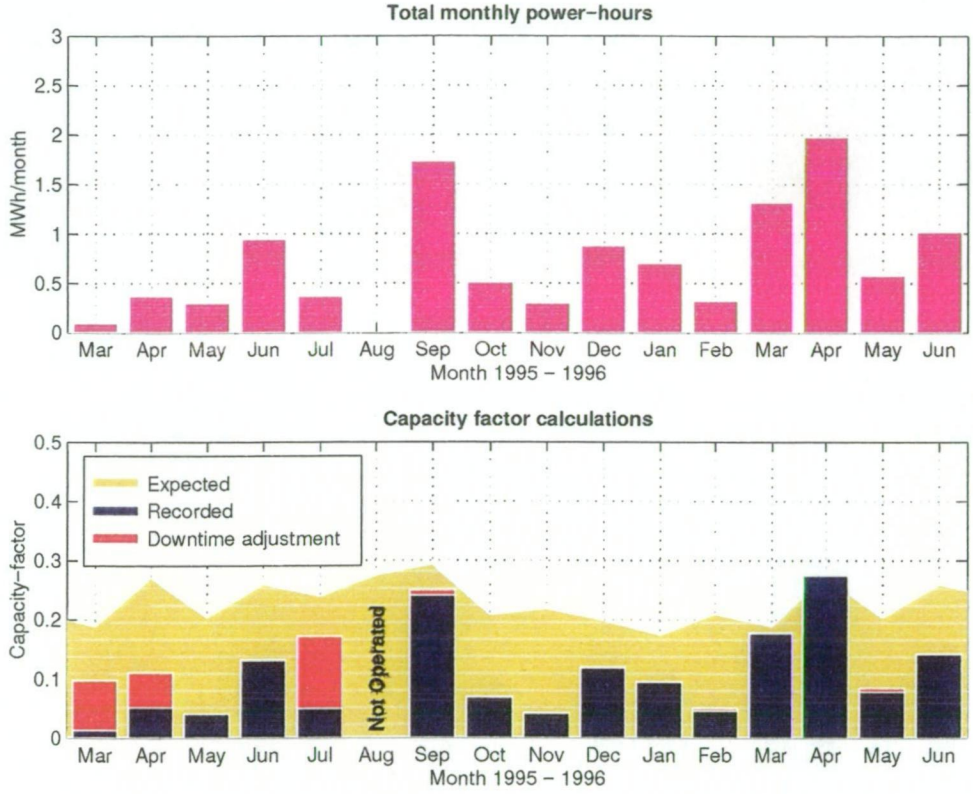

Figure 5.9: Wind turbine performance at Casey March 95 - June 96

Events over this period which required the turbine to be lowered involved:

March 1995 - Broken tail vane.
April 1995 - GEV 7.10 nacelle replacement with repaired Heard Island UM-70X nacelle.
July 1995 - Icing on the regulation bar of the pitch control mechanism and a perforated oil seal in the gearbox (inclement weather delayed re-erection until early September 1995).
February 1996 - Pitch control mechanism re-alignment (resulting in the much improved performance figures for March and April 1996).
May 1996 - Replacement of UM-70X with upgraded GEV 7.10.

Reports from the station have indicated that the GEV 7.10 performs much better than the UM-70X in high winds but the heftier design does not produce as well in light winds. This would account for the low energy totals reported for May and June 1996.

In total, 11.5 MWh had been produced by the unit up until the end of May 1996, far less than that expected from calculations in Chapter 2 (indicated in the lower plot of Figure 5.9 in yellow). The cause for these lower than expected levels has been traced to operational problems. These included:

1. Poor power factor;
2. Ice penetration into one of the inertia bars (fixed September 1995);
3. Gearbox oil leakage (fixed September 1995);
4. Periods of high currents during extreme winds tripping thermal isolators; and
5. High wind variability over a small time period.

The fourth of these operational problems was reported and logged by the station electricians. Unfortunately there was no system to automatically monitor or reset the thermal isolators. To ensure the isolators were connected a manual inspection was required, a task that was need to be conducted on a regular basis during periods of strong winds due to the location of the isolators at the base of the turbine tower. Station logs indicate that losses may have been as high as 50% during production periods due to this problem (i.e. number of inspections that resulted in resetting of isolators).

The effect of the fifth operational problem has yet to be quantified. This requires further observation and measurements of the effect of small period variations in wind speed at the site of the turbine. Preliminary results obtained from measurements initiated at Casey are presented in the next section.

5.4 Wind and solar resource validation programs

The establishment of an 'environmental monitoring network' was also completed as part of the field work program at Casey. This network is designed to validate and extend the knowledge of the wind and solar resources at the four stations.

5.4.1 Environmental monitoring network

To enable the wind speed profile to be determined, three wind monitors were positioned at different heights on a 30 metre VHF radio antenna. The antenna's position within the station confines proved an ideal site to mount monitors, although its proximity to a number of station buildings is of concern. The balloon shed, tank house and operations buildings are all within 30 metres. In the absence of other potential sites to mount the monitors, close to electrical power and communication channels, these objections were overlooked.

To enable solar radiation and PV efficiency levels to be determined, a small PV panel and pyranometer have been positioned on the roof of the operations building at Casey (a wood shield was placed under each instrument to absorb any reflected radiation off the roof). A resistor rated at 100Ω was used in the circuit to provide load to the PV panel.

Outputs from these instruments were then wired to a Datataker DT600 datalogger connected to a PC. This arrangement was envisaged to be operated remotely via the internet from Hobart without the need for on-site supervision. A schematic of this set-up is depicted in Figure 5.10.

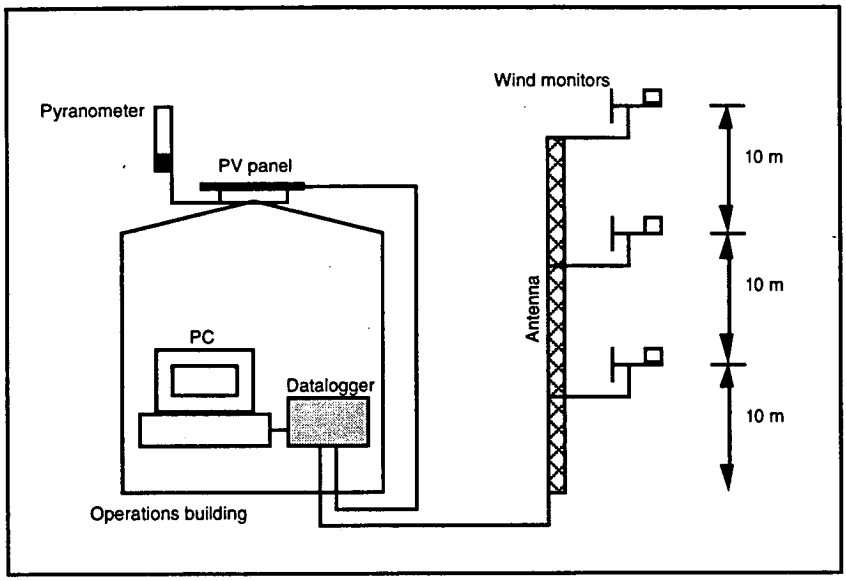

Figure 5.10: Environmental monitoring network schematic for Casey.

The make and model of the monitoring devices is listed in Table 5.5.

Monitoring device	Make	Model	Monitoring technique
Wind monitors	R.M.Youngs	05103	Calibrated current bridge
PV panel	Solarex	MX-5	Calibrated current divider
Pyranometer			Calibrated pulse counter

Table 5.5: Environmental monitoring devices.

The method of monitoring and resultant accuracy of the monitoring devices is listed below:

Wind monitor Flow through propeller was used to determine wind speed, with vane used to determine direction. 100 kΩ (+/-5%) resistors were used with current bridges to give calibrated speed and direction measurements. Accuracy for speed measurements (+/- 2 ms^{-1}), and direction measurements (+/- 5°)

PV panel 100Ω (+/- 5%) load resistor was paralleled with 10 kΩ (+/- 5%) and 1 kΩ (+/- 5%) resistors. Voltage drop across 1 kΩ resistor measured by datalogger. Estimated accuracy for power measurements (+/- 15%).

Pyranometer Pulse countered by datalogger. Accuracy for solar radiation measurements (+/- 5%).

Data using this system was collected at two rates: the first consisting of five minute averages of two second instantaneous measurements, while the second consisted of raw two second instantaneous measurements. The 5 minutes averages were recorded continually, while the 2 second instantaneous measurements were only recorded during periods of high winds. The internal memory of the DT600 allowed over a week or two of 5 minute data, but only a few hours of instantaneous data.

The final operation of the system was delayed due to problems with the establishment of communication protocol and destruction of the 10 metre wind monitor during a blizzard. When fully operational, this system will be used to record information over a number of years, allowing for greater definition of the wind and solar resources.

Analysis of some preliminary information collected while establishing the system, although not complete or comprehensive, does provide some interesting results.

5.4.2 Multi height wind monitoring

As indicated in Chapter 2, the power available from the wind increases with height through the boundary layer. To determine the size of any increases at Casey station, readings from three wind monitors of the environmental monitoring network were sampled over a 7 days interval, beginning 23 March 1995, to construct the profiles presented in Figure 5.11.

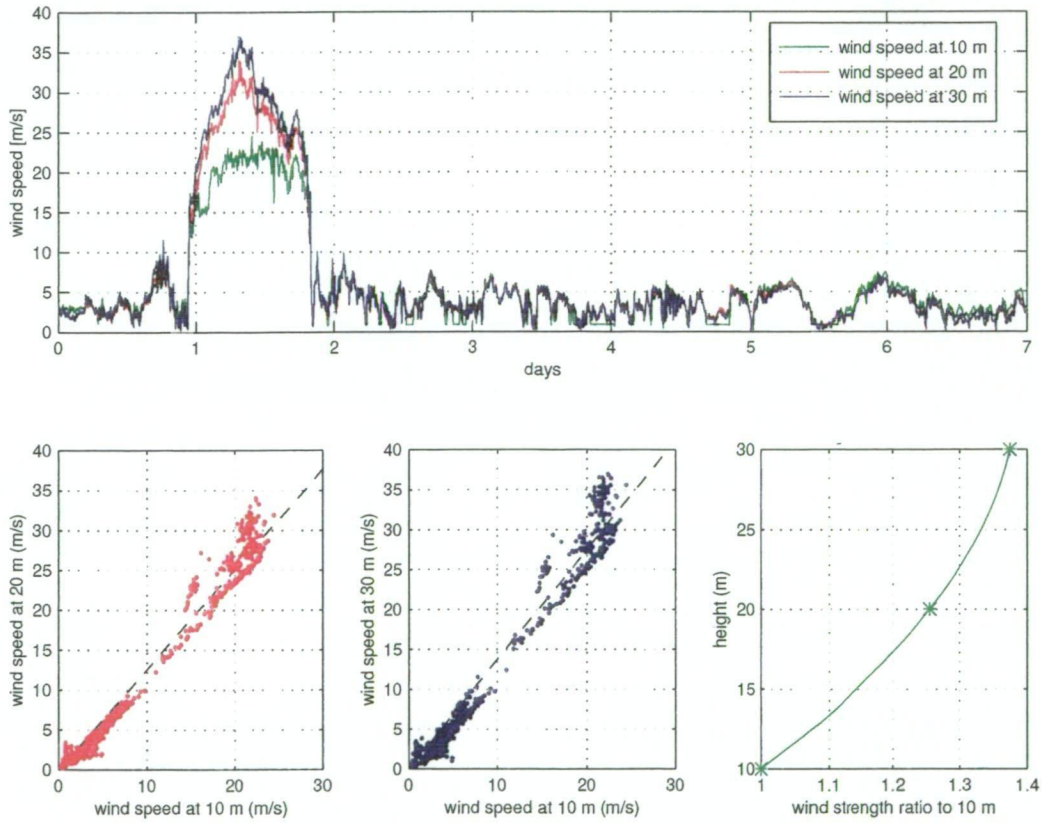

Figure 5.11: Wind increases with height recorded at Casey, March 1995

The magnitude of the increase in wind strength with height can be gauged from the comparisons of the winds at 10m, to those at 20m and 30m (presented in the bottom section of Figure 5.11). Large increases are evident for wind speeds at 20 m and 30 m, in the order of 25% to 37% respectively.

Unfortunately only a limited amount of data was recorded before the 10 m monitor was destroyed in a blizzard. Further work will be required to obtain more data to qualify these observations, which are based on very limited data.

5.4.3 Multi period wind monitoring

The variation of wind speed with height is of importance in determining the amount of wind available for generation, but so too is its variability with time. Highly variable winds could reduce performance and create large power fluctuations. Figure 5.12 indicates two second instantaneous measurements of the wind, with the five minute average superimposed, for a six hour observation period at Casey in November 1995. (Note: wind speeds under 25 m/s were not logged due to data storage limitations resulting in the data gaps in Figure 5.12).

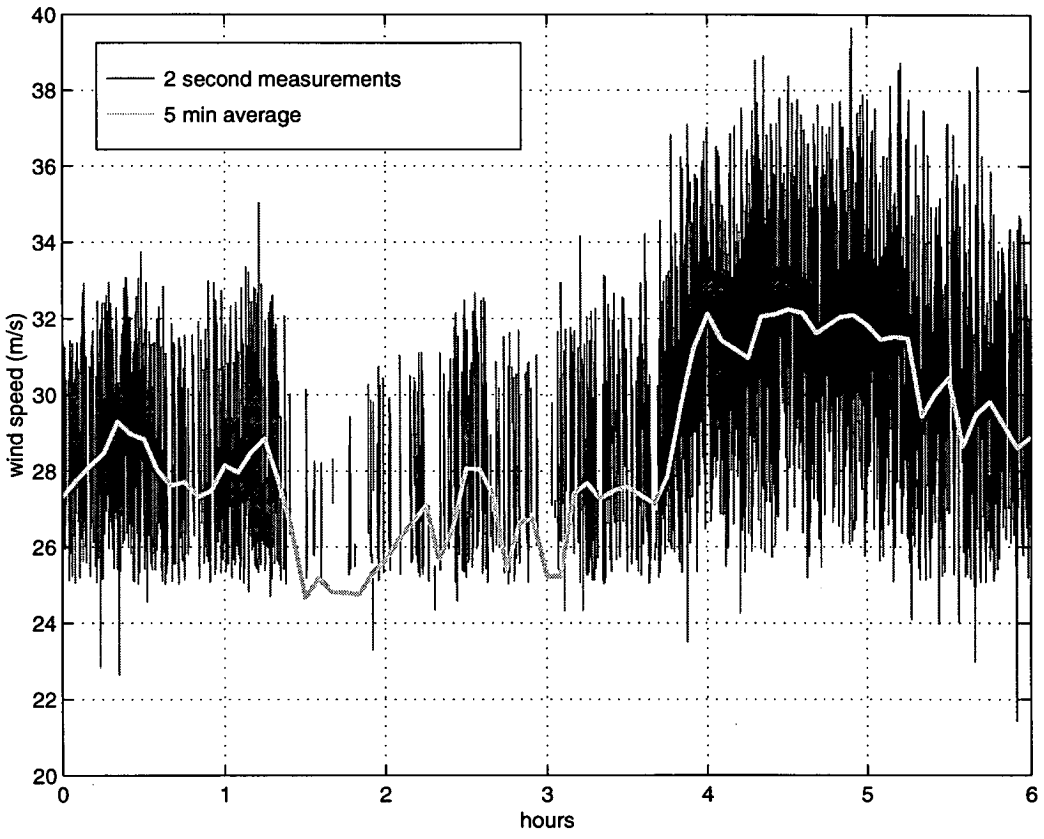

Figure 5.12: Wind variation measurements at Casey - November 1995

Fluctuations of up to +/- 5 ms^{-1} are present in the two second wind. These are quite high and are the most likely cause of the high variation recorded for the UM-70X. Wind turbines intended for use at the stations must employ methods to accommodate these variations.

The five minute average of the wind speed does offer hope. It can be seen that most of the variations are of a small period and able to be smoothed if integrated over a suitable period. For a large turbine rotating at high speed, there will be a natural level of damping from the mechanical inertia of the turbine, which might be able to reduce the effect of these variations. This will come at a cost, with the possibility of fatigue failure increased. Further investigations of the effect of these variations will be needed when more data at this sample rate is available over a longer period.

For the purpose of the wind speed resource determination in Chapter 2, BoM observational data has been used. These consisted of 10 minute averages taken every 3 hours immediately before the hour.

Comparison of the five minute, one hour and BoM standard wind speed measurements (taken at a site 20 metres to the south of the 5 minute and 1 hour averages), are indicated in Figure 5.13 for a 30 day series of observation recorded at Casey in March 1995. The two most significant wind events, in the lower part of the figure, give a clear indication of the difference between the five minute average, hourly average and BoM measurements.

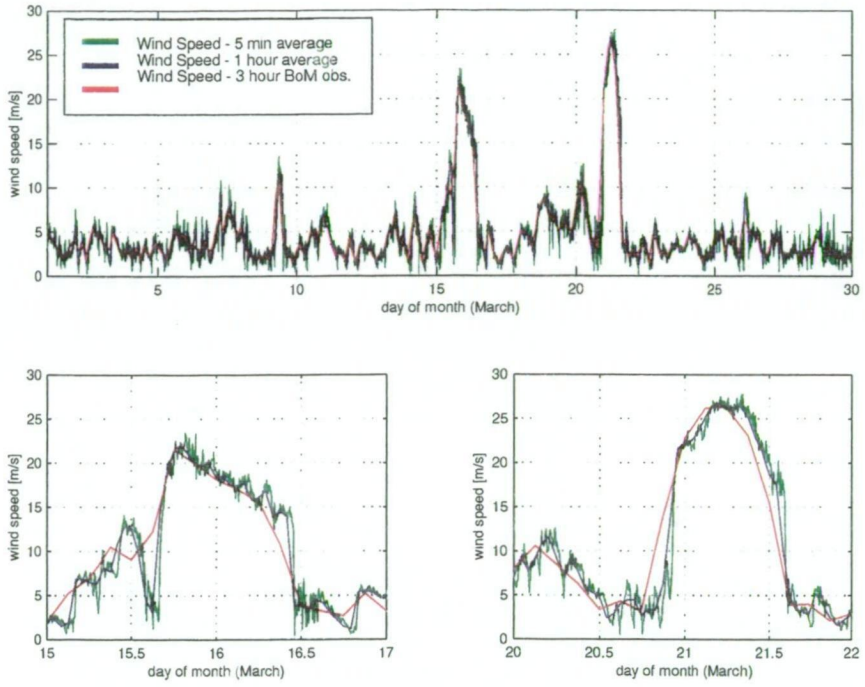

Figure 5.13: Wind averaged over different periods

The hourly average indicates the general trend of the 5 minute averaged data well, with most periods of strong winds captured. BoM observations however appear only to capture the large variations associated with synoptic changes in the wind speed as seen from the upper portion of Figure 5.13. The limited ability for the BoM measurements to give a representation of the five minute or hourly wind average is evident from the lower portion of Figure 5.13 where days 15 to 17 and 20 to 22 have been enlarged.

There are limitations in using BoM observations measurements to evaluate the wind resources of the stations, but in the absence of more data on either a five minute or one hour time basis, all calculations have been based on BoM observations. Collection of more data at each station in the future will allow confirmation of these estimates.

5.4.4 Solar energy measurements at Casey

Measurements of the solar radiation taken at Casey using a pyranometer are given in Figure 5.14 for a sample week beginning 23 March 1995. Estimates for the solar radiation total calculated for a horizontal surface using cloud cover observations and the model presented in Chapter 3, are also indicated in this figure, together with the output from a small 5 W PV panel.

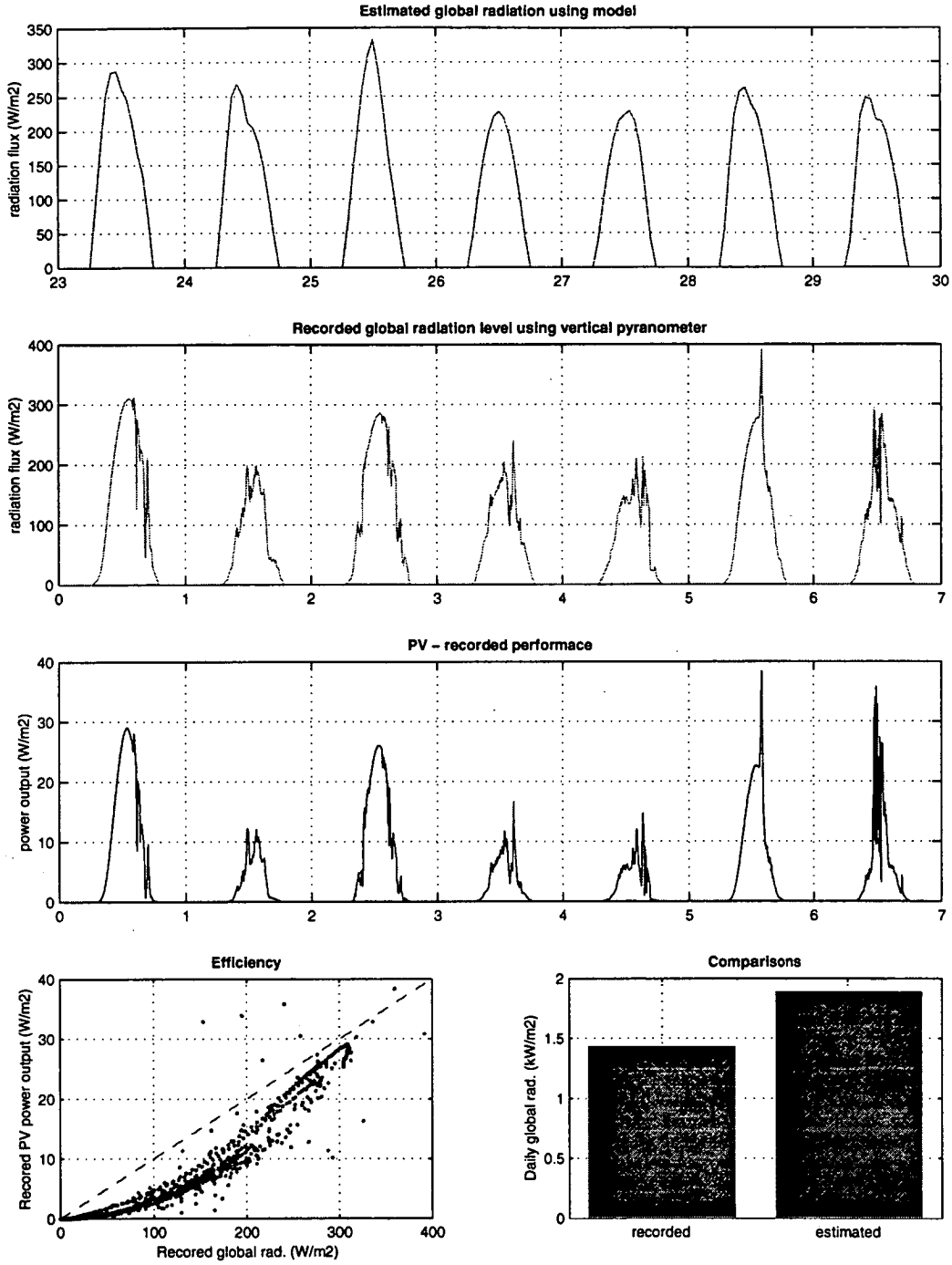

Figure 5.14: Solar energy at Casey, March 1995

Agreement during this time of year is not the best, with global radiation totals overestimated by 20%, indicating limitations to the accuracy of the estimated solar energy reserves in Chapter 3. More readings over a full year will allow direct use of observations in the future. Until these have been obtained, estimates generated in Chapter 3 have been used in all calculations to evaluate solar energy resources.

The performance of the PV panel is presented in the lower left hand corner of Figure 5.13 (with the 10% efficiency level indicated by the broken line). Load on the PV panel was provided for by a 100 Ω resistor under temperatures ranging from zero to -15°C. The performance is quite promising for a commercial cell, especially as the output levels were recorded in less then optimal conditions away from the maximum power point (100 Ω load reduced performance by 30% from power obtainable at maximum power point).

5.5 Electrical energy use breakdowns for Casey

Electrical energy use at the Antarctic stations has the potential to be reduced using load management techniques outlined in Chapter 1. Wasteful and low efficient plant need to be identified and eliminated (or at least minimised), while peak load times could be reduced through the rescheduling of non-essential and intermittent loads.

Such practices are essential if renewable energy systems are to achieve the greatest impact on fuel savings. By reducing loads in general or by shifting loads to times of power production from renewable energy systems, the need for large back-up systems or energy storage systems can be minimised. A breakdown of the stations electrical use is necessary before this will be possible. A detailed and comprehensive energy audit would be the best method to achieve a complete breakdown. In the absence of this, measurements of the load for different buildings have been obtained for Casey allowing for the identification of areas which should be further investigated.

5.5.1 Building diurnal load patterns

Information presented in this section has been obtained from a survey conducted by the wintering station personnel at Casey during 1995. The survey involved the recording of generator loads in the MPH (to determine overall station electrical production levels) and the load from different station buildings around Casey Station. Three monitors were used to obtain the readings: an Elcontrol unit fixed in the MPH, a portable Elcontrol unit connected to a laptop PC and a portable VIP 20 power metering unit (each giving readings to an accuracy of +/- 1 kW). All recordings consist of 4 second averaged measurements taken every ten minutes.

In total, eleven buildings were sampled for approximately eight days each over a four month period. A list of buildings and observation periods are given in Table 5.6. Notable omissions from this list include internal MPH & EPH loads, the workshop and radio transmitter hut loads.

Building		Observation period start	end
Green store		10/7/95	25/7/95
Emergency vehicle shed (EVS)		25/7/95	4/8/95
ANARESAT building		7/8/96	18/8/95
Field store		21/8/96	29/8/95
Domestic Building	- feeder 1	11/9/95	21/9/95
	- feeder 2	13/9/95	24/9/95
Science Building	- feeder 1	21/10/95	30/10/95
	- feeder 2	21/10/95	31/10/95
Waste treatment building		1/11/95	10/11/95
Operations building		10/11/95	18/11/95
Balloon shed		10/11/95	17/11/95
Tank House		18/11/95	25/11/95
Caravans		18/11/95	27/11/95

Table 5.6: Casey energy audit building observation periods

The power readings obtained during the energy survey are presented in Figures 5.15 to 5.17. The diurnal load pattern for each building have been calculated from these readings by averaging readings taken at the same time over the observation period. The standard deviation of the measurements for given time period are also indicated giving an indication of the spread of readings about these calculated means.

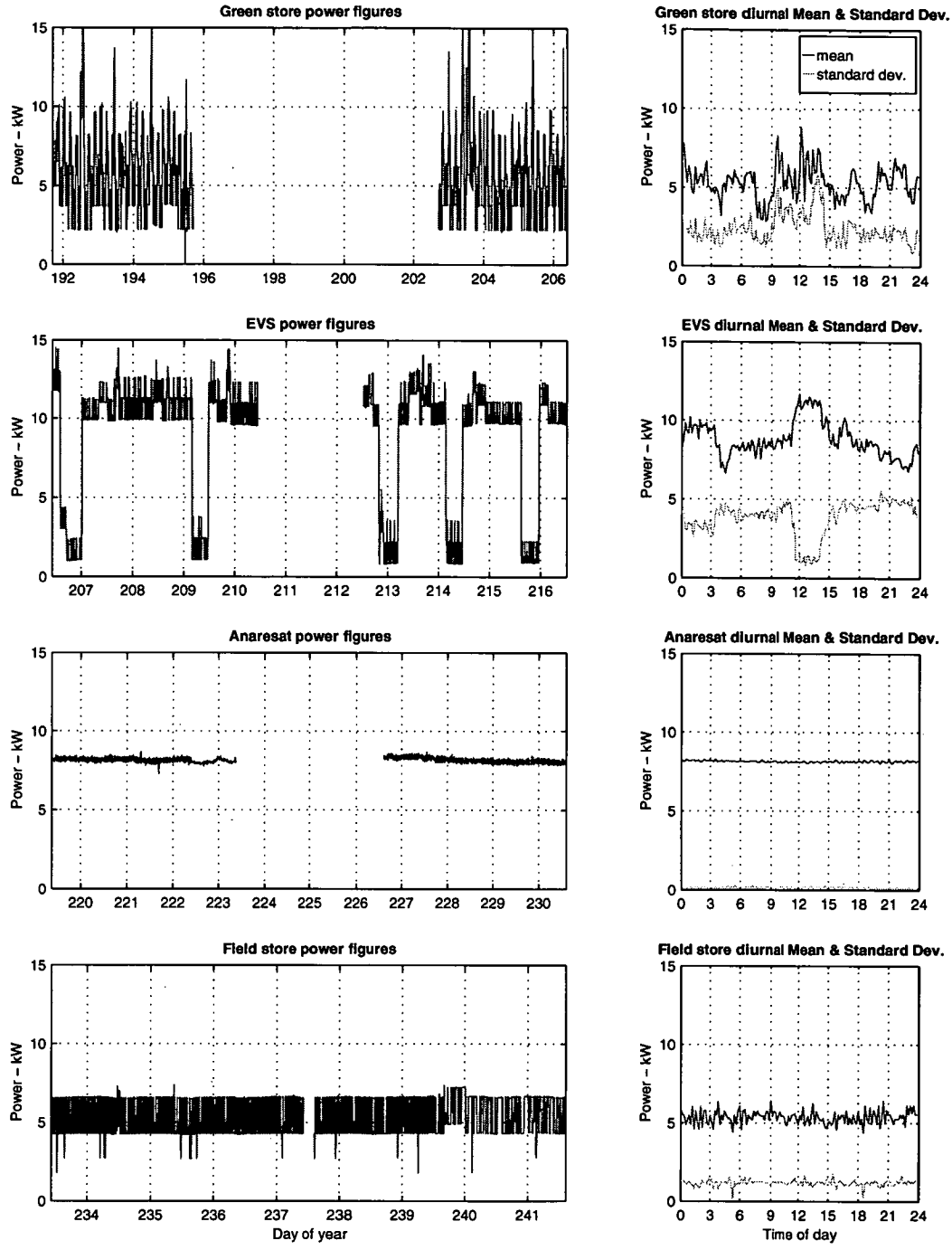

Figure 5.15: Power levels recorded for the Green store, EVS, ANARESAT and Field store, Casey 1995

The green store exhibits a trend for higher energy use during the day, most likely due to lighting, charging fork-lift batteries and loads from the moveable shelving during working hours. Other contributing loads from freezers and dry store heaters, dependent on outside temperature and wind speed, result in the extremely variable load profile over the 8 day interval.

Each of the three other buildings display extremely regular load structures. The EVS indicates a dominant two level power structure, with a small variable load superimposed. Loads in the ANARESAT are extremely constant, resultant from electronic equipment. The Field store exhibits a highly cyclic load profile, most likely due to thermostatically controlled heating.

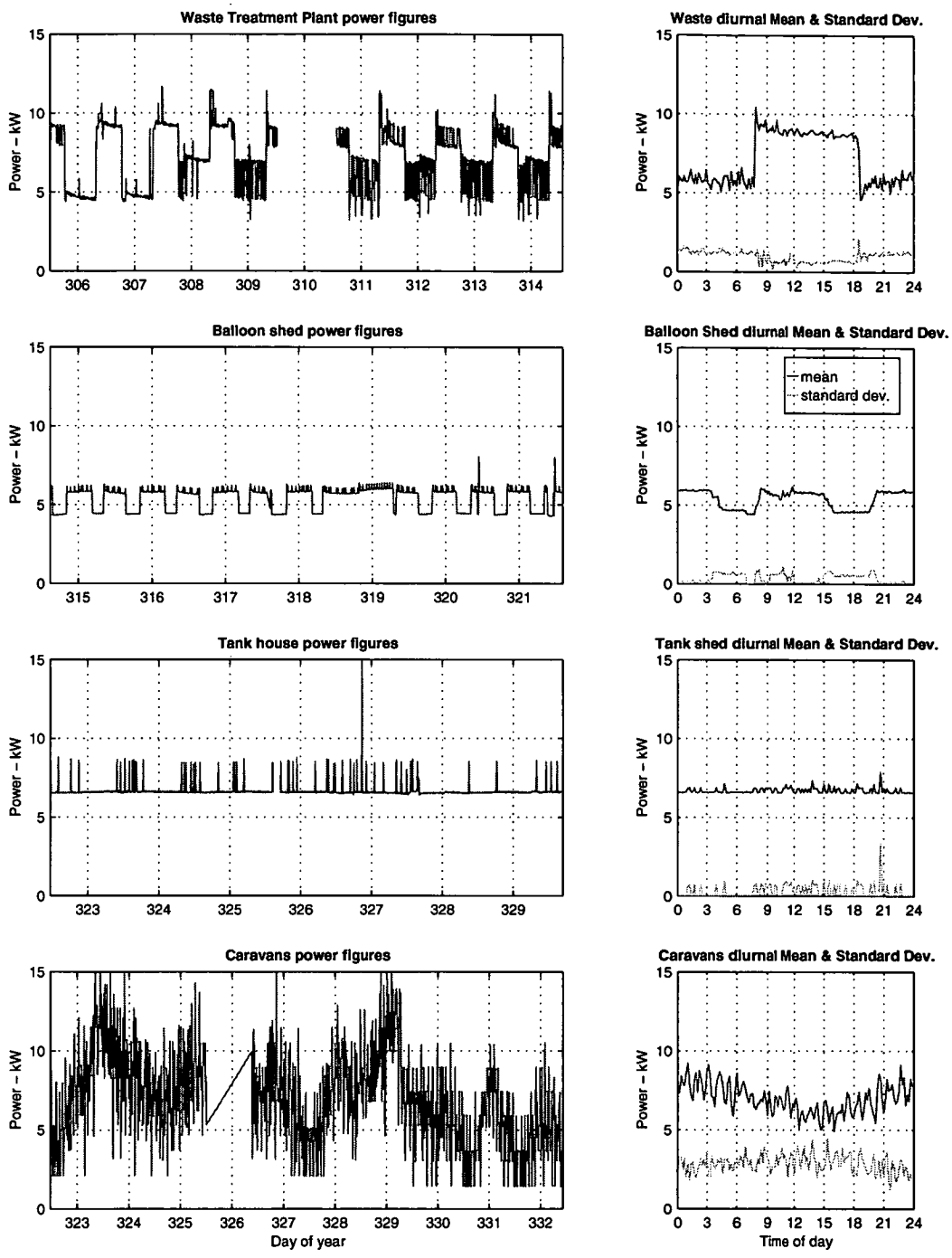

Figure 5.16: Power levels recorded for the Waste shed, Balloon shed, Tank house and Caravans, Casey 1995

Similar regular loads from automatically controlled plant are also evident for the waste treatment house, balloon shed and tank house. Load peaks in the waste treatment house follow pumping and lighting times. Loads from the Balloon shed are highly regular, with the main usage of power coming from an electrolyser unit used to produce hydrogen.

Loading from the caravans is quite variable. The dominant source for loading is from heating and lighting, increasing during the night when occupancy rates are at their highest and outside temperatures are at their lowest.

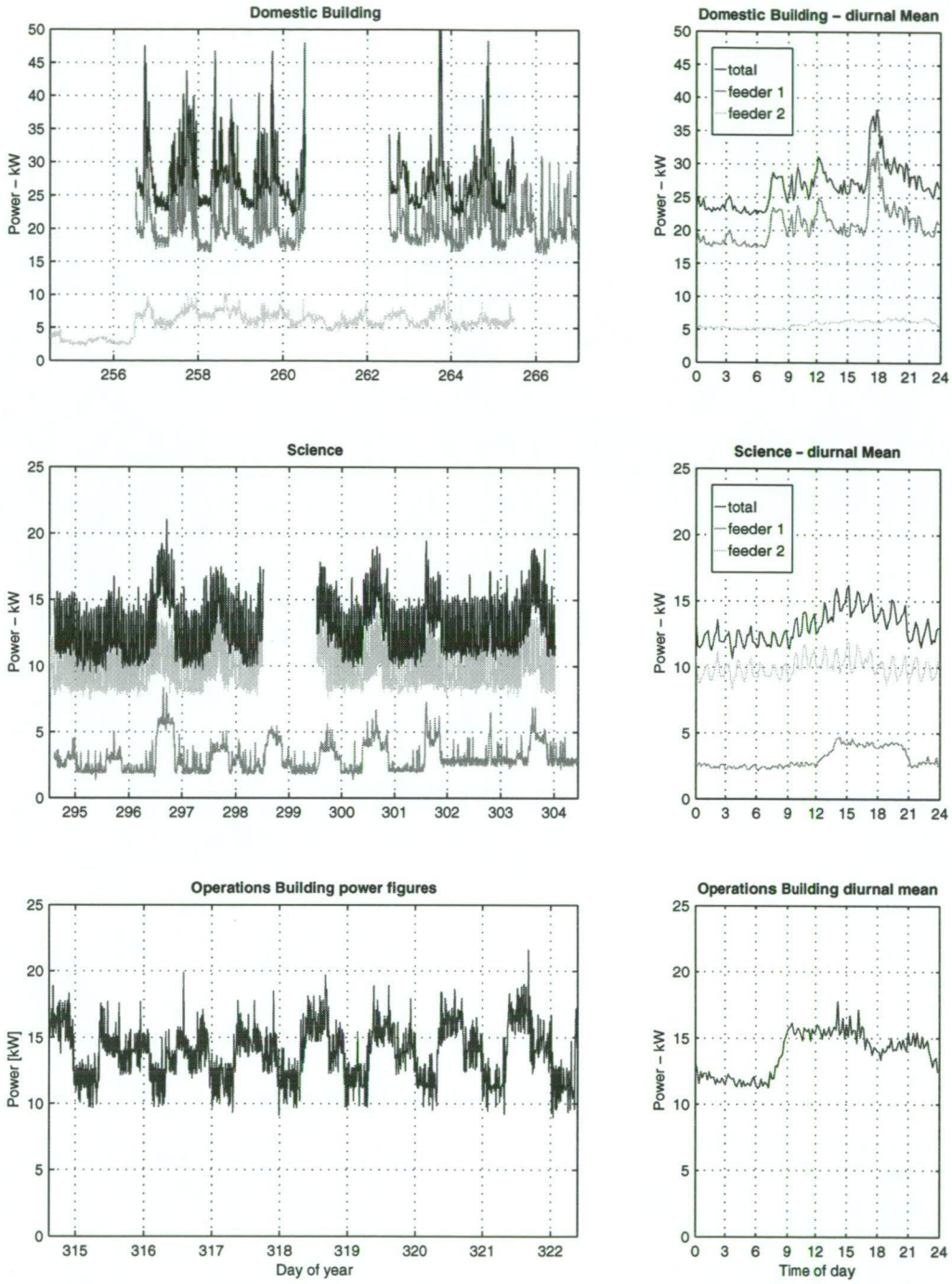

Figure 5.17: Power levels recorded for the Domestic building, Science and Operations, Casey 1995

Loads from the domestic, science and operations buildings are the highest on station. They are also the most variable and the most dependent on work patterns. Clear day maximums are evident in each building, although large base loads are also present. Maximum loads occur in the domestic building around meal preparation and eating times, especially in the evening. The average load increases by 50% over the course of an hour during this period, just before 6pm. Strong periodic loading is evident from the science building, dependent most likely from the cyclic loading of freezers. The short term variations evident in each of these buildings is a characteristic of the work habits of people, with loads often being switched in and out from the use of electronic equipment, including computers and fridges.

Measurements of the total station load were also taken in MPH over the period of the energy survey. Diurnal loading over this period was similar, with a slight trend for decrease coming into the summer. This decrease was small, allowing a cumulative total of the diurnal load profiles of the buildings to be constructed and compared to the average diurnal power output from the MPH. This total is represented in Figure 5.18.

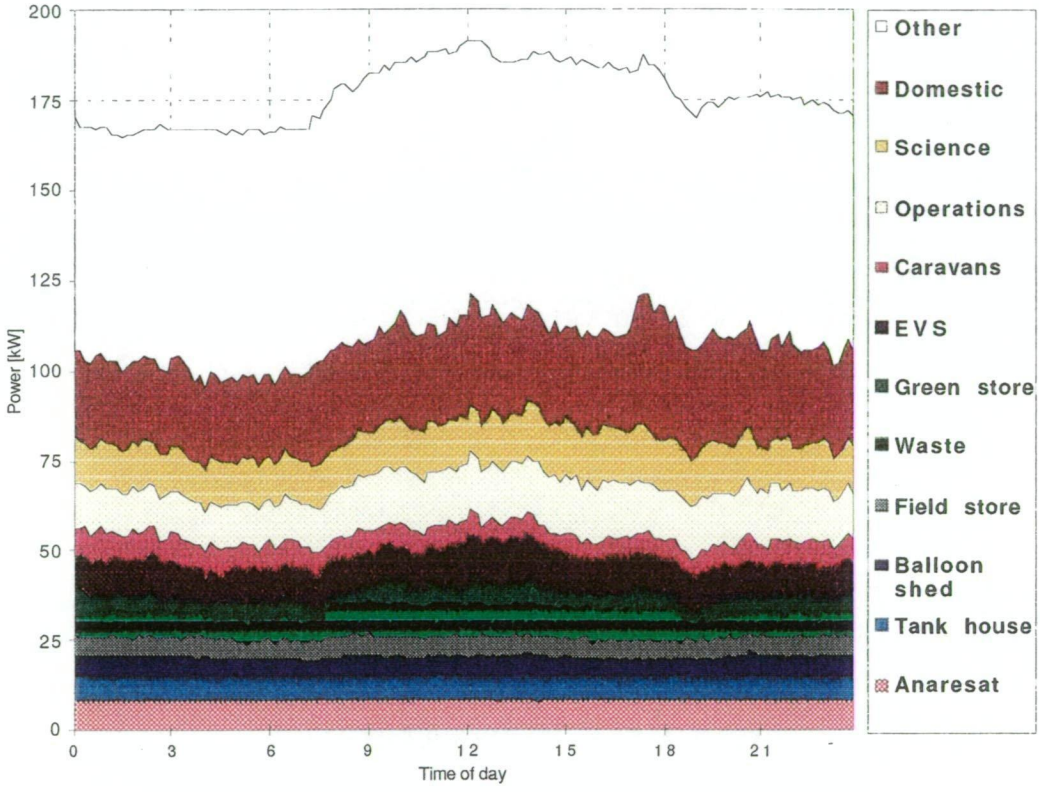

Figure 5.18: Average diurnal load breakdowns for known buildings (cumulative).

Most of the structure is already present from the combined profiles of the sampled buildings. The remaining difference is assumed to be the combination of the internal power-house loads together with the workshop, transmitter loads and any losses from the distribution system although exact agreement is not expected from the averaging technique employed and short sample duration.

5.5.2 Building energy consumption levels

It is apparent from these readings that station buildings loads fall into two groups: those for which regular and periodic loads dominate, and those for which non-regular loads dominate. Furthermore, the buildings identified as having high occupancy rates, tend to exhibit the latter of these load patterns.

A summary of the diurnal load pattern, occupancy rate, and main use of each building is presented in Table 5.7. Building identified as having low occupancy rates tend to exhibit regular load patterns due to the dominate source of load coming from automatic plant and electronic equipment.

Building	Diurnal load patterns		
	loading pattern	occupancy rate	dominant use
Green store	non-regular	medium	food and supply store
EVS	regular	low	emergency vehicle shed/ gym
ANARESAT	regular	low	telecommunications
Field store	regular	low	field equipment store
Domestic	non-regular	high	living/eating/medical/ sleeping/entertainment/
Science	non-regular	high	scientific laboratories/ electronic workshops
Waste	regular	low	sewage treatment plant
Operations	non-regular	high	BoM station/ station management/ electronic laboratory
Balloon shed	regular	low	hydrogen generation plant/ balloon release platform
Tank House	regular	low	water storage
Caravans	non-regular	medium	sleeping

Table 5.7: Diurnal load patterns in Casey station building

Energy consumption levels are presented as a percentage of the total station load in Figure 5.19, calculated by integrating the average 10 minute load of each building and comparing to the station total over the same period.

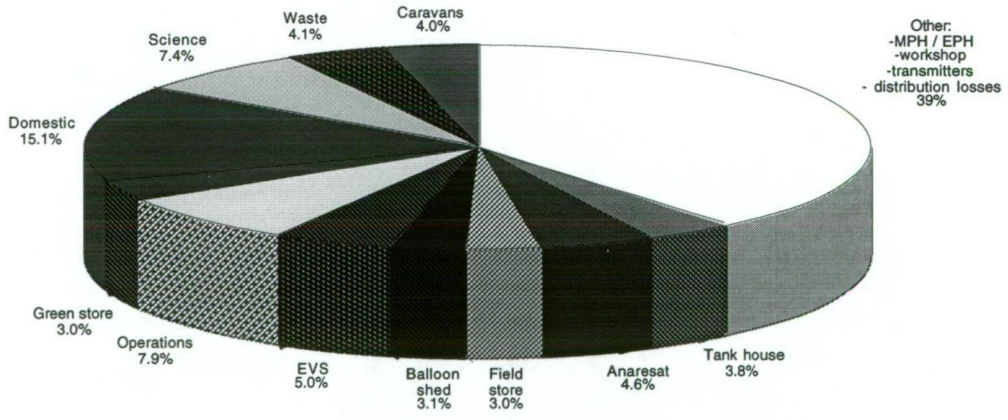

Figure 5.19: Average building energy use expressed as a percentage of average station energy use (Average daily station energy use during sample period equal to 4,487 kWh)

Of concern is the percentage of 'other loads', attributed to workshop loads, radio transmitter loads, distribution losses and internal MPH and EPH loads. Internal loads from within the MPH are the greatest of these unaccounted loads, estimated to average 40 kW by the station electricians. This represents over 21% of the entire station load, well over half of the unaccounted loads. These loads result from control equipment, lighting, charging of the starter batteries of the diesel generator sets, heat distribution system pumps and air circulation system pumps. Minimisation of the these loads has limited potential as all are associated with. essential services.

The average daily energy use for each building is presented in Figure 5.20. This profile has been calculated using an average daily energy usage of 4,487 kWh (based on an average load of 187 kW over the sample period) in-conjuction with the percentages given in Figure 5.19. Of the buildings sampled, energy usage by the domestic building is the largest. At over 600 kWh per day consumption is almost double both that for the operations and science buildings, the next highest energy consumers.

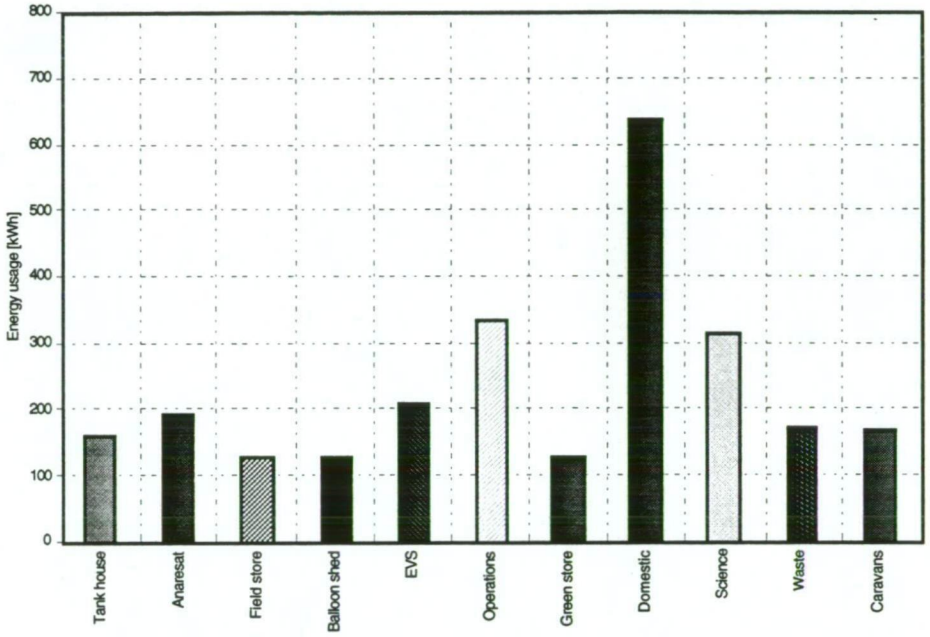

Figure 5.20: Average daily energy consumption levels for observed buildings at Casey

It is interesting to note that these three buildings; the domestic, operations and science buildings, (together with the workshop for which loads were not obtained), have some of the highest occupancy rates on station. From this figure and other given in this section, the load at the stations can be divided into three areas:

1. Internal powerhouse loads and distribution losses.
2. Automatic plant loads.
3. People dependent loads.

Reducing base loads and shifting station loads to periods of high wind and/or or solar radiation exposure would allow for better fuel savings from a renewable energy generation system. To achieve this the potential for reducing loads and shifting loads could be sort in each of these areas identified above.

For internal powerhouse loads and distribution losses, the scope for reducing loads is heavily dependent on the current engineering practices and equipment installed at the stations. As mentioned in Chapter 4, as old plant is replaced, new more efficient plant is actively being phased in. Automatic plant loads have potential for shifting, especially if operation times are not critical, but only for non-essential and interruptable loads.

People dependent loads are heavily dependent on human factors, resulting in extra loads during activity periods during the day. Shifting load peaks to high renewable energy production periods could be achieved by encouraging station personnel to save energy and use flexible work schedules. While this is possible in theory, it would require extensive planning and above all enthusiasm from all involved. Given the autonomous nature of most projects, compounded by tight schedules, this may not be practical and would tend to vary quite significantly from season to season.

5.6 Summary

Field work conducted at Casey involved the installation of a UM-70X wind-turbine, the establishment of an environmental monitoring network and the recording of building load patterns.

Performance of the UM-70X at both Heard Island and Casey has been promising, although power produced from the unit was below expectations at both sites. Limited storage potential was identified as a cause for lower than expected energy production totals at Heard Island where, during windy periods, the UM-70X produced more energy than could be used. At Casey, where storage was not an issue as power was fed directly into the grid, other problems were identified as contributing to the reduced performance levels. These include:

- poor power factor;
- ice penetration;
- gear box oil seals; and
- high currents in strong winds.

Short period fluctuations were observed in the power output of the UM-70X. This is a cause for concern, if a significant proportion of the station energy needs are to be supplied by wind turbines, necessitating some form of power regulation method. Data obtained from the environmental monitoring network indicated that small period wind speed variations, the most likely cause of the power fluctuations, are quite significant at Casey.

Data from the environmental network also allowed comparison to be made between BoM wind speed measurements (consisting of 10 minute averages taken every 3 hours), and five minute and one hour averages of the wind. Indications are that the BoM wind speed measurements capture the larger fluctuations but differ significantly with 5 minute averages and fluctuations that will occur during a storm period.

Solar radiation measurements obtained from the environmental network over a 7 day sample week in March were significantly lower than estimates from the solar radiation model described in Chapter 3. However, agreement was to within 80%, offering same positive implication for use of model estimates to predict solar generation periods.

Recording of building load patterns at Casey has allowed a more detailed understanding of station load causes to be developed. Two types of loads were identified: regular and periodic loads in low occupancy buildings, and non-regular highly variable loads in high use building. Automatic plant and electronic equipment were identified as the cause for regular loads, while climate and work pattern induced loads account for the non-regular loads. These breakdowns are similar to those identified for the station load model used in Chapter 4 to generate load sequences.

Chapter 6

Modelling

6.1 Introduction

The potential for large fuel savings using renewable energy systems is in part dependent on the match between consumption periods and renewable energy production periods. High renewable energy reserves are only useful if the power that can be extracted from them is useable. By sizing the renewable plant correctly, the match between production and consumption can be optimised, maximising returns for a given investment. To enable the optimal sizing for wind and solar energy to be determined, simulation models have been developed.

6.2 Renewable Energy Systems

The incorporation of a renewable energy generation component into diesel generation systems results in a hybrid system. Small scale hybrid systems, involving wind and/or a solar generation plant in conjunction with diesel generators, have been established in many places around the world. These systems, referred to as RAPS (Remote Area Power Systems) or village power systems, are usually of the order of 10 kW to 1 MW. A description of the set-up of some of these systems, potentially suitable for use at the stations, is provided in this section.

6.2.1 Low penetration systems

In the simplest arrangement, power from wind or solar plant is used to displace diesel fuel that would have been used by diesel generator sets. In these systems the diesel generator is kept operational at all times, with periods of low wind adequately covered. When high winds are present, the wind turbine is synchronised onto the grid in parallel with the diesel generator. Use of an induction generator directly connected to the AC power network as indicated in Figure 6.1 below allows for a very simple arrangement.

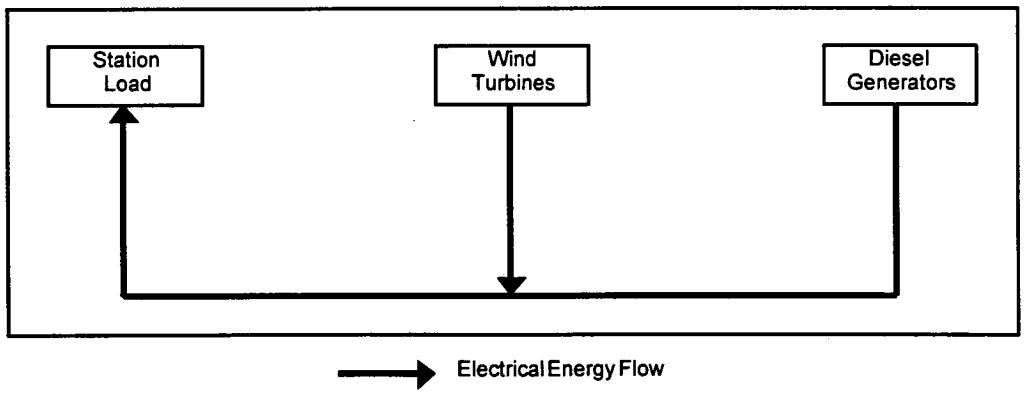

Figure 6.1: Hybrid energy system: Wind / diesel

In hybrid systems the penetration level is defined as the fraction of the total load generated by renewable plant. A renewable energy system with high penetration levels the most often will result in the best fuel savings.

The use of variable speed DC wind turbines and PV arrays together with DC to AC invertors as indicated in Figure 6.2 is one method to increase the renewable penetration level and provide alternate periods for production. Provision for a load dump, allowing power to be diverted from the system, may be required if oversupply is an issue.

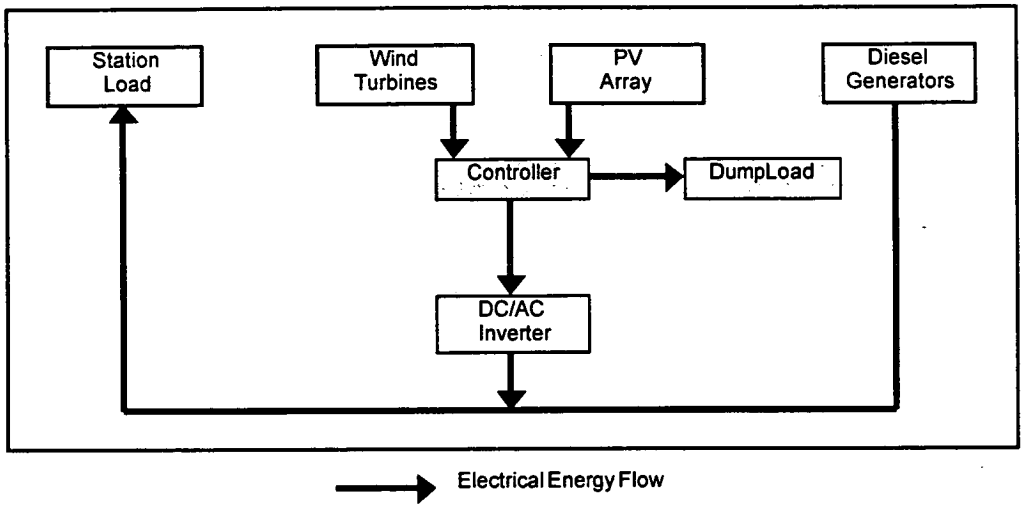

Figure 6.2: Hybrid energy system: Wind / solar/ diesel with dump load.

Control and operation of these systems is not straight forward. A number of complex and expensive problems exist, potentially compromising any financial savings brought about through reduced fuel use. Issues of concern include:

1. **Frequent diesel cycling:** The fluctuating nature of power output from renewable power plant (particularly wind turbines), combined with variable consumer load, can result in an unacceptably high levels of diesel start/stop cycles with correspondingly short run periods. This can lead to regular cold starting of diesel plant, over use of the starting battery, and increased wear, all reducing the operational life time of the diesel engine;

2. **Diesel under-loading:** In systems where diesels are used to meet any load deficits, unfavourable load conditions can result in prolonged periods of low-loading. Operation of diesel plant at less than 30-50% of their rated power is not recommended as it gives rise to increased wear and maintenance and leads to inefficient running;

3. **Low utilisation of renewable plant:** In poorly designed systems, where production periods do not correspond with demand periods, large quantities of renewable energy will be dumped;

4. **Poor quality of supply:** Short-term variations in output from renewable power plant (particularly wind turbines) can result in large voltage and frequency excursions [Bass, 1987].

If a limit is imposed on the amount of renewable power production, these problems can be minimised. Low penetration systems avoid diesel under-loading and allow adequate power regulation to be maintained by the governor systems of any remaining diesel plant on-line. Penetration levels of up to 56% have been reported as possible without significant problems [Malatestas, 1987]. Power utility companies such as Tasmania's Hydro Electric Commission (HEC) in the King Island wind farm project, tend to be more conservative, employing a 40% penetration limit [Caney, 1995].

A heating dump load could be used to maintain a 40% penetration level limit, an approach that has been considered for the Australian stations in the next section.

6.2.2 High penetration systems

While low penetration systems are effective, the size of fuel savings possible are limited. Greater fuel savings can be obtained from high penetration systems. High renewable penetration systems require advanced control systems in order to maintain continuous supply at a reasonable quality. A compromise between fuel savings and protection of plant from undue wear and tear is necessary in these systems to enable the overall costs to be minimised [Infield, 1992].

Resistive dump loads (or if possible switchable non-essential loads) have been used in some cases to provide frequency regulation and protection of oversupply. This can alleviate some problems arising in high renewable penetration systems, although low loading and inefficient fuel use are still of issue. Moreover, with fuel consumption in a diesel generator under zero load estimated to represent 10-15% of that when under full load, significant advantages could be achieved if the entire diesel plant could be disengaged [Cramer, 1989]. Intermittent diesel usage is not straight forward, with supply continuity and high diesel cycling of concern. Experience gained from a number of operational systems indicates that attempting to turn off the diesel in a manner which preserves continuity of supply, is problematic for systems without some form of short term energy storage [Infield, 1990a].

Examination of the spectral composition of the wind speed indicates that fluctuations can be separated into two groups: turbulence in the order of seconds to minutes, and synoptic variations in the order of hour to days [Infield, 1990a]. This indicates storage should be separated into two categories: short term storage for control regulation, and long term storage for increased production and consumption matching. Short term energy storage need only be sized on a time scale in the order of minutes, allowing adequate power stabilisation and sufficient time for backup systems to be brought on line.

Several different storage methods have been suggested including batteries, hydraulic accumulators, and flywheels [Linders, 1989]. A possible configuration, consisting of storage in the form of a floating battery system is indicated Figure 6.3. Power electronics could be used in this system to regulate the voltage and frequency of the network through control of a line commutated inverter, with arrangements for a resistive dump load to prevent overcharging of the battery system.

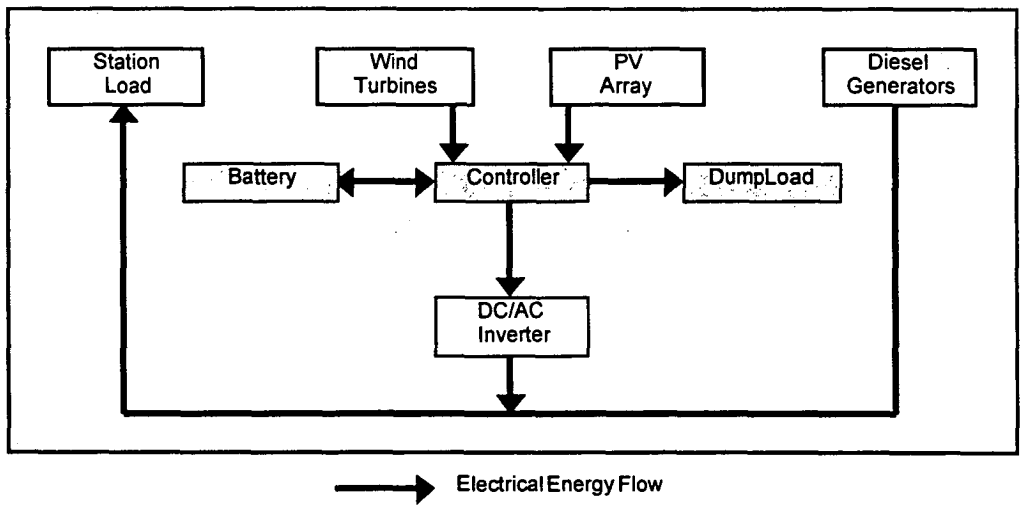

Figure 6.3: Hybrid energy system: Wind / solar/ diesel with battery storage

Whether in combination with mechanical clutches, flywheels or stand-alone, battery storage is expensive, limiting the size of economical systems. This is because:

- systems must be sized to handle the maximum expected charge rate;
- power electronics are necessary to enable proper power control and prevent overcharging; and
- frequent cycling will reduce the operational life time of batteries.

6.2.3 Over sized systems with mass storage

Advanced fully renewable systems, eliminating the need for diesel supplementation, are only possible with the addition of mass storage. The size of this storage must be of the order of hours to days to compensate for long term diurnal and synoptic fluctuations.

A concept that has been proposed as a possible storage system is a hydrogen loop [Linders, 1989; Dienhart, 1994]. In these systems, hydrogen is generated by electrolysis using excess electricity generated from oversized renewable plant. The hydrogen is then stored in pressurised storage tanks until needed, at which point fuel cells are used to generate electrical and thermal power. A system comprising hydrogen storage is represented in Figure 6.4, as outlined for the Antarctic stations by Guichard (1994):

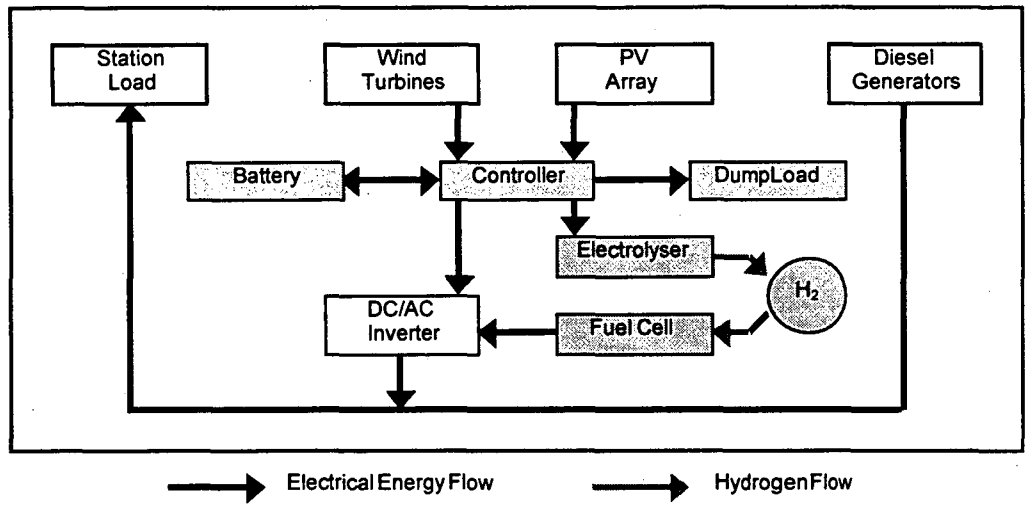

Figure 6.4: Hybrid energy system: Wind / solar / diesel with battery and hydrogen storage

The concept of hydrogen storage, although proposed in many reports since the 1970s, does not yet exist in commercial operation. With closed loop efficiencies of between 25% to 42% reported for experimental systems, their cost effectiveness has yet to be established [Kauranen, 1994].

6.3 Simulation models

The sizing of components in any renewable energy system will be a function of the load, the renewable energy resources available at a site, and the matching of their serial structure. The high base loads of the stations are potentially well suited for simple diesel displacement systems, while low correlation of station load with wind speed indicate that high penetration systems could be problematic. To investigate these possibilities, simulation models have been constructed.

6.3.1 Hybrid energy system outlines

An excellent summary of current wind/diesel system modelling in Europe can be found in the paper 'Wind/Diesel system modelling and design' [Infield, 1990b]. Models described in this paper are directed towards the fulfilment of two goals: the first is to estimate the overall performance of a hybrid energy system in terms of fuel savings and diesel cycling; while the second is to predict the stability and quality of supply from different control strategies. A performance type model has been selected to investigate the renewable energy potential of the Antarctic stations.

Simulation models have been developed using a balance of power production to consumption, as outlined by Skarstein (1989). Constant efficiencies have been assumed for all generation plants as described by Dienhart (1994) and Kauranen (1994). Models have been developed to investigate the following configurations:

Diesel only systems: where all power is produced using diesel generator sets, used to establish consumption patterns for comparison purposes;

40% penetration systems: involving renewable power generation plant restricted to 40% of station load allowing adequate frequency and voltage regulation. Any additional power produced above the 40% of station load is dumped;

100% penetration systems: involving inclusion of power regulation equipment, stabilising load over the one-hour time step. This allows for full load penetration of renewables and possible intermittent diesel usage. Any additional power production above station load is dumped;

Battery storage systems: involving inclusion of storage in the form of batteries, with two-way inverters sized to take all excess power produced from renewables above station load and provide full station load during periods of insufficient renewable energy generation. If maximum energy storage is reached, any additional power above station load is dumped; and

Hydrogen storage systems: involving inclusion of bulk storage systems with a hydrogen loop employed for long term storage and limited battery system for short term storage.

An one-hour time step has been used for each model at which a power balance equation is solved allowing calculation of the load proportion provided by the diesel generator sets. Fuel totals are then derived from these loads. Any additional fuel needed to compensate for lower thermal energy generation from the diesel generator sets are not included in these totals, although net fuel savings including extra fuel use by the boilers to compensates for this effect are indicated in Chapter 7.

Programs were written in the MATLAB programming language and run on a UNIX platform. For non storage models, the power balance equation is solved using vectors. For storage models an iterative process is employed, solving the storage state at each time step, for use in the next. All model runs were performed at the Antarctic CRC (Cooperative Research Centre) at the University of Tasmania.

6.3.2 Input fields

Time series sequences for the station load, wind turbine power and photovoltaic power form the basis for comparison in the power balance models. Input fields have been obtained for each station over the period 1992 to 1995 allowing for a four year simulation period. A list of all variables used in the models as well as their dimensions and status are given in Table 6.1.

Variable	Description	Units	Status
P_L	Station load	[kW]	Given
P_W	Wind turbine power	[kW]	Given
P_S	Photovoltaic power	[kW]	Given
P_G	Diesel Generator power	[kW]	Calculated
P_D	Dump load	[kW]	Calculated
P_C	Control loads	[kW]	Calculated
W_B	Battery storage level	[kWh]	Calculated
B_c	Maximum battery charge rate	[kW]	Given
B_d	Maximum battery discharge rate	[kW]	Given
B_m	Maximum battery storage level	[kWh]	Given
η_B	Battery storage efficiency	-	Calculated
η_c	Battery charge efficiency	-	Given
η_d	Battery discharge efficiency	-	Given
W_H	Hydrogen storage level	[kWh]	Calculated
H_{el}	Maximum electrolyser charge rate	[kW]	Given
H_{fc}	Maximum fuel cell discharge rate	[kW]	Given
H_m	Maximum hydrogen storage level	[kWh]	Given
η_H	Hydrogen storage efficiency	-	Calculated
η_{el}	Electrolyser efficiency	-	Given
η_{fc}	Fuel cell efficiency	-	Given

Table 6.1: Simulation model variables and dimensions

Wind power capacity factors were constructed using BoM wind speed readings (taken every 3 hours at 10 metres) linearly interpolated onto an one hour grid. To calculate wind capacity factors the average recoverable power over a given hour, $P_{rec}(t)$, is assumed to equal that given by the power curve for the interpolated hourly wind speed V_i (as given in the equation below):

$$P_{rec}(t) = \int_0^\infty w(V).p(V).dV \approx w(V_i)\int_0^\infty p(V_i).dV = w(V_i) \qquad (6.1)$$

Using the 1-hour linearly interpolated wind speed records, V_i, allows for calculation of wind capacity factors, $C_w(t)$, at a given hour, t, using the power curve w for the UM-70X wind-turbine (rated at 10 kW).

$$C_w(t) = \frac{P_{rec}(t)}{rated \quad power} \approx \frac{w(V_i)}{10 \quad [kW]} \qquad (6.2)$$

The recoverable wind turbine power $P_w(t)$, is then calculated using the total rated power of all wind generation plant G_w:

$$P_w(t) = G_w.C_w(t) \qquad (6.3)$$

Solar power capacity factors were constructed for a PV array without tracking, fixed at the optimal tilt angle to maximise exposure, calculated from 1-hour global radiation estimates based on BoM cloud observations as described in Chapter 3. Using these 1-hour solar radiation estimates over 1992-95, $G_i(t)$, allows for calculation of solar capacity factors $C_s(t)$, relative to a standard rate of 1 kW/m^2 (assuming PV performance is independent of temperature and intensity as described in Chapter 3).

$$C_s(t) = \frac{G_i(t)}{standardised \quad insolation \quad rate} \approx \frac{G_i(t)}{1 \quad [kWm^{-2}]} \tag{6.4}$$

The recoverable Photovoltaic power $P_s(t)$, is then determined relative to the rated size of the PV array G_s:

$$P_s(t) = G_s.C_s(t) \tag{6.5}$$

Hourly station load time series, $P_L(t)$, were constructed using the method described in Chapter 4, Section 4.4.3, where synthetic load sequences for each station were generated based on temperature, wind speed, population and the monthly average station load for the period 1992-1995.

Having the station load, $P_L(t)$, wind turbine output power for a given installed capacity, $P_w(t)$, and photovoltaic array output for a given rated array, $P_s(t)$, each model will calculate time series for diesel generator power $P_D(t)$. Based on these series, fuel consumption levels will be calculated.

Each station powerhouse is controlled by a Programmable logic control (PLC), which determines how many generating units are on-line at any time. If the load increases beyond the rated capacity of the number of units currently connected, another unit is brought into service, or if the load drops and low loading results, a unit is phased out of service and shut down. For the purpose of modelling over a one-hour time step, the number of generators connected and their average load is important. If we assume that whenever the average load on a diesel generator equals 130 kW, another unit is brought on-line, the simple guide presented in Table 6.2 indicates the number of units on-line given the combined generator load.

Combined generator load	No. of generators on-line
0-130 kW	1
130 - 260 kW	2
260 - 390 kW	3
390 - 520 kW	4

Table 6.2: Number of diesel generators on-line for a given combined diesel generator load

Equal loading is assumed for each generator over the one hour time interval with any intra-hour cycling above or below the limits indicated in Table 6.2 beyond the resolution of the models.

The total fuel consumption is dependent on the number of diesel units on-line and their average load. Higher loading on a generator will result in better fuel efficiency, as long as the unit isn't overloaded. To model these effects, the fuel consumption for each generator on-line will be assumed to increase linearly from a base level at $P_{gen} = 0$, to a maximum at $P_{gen} = 130$. This results in the total fuel consumption being a function of the load on the generators as well as the number of units engaged. The equation below gives the total fuel consumption over one hour, *Fuel*, given the number of generators on line, *Gens*, and their combined loading, P_G:

$$Fuel \text{ [litres]} = A * P_G + B * Gens \tag{6.6}$$

To solve this equation for A and B, a least squares line of best fit has been used. In this analysis, an error function S is defined as the square of the difference between observed fuel consumption *Fuel* and calculated fuel consumption *Fuel'*. Using observed generator load P_G, fuel consumption *Fuel* and the number of generators *Gens*, variables A and B are then chosen to minimise the error function S as indicated below:

$$S = \sum [Fuel - Fuel']^2 = \sum [Fuel - A * P_G - B * Gens]^2 \tag{6.7a}$$

$$0 = \frac{\partial S}{\partial A} = \sum P_G * Fuel - A \sum P_G{}^2 - B \sum P_G * Gens \tag{6.7b}$$

$$0 = \frac{\partial S}{\partial B} = \sum Gens * Fuel - A \sum P_G * Gens - B \sum Gens^2 \tag{6.7c}$$

Equations 6.7 were solved using hourly fuel consumption levels and diesel generator loads calculated from the data presented in Figure 4.9, collected at each station over 1992-1995. This data, together with the resultant fuel equation is presented in Figure 6.5.

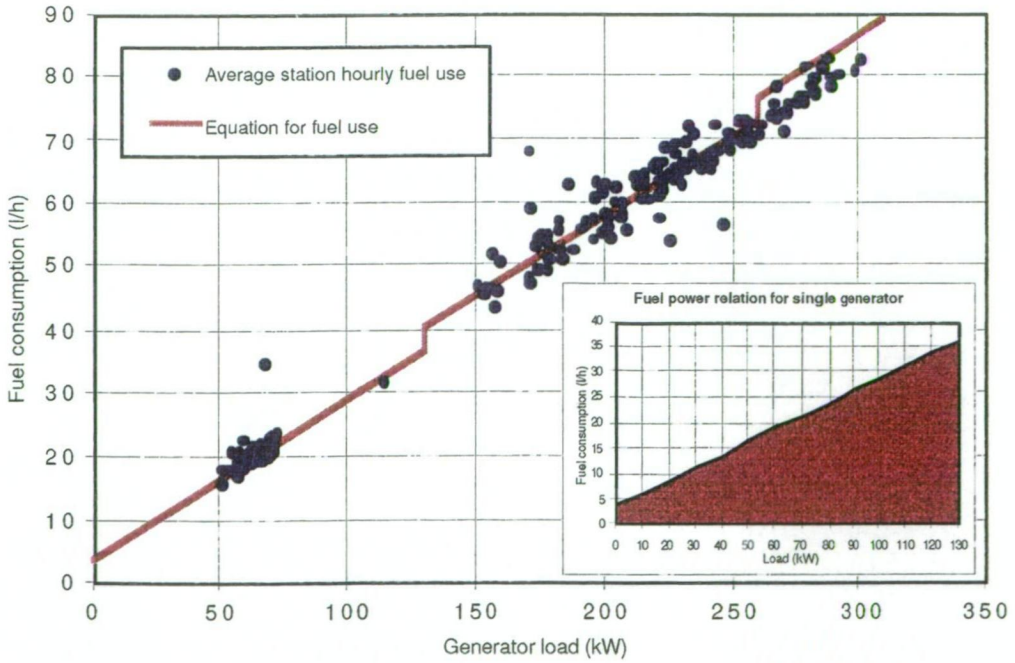

Figure 6.5: Least squares line of best fit for fuel use (based on monthly station reports).

The discontinuities in the fuel use equation have been added to take into account the extra fuel used when additional generators are brought into service. The fuel consumption for a single generator (superimposed onto Figure 6.5) indicates that fuel consumption at zero loading will be 10.3% of that at maximum loading (130 kW).

Using this fit, values of A and B were determined to give the following equation for the fuel.

$$Fuel\ [\text{litres}] = 0.2513*P_G+3.753*Gens \tag{6.8}$$

To solve for the generator load, P_G, the following models have been used.

6.3.3 Diesel only model

In the current system, all station electrical needs are met through the use of the diesel generator sets. If the station electrical power load is given by P_L, and electrical power generated by the diesel generator sets is given by P_G, the power balance is simply:

$$0 = P_G - P_L \tag{6.9}$$

Using the magnitude of the total load on the diesel generators, P_G allows solution of the total fuel consumption level *Fuel*, as well as the number of generators *Gens* and their average load.

6.3.4 40% penetration limited model

To allow for up to 40% renewable penetration of the load by renewables, extra terms representing power production from wind P_W and solar P_S energy generation plant have been included in the power balance equation (note P_W and P_S represents the net power output of a generation system including any inverter losses due to DC/AC conversion). A term representing the excess power diverted to a dump load P_D, has also be included to ensure renewable penetration does not exceed 40% of the station load P_L. This results in the power balance equation:

$$0 = P_G - P_D + P_W + P_S - P_L \tag{6.10}$$

together with the constraint,

$$P_D = \begin{cases} P_W + P_S - 0.4P_L & ,(P_W + P_S - 0.4P_L > 0) \\ 0 & ,(P_W + P_S - 0.4P_L \leq 0) \end{cases}$$

Using the constraint, Equation 6.10 can be solved for the diesel generated power P_G and hence number of generators *Gens*, allowing the average load on each generator to be solved, and the total fuel consumption level *Fuel*. This approach will be used for a number of different rated renewable energy systems, allowing the amount of fuel savings to be determined for a range of different sizes and mixes of wind and solar generation plant.

6.3.5 100% penetration model

For renewable energy penetration up to 100% penetration, regulation of the voltage and frequency will be necessary. To model effects from regulation equipment and inverters, a parasitic control load P_C has been introduced to the power balance equation. The value of this dump load will be assumed to be in direct proportion (10%) to the amount of renewable energy production power above 40%. Equation 6.11 gives the resultant power balance:

$$0 = P_G - P_D - P_C + P_W + P_S - P_L \tag{6.11}$$

together with the constraints (where the net power $P_{net} = P_W + P_S - P_L - P_C$),

$$P_C = \begin{cases} 0.1(P_W + P_S - 0.4P_L) & ,(P_W + P_S - 0.4P_L > 0) \\ 0 & ,(P_W + P_S - 0.4P_L \le 0) \end{cases}$$

$$P_D = \begin{cases} P_{net} & ,(P_{net} > 0) \\ 0 & ,(P_{net} \le 0) \end{cases}$$

Two methods will be used to calculate the total fuel consumption for 100% penetration systems. The first assumes that at least one diesel generator must remain on line at all times to provide regulation, while the second assumes the presence of limited storage for load regulation and continuity allowing all diesel units to be stopped (a situation that will only apply if the average diesel load P_D over the 1 hour time step is zero). Although no energy penalty has been included to model this second situation, the number of times that all the diesels have been stopped is indicated on the diesel loading curves by a zero load.

6.3.6 Battery storage model

To model battery storage systems extra terms representing the **available** battery storage energy over an hour W_B, and conversion efficiency η_B, have been introduced into the power balance equation. The amount of power going into and out of this storage is equivalent to the rate of change of this storage energy, hence the derivative in the energy balance of Equation 6.12.

$$\eta_B \frac{d(W_B)}{dt} = P_G - P_D - P_C + P_W + P_S - P_L \tag{6.12}$$

together with the constraints (where the net power $P_{net} = P_W + P_S - P_L - P_C$),

$$P_C = \begin{cases} 0.1(P_W + P_S - 0.4P_L) & ,(P_W + P_S - 0.4P_L > 0) \\ 0 & ,(P_W + P_S - 0.4P_L \le 0) \end{cases}$$

$$P_D = \begin{cases} P_{net} - B_c & ,(P_{net} > B_c) \;\&\; (W_B < B_m) \\ P_{net} & ,(P_{net} > 0) \;\&\; (W_B \ge B_m) \\ 0 & ,otherwise \end{cases}$$

$$P_G = \begin{cases} -P_{net} + B_d & ,(-P_{net} \geq B_d) \quad \& \quad (W_B > 0) \\ -P_{net} & ,(-P_{net} \geq 0) \quad \& \quad (W_B \leq 0) \\ 0 & ,otherwise \end{cases}$$

$$\eta_B = \begin{cases} \eta_d & ,(P_{net} - P_D + P_G < 0) \\ 1/\eta_c & ,(P_{net} - P_D + P_G > 0) \end{cases}$$

and to check for overcharging at the end of each time step, the adjustment:

$$P_D = \begin{cases} P_D & ,if \quad (W_B \leq B_m) \\ P_D + \eta_c(W_B - B_m) & ,if \quad (W_B > B_m) \end{cases}, \quad W_B = \begin{cases} W_B & ,if \quad (W_B \leq B_m) \\ B_m & ,if \quad (W_B > B_m) \end{cases}$$

The maximum amount of energy that can be stored by the battery is represented by B_m. This term is defined as the **available** battery storage and may differ from the **actual** battery storage to prevent very low state-of-charge (SOC) levels. The maximum rate of charge B_c and discharge B_d of the battery system will be set to the size of the generation plant. This will allow any excess renewable power to be stored by the batteries or any station load not met by renewables to be provided for by the batteries. If there is not sufficient storage to meet the entire station load not met by renewables within a given time step, the batteries will not be used in an attempt to model the prevention of deep discharge. Efficiencies of 90% into storage (charge efficiency η_c) and 90% out of storage (discharge efficiency η_d) have been assumed, resulting in a combined efficiency for battery storage of 81%, as reported in simulations by Kauranen (1994).

Equation 6.12 together with the constraints allow for the solution of the battery storage energy level, W_B, using a first order Taylor series expansion approximation for the derivative at each time step. In cases when W_B is less to zero due to internal rounding errors or in the solution of the Taylor series, W_B is set to zero for the next time step. The diesel power time series, P_G, is also calculated at for time step to allow the fuel consumption level to be determined.

6.3.7 Hydrogen loop storage model

With the introduction of hydrogen storage, the power balance equation becomes much more complicated, as would any control strategy and control system. Provision has been made for short term battery storage to complement a longer term hydrogen storage circuit comprising an electrolyser, storage tank and fuel cell. The resultant power balance equation includes extra terms for the hydrogen energy storage level, W_H, and conversion efficiency, η_H, leading to the expression:

$$\eta_H \frac{d(W_H)}{dt} + \eta_B \frac{d(W_B)}{dt} = P_G - P_D - P_C + P_W + P_S - P_L \qquad (6.13)$$

together with the constraints (defining the net power $P_{net} = P_W + P_S - P_L - P_C$),

$$P_C = \begin{cases} 0.1(P_W + P_S - 0.4P_L) & ,(P_W + P_S - 0.4P_L > 0) \\ 0 & ,(P_W + P_S - 0.4P_L \leq 0) \end{cases}$$

$$P_D = \begin{cases} P_{net} - B_c - H_{el} & ,(P_{net} > B_c + H_{el}) \;\&\; (W_B < B_m) \;\&\; (W_H < H_m) \\ P_{net} - B_c & ,(P_{net} > B_c) \;\&\; (W_B < B_m) \;\&\; (W_H > H_m) \\ P_{net} - H_{el} & ,(P_{net} > H_{el}) \;\&\; (W_B > B_m) \;\&\; (W_H < H_m) \\ P_{net} & ,(P_{net} > 0) \;\&\; (W_B \geq B_m) \;\&\; (W_H \geq H_m) \\ 0 & ,otherwise \end{cases}$$

$$P_G = \begin{cases} -P_{net} - B_d - H_{fc} & ,(-P_{net} \geq B_d + H_{fc}) \;\&\; (W_B > 0) \;\&\; (W_H > 0) \\ -P_{net} - B_d & ,(-P_{net} \geq B_d) \;\&\; (W_B > 0) \;\&\; (W_H \leq 0) \\ -P_{net} - H_{fc} & ,(-P_{net} \geq H_{fc}) \;\&\; (W_B \leq 0) \;\&\; (W_H > 0) \\ -P_{net} & ,(-P_{net} \geq 0) \;\&\; (W_B \leq 0) \;\&\; (W_H \leq 0) \\ 0 & ,otherwise \end{cases}$$

$$\eta_B \frac{d(W_B)}{dt} = \begin{cases} P_{net} - P_D + P_G & ,(-B_d < P_{net} - P_D + P_G < 0) \;\&\; (W_B > 0) \\ P_{net} - P_D + P_G & ,(0 < P_{net} - P_D + P_G < B_c) \;\&\; (W_B < B_m) \\ -B_d & ,(P_{net} - P_D + P_G \leq -B_d) \;\&\; (W_B > 0) \\ B_c & ,(P_{net} - P_D + P_G \geq B_c) \;\&\; (W_B < B_m) \\ 0 & ,otherwise \end{cases}$$

$$\eta_B = \begin{cases} \eta_d & ,(P_{net} - P_D + P_G < 0) \\ 1/\eta_c & ,(P_{net} - P_D + P_G > 0) \end{cases}$$

$$\eta_H = \begin{cases} \eta_{fc} & ,\left(P_{net} - P_D + P_G - \eta_B \frac{d(W_B)}{dt} < 0\right) \\ 1/\eta_{el} & ,\left(P_{net} - P_D + P_G - \eta_B \frac{d(W_B)}{dt} > 0\right) \end{cases}$$

and to check for overcharging at the end of each time step, the adjustments:

$$P_D = \begin{cases} P_D & ,if \;\; (W_B \leq B_m) \\ P_D + \eta_c (W_B - B_m) & ,if \;\; (W_B > B_m) \end{cases}, \quad W_B = \begin{cases} W_B & ,if \;\; (W_B \leq B_m) \\ B_m & ,if \;\; (W_B > B_m) \end{cases}$$

$$P_D = \begin{cases} P_D & ,if \;\; (W_H \leq H_m) \\ P_D + \eta_{el} (W_H - H_m) & ,if \;\; (W_H > H_m) \end{cases}, \quad W_H = \begin{cases} W_H & ,if \;\; (W_H \leq H_m) \\ H_m & ,if \;\; (W_H > H_m) \end{cases}$$

Priority has been given for battery storage to be used before hydrogen storage, with power diverted into hydrogen storage only if battery storage is full. Likewise, for any deficiencies, power will be first taken from battery storage and then from hydrogen storage. If both battery and hydrogen storage has been depleted, any shortfalls will be met by the diesel generators. This may not be the best method to allow for the greatest fuel saving and least plant wear, but due to the limited resolution of the model, further investigations have not been conducted.

As for battery storage, it has been assumed that the electrolyser charge rate H_{el} is of sufficient size to allow all excess power to be converted into hydrogen, and the fuel cell discharge rate H_{fc} of sufficient size to provide full station load if hydrogen storage levels permit. Partial discharge of the battery and hydrogen systems have been suppressed if when combined they cannot meet the desired total station load over a time step.

Efficiencies of 60% into storage (electrolyser efficiency η_{el}), and 50% out of storage (fuel cell efficiency η_{fc}) have been assumed, resulting in a combined efficiency for hydrogen storage of 30%, similar in magnitude to values reported by Kauranen (1994). Using Taylor series expansions for the derivatives allows Equation 6.13 to be solved for each time step, allowing fuel consumption levels to be calculated from the diesel generator load P_G. As for the battery storage level, when the hydrogen storage level W_H is less to zero due to internal rounding errors or in the solution of the Taylor series, it is set to zero for the next time step.

6.4 Modelling results for simple hybrid energy systems

Systems not involving storage of any kind will be considered as simple hybrid systems. These are envisaged to operate along side the existing diesel generators, displacing fuel use when conditions suitable for power generation from the wind or sun occur. For comparison purposes, the current system using only diesel generators is described first. Power production and fuel consumption levels calculated for this system have been used as a reference to calculate fuel savings for hybrid energy systems.

6.4.1 Current system

Using the model for diesel only systems presented in Section 6.3.3 and the station load series described in Section 4.4.3, allows for calculation of hourly values of each stations diesel generator loads and number of on-line generators. Averages of these quantities together with a profile of the diesel generator loading patterns are presented in Figure 6.6 for each station over the period 1992 to 1995. Four day averages have been used in all figures to allow easy visual interpretation. (Note: An artifact of this averaging process may result in the third generator appearing to engage early).

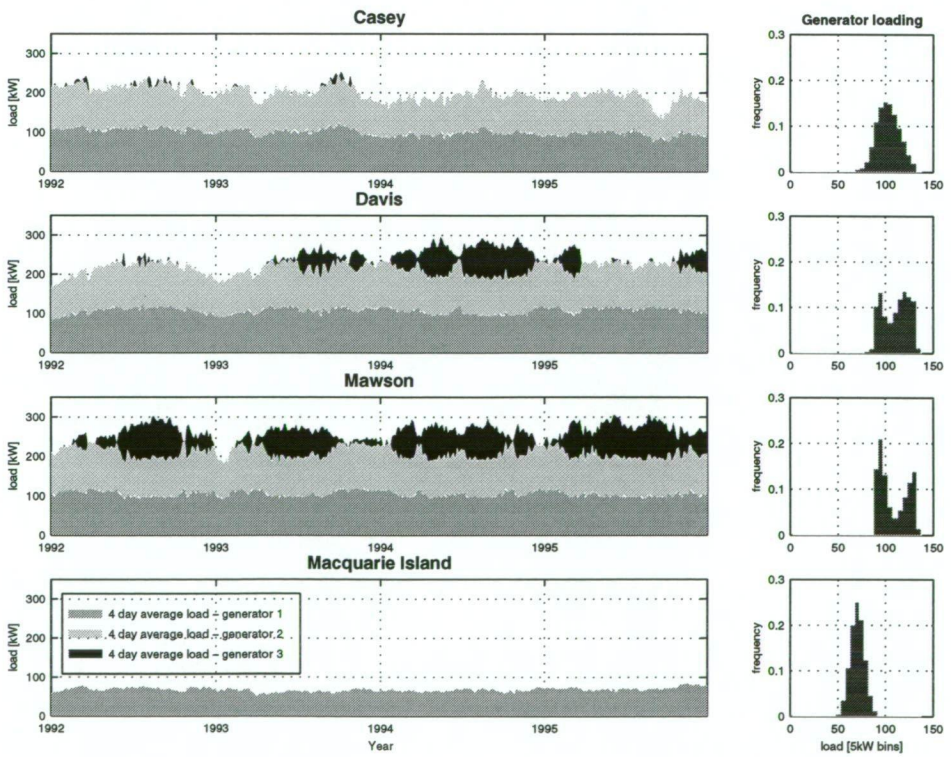

Figure 6.6: Average monthly station load together with diesel generator loading (1992-95)

Two diesel units are usually employed to meet the loads at the continental stations while a third unit is often needed at Mawson and Davis. Generator loading at Casey is centred around 100 kW, while for Mawson and Davis the periodic use of a third unit results in the two peaked distribution. Macquarie Island loads are able to be met by a single unit at all times, with an average load centred about 70 kW. The periodic use of the third generator at the continental stations is also evident from the results presented in Table 6.3 where the average number of generators on-line, average load per generator and average number of start/stop cycles of duration equal to or greater than one hour are presented. (Note: Averages based on data over the simulation period 1992-95).

Site	Diesel generators			Total fuel use	
	Average on-line	Average load (kW)	Stop/start cycles(y^{-1})	Average (kl/y)	Difference with actual
Casey	2.0	100	28	509	-1%
Davis	2.2	108	137	599	+5%
Mawson	2.5	106	222	658	+4%
Macquarie Island	1.0	68	0	183	+1%

Table 6.3: Generator loading and fuel use as estimated from diesel only energy model.

The differences between these estimates and the reported totals from the stations (presented in Section 4.2) for the years 1992-1995 are also provided for reference. The ratio of fuel savings derived from the use of renewable generation plant in the other models have been calculated against these values.

6.4.2 Wind/Solar/Diesel systems - low penetration

Estimated fuel savings indicated from the 40% penetration limited model are presented in Figure 6.7 for the indicated wind and solar generating capacities. These ratios indicate the average fuel savings calculated for the stations over the years 1992-95.

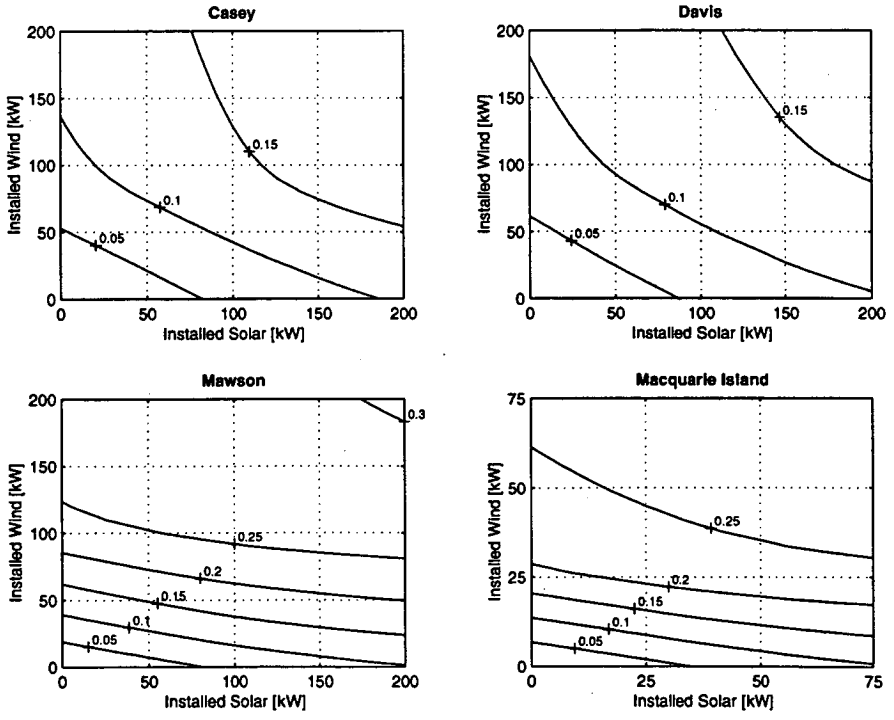

Figure 6.7: Fuel savings met through a 40% renewable penetration limited wind/ solar/diesel energy system

The graphs in Figure 6.7 have been calculated by estimating the fuel savings for different combinations of wind/solar/diesel systems from pure wind/diesel to pure solar/diesel and including all 20 kW wind/solar combinations in between. The fuel saving ratios were determined by comparing the calculated fuel use of the relevant wind/solar/diesel system to that of the diesel only system (presented in Table 6.3), with the indicated contour lines fitted using a bi-linear MatLAB routine. This method has been used throughout the remainder of this section.

Further information for standard sized systems from the 40% renewable penetration model has been presented in Table 6.4. Dumped renewable energy represents power produced from the combined wind and solar plant that could not be used (ie. over the 40% renewable penetration limit). The combined renewable output is equal to the sum of this dumped energy and the indicated useful renewable energy. Station load ratios represent the proportion of each station's energy needs met by the renewable energy system.

Site	Installed plant		Renewable Energy			Fuel savings		Diesel generators		
	wind (kW)	solar (kW)	useful (MWh/y)	dumped (MWh/y)	station load (%)	(kl/y)	(%)	Average on-line	Average load (kW)	Stop/start cycles(y^{-1})
Casey	100	-	169	19	10%	47	9%	1.9	96	147
	100	100	271	37	15%	73	14%	1.9	93	211
	200	-	209	166	12%	57	11%	1.9	97	200
Davis	100	-	170	7	8%	46	8%	2.1	104	149
	100	100	278	23	13%	76	13%	2.1	101	146
	200	-	230	124	11%	62	10%	2.1	102	178
Mawson	100	-	539	7	24%	150	23%	2.1	96	130
	100	100	623	63	27%	172	26%	2.1	93	118
	200	-	650	442	28%	179	27%	2.1	91	129
Macquarie Island	50	-	177	93	30%	45	24%	1.0	48	0
	50	50	195	128	33%	49	27%	1.0	47	0
	100	-	197	344	33%	49	27%	1.0	46	0

Table 6.4: Estimated performance of wind/solar systems limited to 40% of load (Note: Fuel savings ratios may appear to differ with figure 6.6 due to round off errors)

Returns for Mawson are excellent, with a 100 kW wind (only) system able to produce 24% of the stations needs, almost three time the power production for a similar sized unit at Casey or Davis. Macquarie Island also has excellent returns, with a 50 kW wind system expected to meet 30% of the stations electrical energy needs. At Mawson the addition of 100 kW of wind power plant has the added advantage of decreasing the frequency that a third generator is needed to be brought into service. For these low renewable penetration cases, the percentage savings in fuel are only a few percent below the energy percentage met by renewables, an indication that the diesel generators are not subject to low loading.

Mixed systems (comprising 100 kW wind and 100 kW solar at the continental stations, 50 kW wind and 50 kW solar at Macquarie Island), offer methods to increase the ratio of the total station energy met by renewables. Increases are more promising at Casey and Davis, where the additional energy production results in additional fuel savings of 5%. At Mawson and Macquarie Island, the high production times from wind plant tend to limit the potential for solar plant to provide additional useful renewable energy before the 40% renewable penetration is reached. This results in additional fuel savings being limited to 2% at Mawson and 3% at Macquarie Island.

The use of large wind systems, approaching the average station load, offers poor returns for 40% penetration limited systems. A doubling of wind systems (to 200 kW at the continental stations, and to 100 kW at Macquarie Island), results in large dump loads and relatively small additional fuel savings. The reason for these poor returns can be seen from the power production series, presented in Figures 6.8 to 6.11.

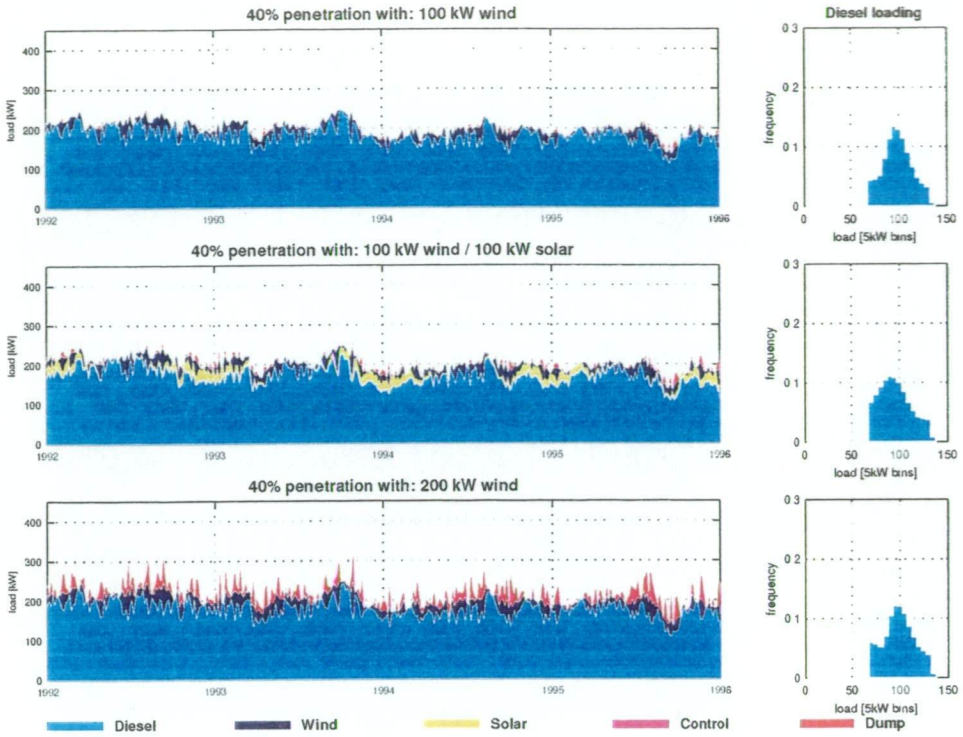

Figure 6.8: Casey - four day average of the contribution of wind and solar energy systems, with renewables limited to 40% penetration of load [1992-1995].

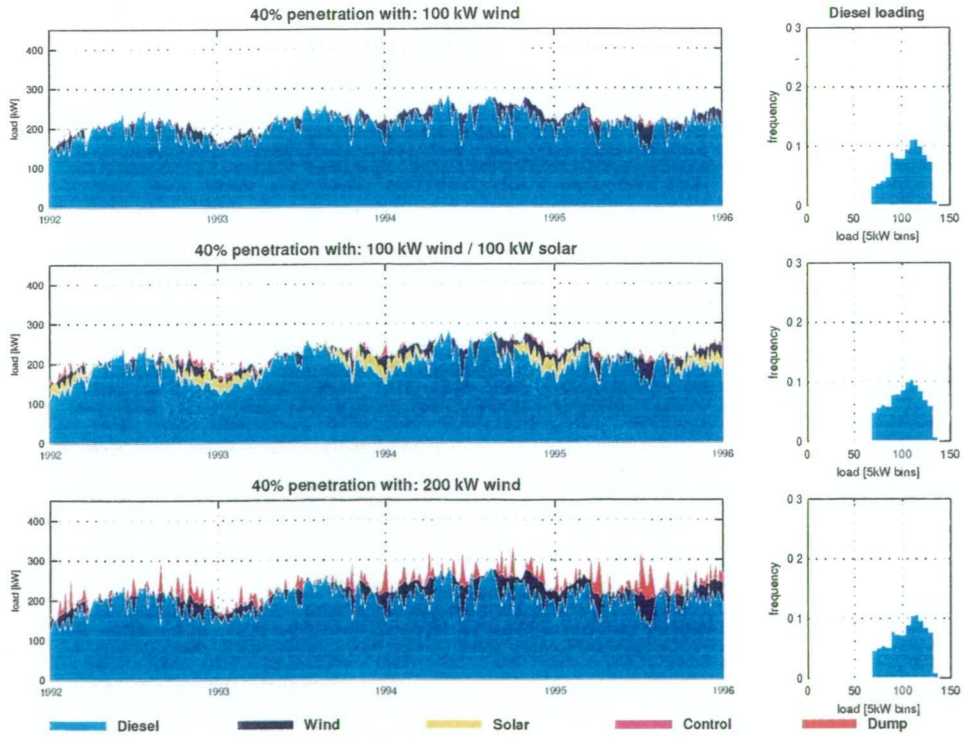

Figure 6.9: Davis - four day average of the contribution of wind and solar energy systems, with renewables limited to 40% penetration of load [1992-1995].

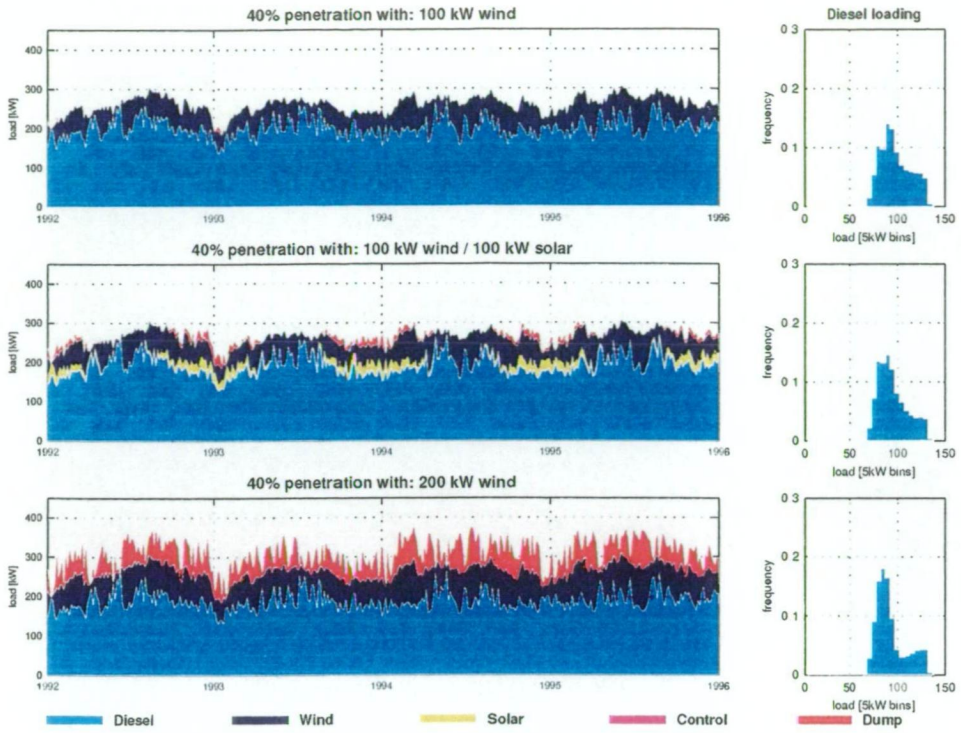

Figure 6.10: Mawson - four day average of the contribution of wind and solar energy systems, with renewables limited to 40% penetration of load [1992-1995].

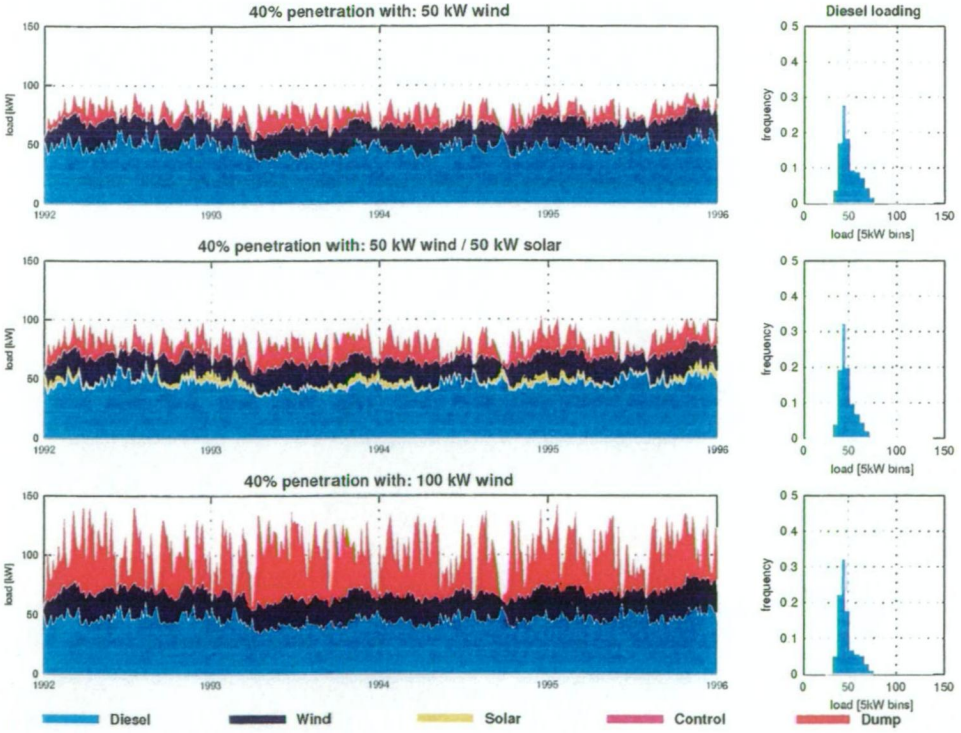

Figure 6.11: Macquarie Island - four day average of the contribution of wind and solar energy systems, with renewables limited to 40% penetration of load [1992-1995].

These plots represent four day averages of the contribution of wind, solar and diesel to the station load, and any dump loads that result under a 40% renewable penetration limited control system. For large sized wind only systems, saturation of the amount of useful power quickly occurs, resulting in high dump loads.

For mixed wind and solar systems, less frequent wind resources at Casey and Davis result in solar energy production periods being out of phase with high wind production times to a greater degree. This result in lower dump loads than for wind only systems of the same installed capacity at the two stations where, as seen in Figures 6.8 to 6.9, irregular winds result in short production periods. More consistent wind resources at Mawson and Macquarie Island result in a different situation. The four day averages for these stations, presented in Figures 6.10 and 6.11 have more consistent production periods with high four day averages for wind only systems.

A 40% renewable load limited system offers the simplest method to include a renewable power generation component to the stations, and where capital investment is required only for the wind turbines and photovoltaic systems. For higher fuel savings, 100% penetration systems must be used, where renewable power plant are able to provide the full station load through the inclusion of power regulation equipment.

6.4.3 Wind/Solar/Diesel systems - high penetration systems

Substantial increases in fuel savings are possible with power regulation systems. Figure 6.12 indicates the fuel savings ratios calculated using the 100% penetration model described in Section 6.3.5. Systems with wind and solar generation up to 400 kW (each) have been investigated for Casey, Davis and Mawson; and 150 kW for Macquarie Island.

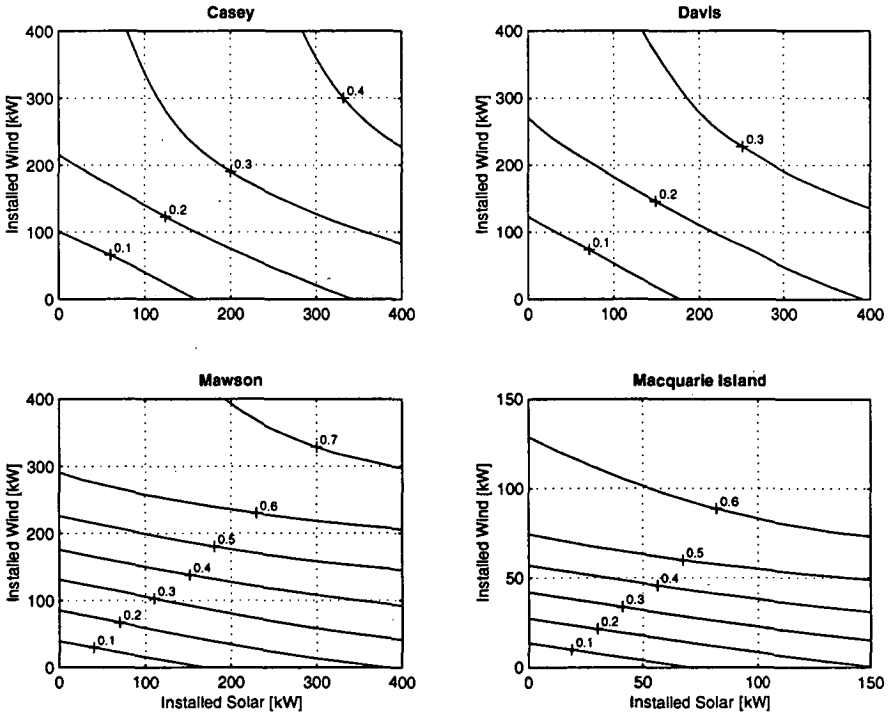

Figure 6.12: Fuel savings at the Australian Antarctic stations from high penetration renewable energy systems

Mawson and Macquarie Island continue to present extremely promising results, where fuel savings of up to 50% can be achieved through the use of wind only systems of 250 kW and 75 kW capacity respectively.

At Casey and Davis wind only systems are not as promising, with fuel savings approaching 20%. Combining wind with solar at these stations does allow for increased fuel savings up to 31% at Casey, and 26% at Davis.

Information on the breakdown of energy production, fuel savings and generator loading is presented in Table 6.5 for standard sized wind and solar power plant. Low dump loads occur at the continental stations for systems with 200 kW of installed wind, even when combined with equivalent sized solar systems.

Site	Installed plant		Renewable Energy			Fuel savings		Diesel generators		
	wind (kW)	solar (kW)	useful (MWh/y)	dumped (MWh/y)	station load (%)	(kl/y)	(%)	Average on-line	Average load (kW)	Stop/start cycles(y^{-1})
Casey	200	-	372	4	20%	97	19%	1.8	86	205
	200	200	600	16	33%	157	31%	1.6	79	323
	400	-	539	211	28%	132	26%	1.7	77	267
Davis	200	-	353	> 1	17%	95	16%	2.0	99	241
	200	200	595	7	28%	158	26%	1.8	91	301
	400	-	567	140	27%	143	24%	1.9	87	287
Mawson	200	-	1,092	> 1	48%	296	45%	1.5	89	382
	200	200	1,345	26	59%	358	54%	1.4	74	377
	400	-	1,716	469	75%	431	65%	1.3	42	354
Macquarie Island	100	-	450	90	76%	105	57%	1.0	20	0
	100	100	504	142	85%	116	63%	1.0	16	0
	150	-	517	293	87%	115	63%	1.0	15	0

Table 6.5: Estimated performance of wind/solar systems with power conditioning

Problems are evident for oversized wind systems, sized greater than the average station load, at Mawson and Macquarie Island. These include:

- Large dump loads are evident for these systems.

- Extra fuel savings limited (Macquarie Island).

- Poor diesel generator average loading resulting in high diesel idling.

The serial structure of power production for 100% penetration systems is indicated in Figures 6.13 to 6.16. At Casey and Davis, the variability and irregularity of wind resources once again place limits to the production periods from wind plants resulting in the lower fuel savings compared to similar size plant at Mawson and Macquarie Island.

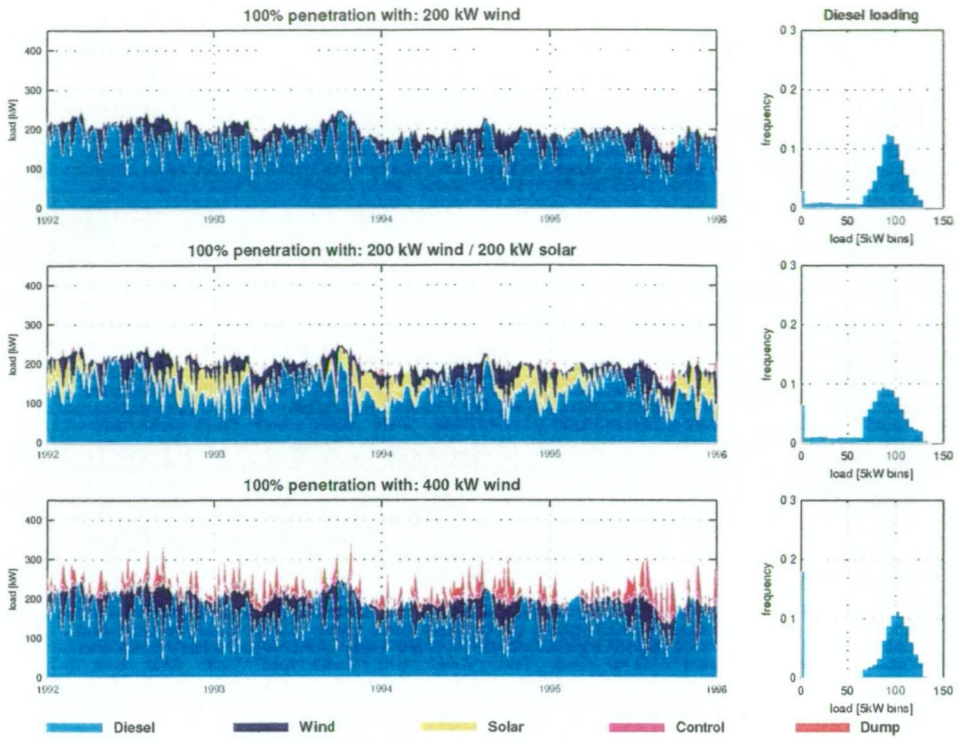

Figure 6.13: Casey - four day average of the contribution of wind and solar energy systems, allowing 100% penetration of load by renewables [1992-1995].

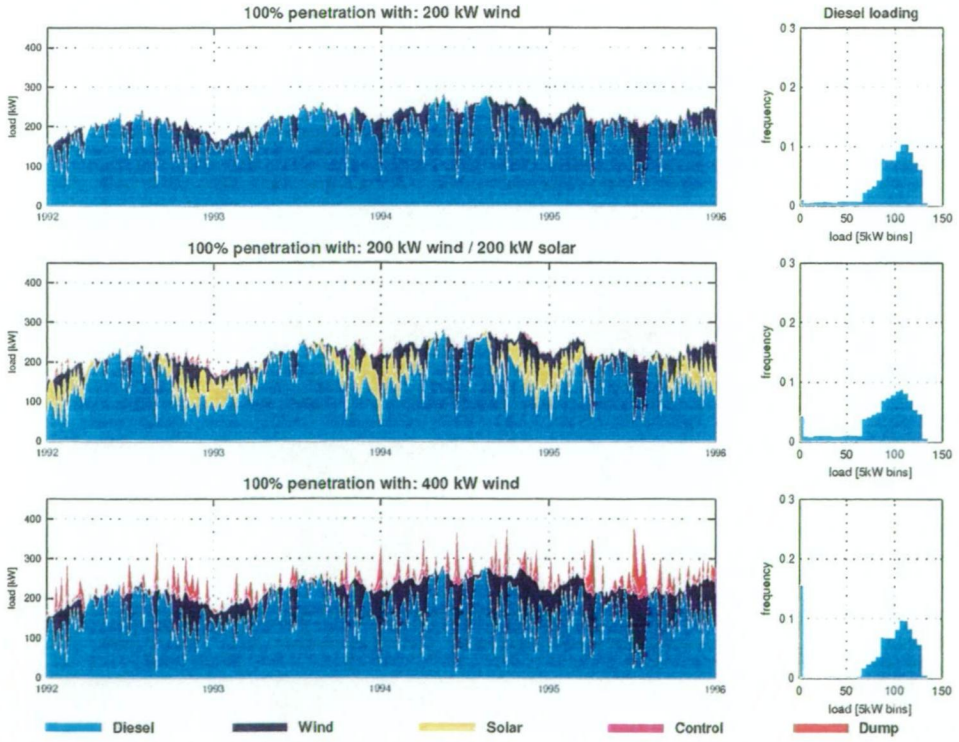

Figure 6.14: Davis - four day average of the contribution of wind and solar energy systems, allowing 100% penetration of load by renewables [1992-1995].

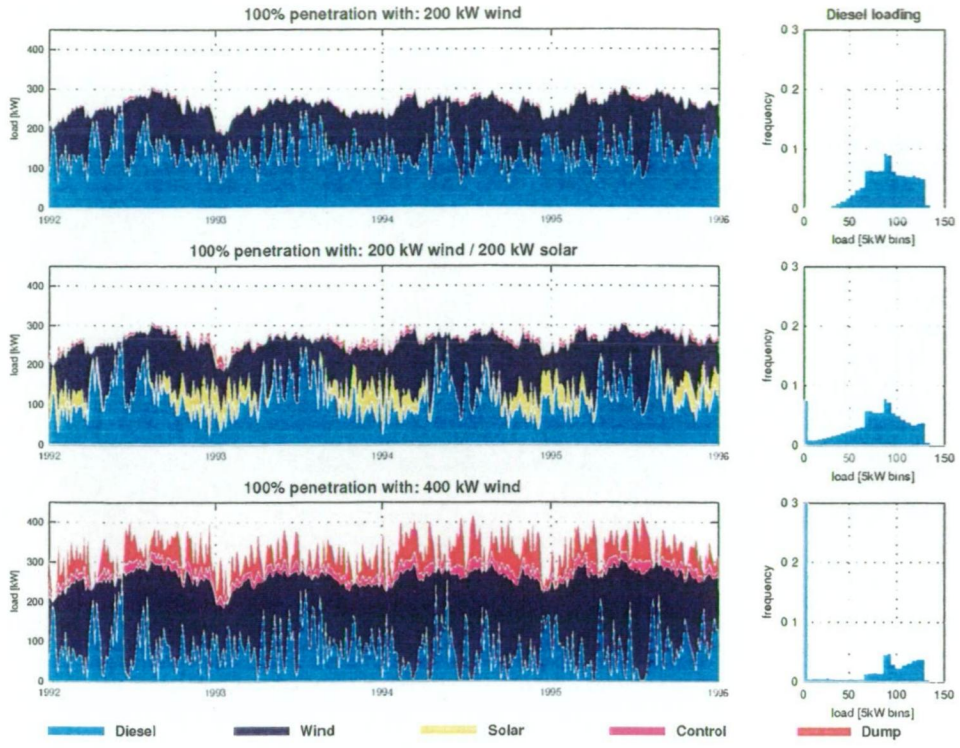

Figure 6.15: Mawson - four day average of the contribution of wind and solar energy systems, allowing 100% penetration of load by renewables [1992-1995].

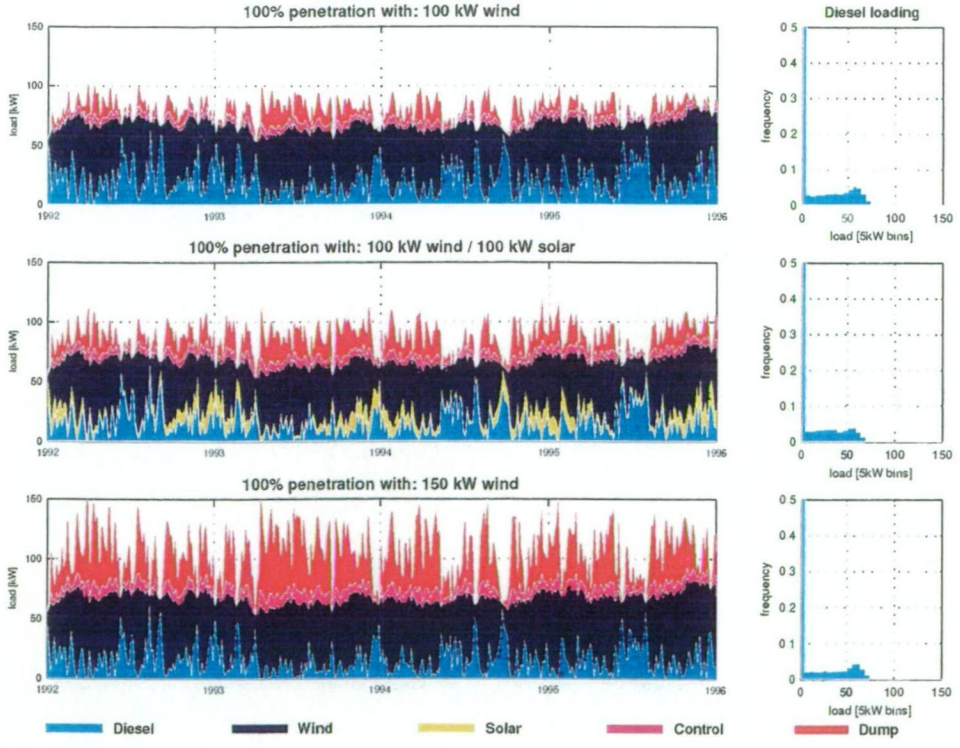

Figure 6.16: Macquarie Island - four day average of the contribution of wind and solar energy systems, allowing 100% penetration of load by renewables [1992-1995].

The diesel generator load profiles indicate that oversized systems result in significant periods of zero diesel generator loading. In such cases, increased fuel savings are possible through intermittent stopping of all generators. In order for this to be possible, sufficient short term storage of duration less than one hour for the purpose of modelling has been assumed. This will not affect the energy production amounts as the storage is only useful to provide voltage and frequency regulation and continuity of supply. To model these conditions, fuel consumption has been set to zero whenever the calculated combined diesel generator load is zero, resulting in the values presented in Table 6.6.

Site	Installed plant		Fuel savings				Diesel generators		
	wind (kW)	solar (kW)	total (kl/y)	increase (kl/y)	total (%)	increase (%)	Average on-line	Average load (kW)	Stop/start cycles(y^{-1})
Casey	200	-	98	1	19%	> 1%	1.8	89	265
	200	200	159	2	31%	> 1%	1.6	84	440
	400	-	138	6	27%	1%	1.5	94	423
Davis	200	-	95	> 1	16%	> 1%	2.0	100	245
	200	200	159	1	27%	> 1%	1.8	94	351
	400	-	148	5	25%	1%	1.7	102	395
Mawson	200	-	296	> 1	45%	> 1%	1.5	89	385
	200	200	361	3	55%	1%	1.3	81	514
	400	-	449	18	68%	3%	0.9	92	625
Macquarie Island	100	-	120	15	66%	9%	0.5	39	271
	100	100	134	18	73%	10%	0.3	35	290
	150	-	135	20	74%	11%	0.4	41	260

Table 6.6: Estimated performance of wind/solar systems with power conditioning and intermittent diesel stopping

Increased fuel savings result for large oversized systems, especially at Mawson and Macquarie Island. Macquarie Island gives the most promising savings, a consequence of the high instance of zero loading on the diesel generator. These increases in fuel savings come from better loading on the diesels, with increases in stop/start cycles reducing times of low loading. To obtain further fuel savings, and a reduction in diesel stop/start cycles, inter hourly storage systems are required.

6.5 Modelling results for storage systems

Finding a suitable storage medium is the major difficulty for renewable energy power generation systems. Storage requirements can be minimised through efficient scheduling of loads, including the shifting of any non-critical interruptable loads to periods of high renewable power production, as outlined in Chapter 5. This could prove more effective than the installation of costly storage. For this reason, only systems able to meet up to 80-90% of current demands will be investigated. In many cases the sizing and cost of systems required to meet the addition 10%-20% is unrealistic, requiring huge investments for small additional improvements.

6.5.1 Battery storage systems

Addition of battery storage up to 8000 kWh and 1600 kWh (approximately a 1 day load based on peak consumption) for the continental stations and Macquarie Island respectively, results in the fuel savings ratios given in Figure 6.17 (for wind/diesel /battery systems) and Figure 6.18 (for wind/solar/diesel/battery systems). These values have been calculated using the model presented in Section 6.3.6.

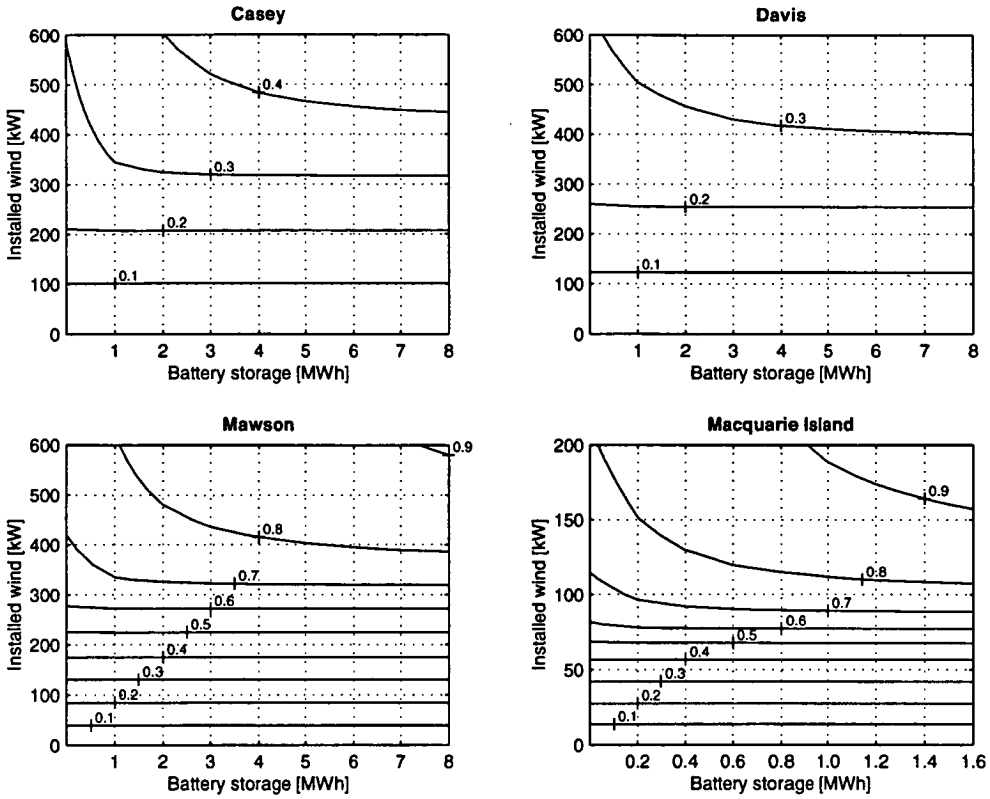

Figure 6.17: Fuel savings ratios for wind/diesel systems with battery storage
(up to 8 MWh at Casey, Davis and Mawson; and 1.6 MWh at Macquarie Island) [1992-95].

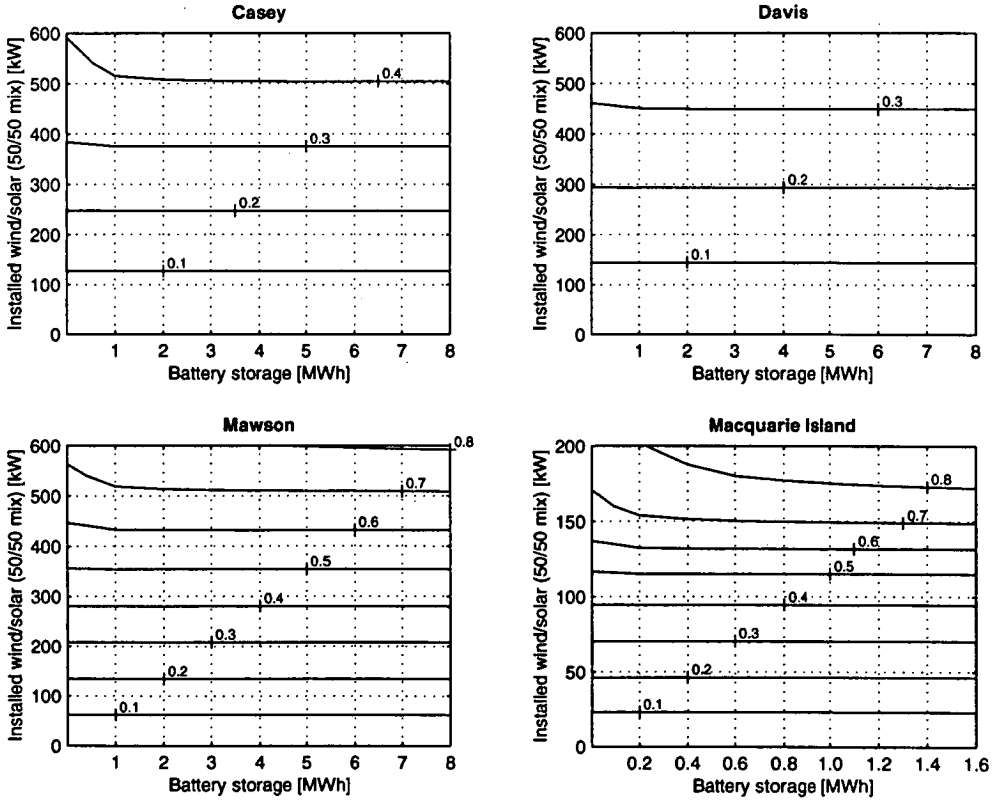

Figure 6.18: Fuel savings ratios for wind/solar/diesel systems with battery storage
(up to 8 MWh at Casey, Davis and Mawson; and 1.6 MWh at Macquarie Island) [1992-95].

Battery storage is extremely expensive, with large fuel savings and decreased cycling the only way to justify its use. Benefits from the use of battery storage, sufficient to meet 6 hours of continuous station load, is indicated in Table 6.7.

Site	Installed plant		Renewable Energy			Fuel savings		Diesel generators		
	wind (kW)	solar (kW)	useful (MWh/y)	dumped (MWh/y)	station load (%)	(kl/y)	(%)	Average on-line	Average load (kW)	Stop/start cycles(y^{-1})
Casey	400	-	685	65	34%	173	34%	1.4	95	344
	400	200	901	90	46%	230	45%	1.2	90	440
	400	400	1,109	124	56%	282	55%	1.0	88	499
	600	-	838	287	40%	203	40%	1.3	95	363
Davis	400	-	650	57	28%	168	28%	1.6	104	353
	400	200	875	79	38%	227	38%	1.5	99	409
	400	400	1,093	109	47%	281	47%	1.2	99	494
	600	-	787	252	34%	202	34%	1.5	104	391
Mawson	400	-	1,943	241	77%	503	76%	0.6	98	426
	400	200	2,106	358	83%	542	82%	0.5	95	361
	400	400	2,222	521	86%	567	86%	0.4	95	311
	600	-	2,215	1,063	83%	546	83%	0.4	100	330
Macquarie Island	100	-	494	46	76%	134	74%	0.4	44	153
	100	50	527	66	81%	143	78%	0.3	41	143
	150	-	570	240	84%	151	83%	0.2	47	111
	200	-	615	464	87%	157	86%	0.2	49	100

Table 6.7: Estimated performance of wind/solar systems with storage (2000 kWh battery for Casey, Davis and Mawson; 400 kWh for Macquarie Island).

Extension to 24 hours, involving a four-fold increase in battery storage size, result in the increases presented in Table 6.8.

Site	Installed plant		Renewable Energy			Fuel savings		Diesel generators		
	wind (kW)	solar (kW)	useful (MWh/y)	dumped (MWh/y)	station load (%)	(kl/y)	(%)	Average on-line	Average load (kW)	Stop/start cycles(y^{-1})
Casey	400	-	747	3	37%	187	37%	1.3	96	324
	400	200	981	10	50%	249	49%	1.1	90	405
	400	400	1,205	27	60%	305	60%	0.9	89	427
	600	-	1,024	101	49%	247	49%	1.1	96	296
Davis	400	-	697	10	30%	179	30%	1.6	104	339
	400	200	938	17	41%	242	40%	1.4	100	382
	400	400	1,174	28	50%	300	50%	1.2	100	438
	600	-	949	112	39%	234	39%	1.4	105	340
Mawson	400	-	2,083	102	81%	536	81%	0.5	98	321
	400	200	2,255	209	88%	577	88%	0.3	95	231
	400	400	2,348	395	91%	596	91%	0.2	96	179
	600	-	2,426	852	90%	594	90%	0.2	98	158
Macquarie Island	100	-	519	21	79%	141	77%	0.3	45	123
	100	50	557	36	85%	151	83%	0.2	42	100
	150	-	616	194	90%	163	89%	0.1	48	57
	200	-	662	418	93%	170	93%	0.1	49	42

Table 6.8: Estimated performance of wind/solar systems with storage (8000 kWh battery for Casey, Davis and Mawson; 1600 kWh for Macquarie Island).

To calculate these results, the maximum charge rate of the battery systems has been sized to allow all excess energy above station load to be converted into storage, equivalent to the rating of the combined installed wind and solar generation plant.

Impressive fuel savings are clearly evident at Mawson and Macquarie Island. Comparison between the 100% penetration systems and battery systems indicate that although inclusion of inter-hourly battery storage leads to higher fuel savings, these are only possible with large increases in renewable generation plant to that well above the average daily load. The capital costs associated with these increases, in addition to the cost of battery storage system, are large when considering the projected additional fuel savings over 100% penetration systems.

The use of these systems will also result in large dump loads once storage limits are reached. Fail-safe methods must be included in any system to make sure that periods of high power production do not result in damage to the charging systems. The need for fast reliable control systems allowing rapid diversion of power into a dump load is an absolute necessity in these systems, further increasing capital costs.

6.5.2 Hydrogen storage systems

Hydrogen storage has been suggested as a future possibility allowing mass storage in place of batteries, allowing diesel backup systems to be minimised and eventually eliminated. At this stage no closed loop commercial operations of the type envisaged for the Antarctic stations have been constructed, but future advancements in electrolysers and fuel cells could make the use of hydrogen storage common place.

To investigate savings possible from its use, hydrogen storage combined with a limited battery storage (equivalent to one hour), have been investigated at the stations. A 60% efficiency into storage and a 50% efficiency out of storage has been assumed, resulting in a combined closed loop efficiency of only 30%. Assuming these values, the fuel savings ratios presented in Figure 6.19 (for wind systems) and Figure 6.20 (wind/solar systems) have been calculated for hydrogen systems sized at 32 MWh and 7 MWh (approximately 5 days load based on peak consumption) for the continental stations and Macquarie Island respectively.

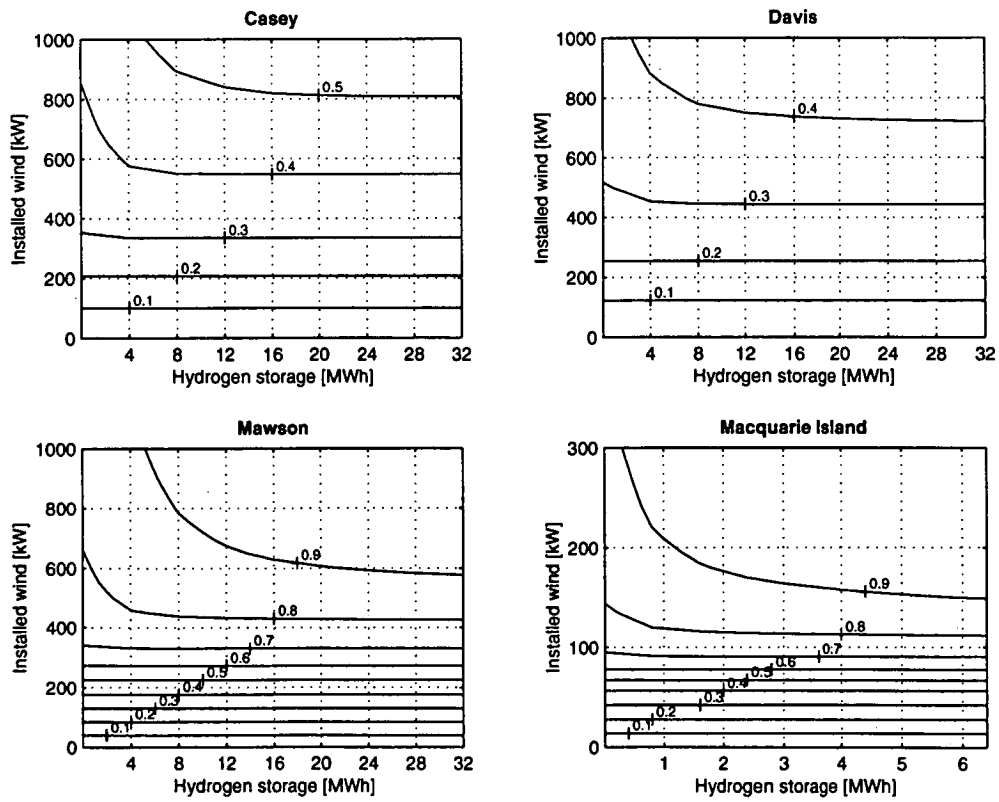

Figure 6.19: Comparison of wind systems, 40% limited penetration, 100% penetration and with hydrogen storage up to 32 MWh [1992-95].

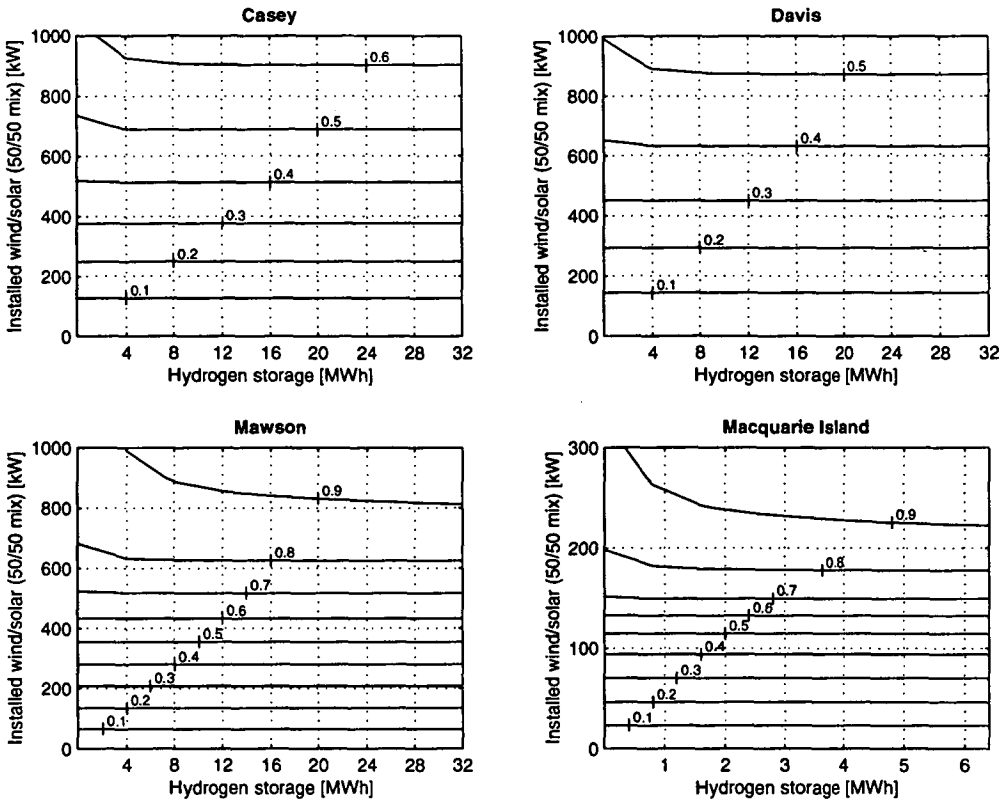

Figure 6.20: Comparison of wind/solar systems, 40% limited penetration, 100% penetration and with hydrogen storage up to 32 MWh [1992-95].

Similar issues are evident for these systems as with battery systems. A huge increase in generation plant, combined with the provision for mass storage, only results in small increases in fuel savings over systems allowing intermittent diesel stopping.

The main problem with mass storage systems is filling this storage. Extremely large over-sizing of wind and solar capacities is required, especially for a system with 30% closed loop efficiency, combined with large into storage conversion plant. In these estimates, all renewable energy available from excess production has been assumed to be able to be converted by electrolysis into hydrogen. This would require the electrolyser to be of equivalent size to the renewable generating plant.

Capital costs from the large generation plant, electrolysers and fuel cells will be high especially compared with the increase in fuel savings brought about from the use of hydrogen systems.

6.6 Summary

Matching station load demand with wind and solar production periods, through the use of 1-hour time step models, indicate that significant fuel savings can be achieved at some of the Australian Antarctic stations through the use of renewable energy systems.

A 100 kW wind system, connected to the existing system with load penetration limited to 40%, could provide 10% of the energy needs at Casey, 9% at Davis, while up to 24% at Mawson. A smaller 50 kW wind system, connected the same way with penetration limited to 40%, would be able to provide 30% of the energy needs at Macquarie Island. This amounts to annual fuel savings of 47,000 litres; 46,000 litres; 150,000 litres and 45,000 litres for Casey, Davis, Mawson and Macquarie Island respectively.

Extension to a 200 kW wind system, in conjunction with the inclusion of power regulation equipment allowing 100% penetration, would allow for 20% of the energy needs to be met at Casey, 17% at Davis and 48% at Mawson. A 100 kW wind system in conjunction with power regulation equipment, would be able to provide 76% of the energy needs at Macquarie Island. This would result in annual fuel savings estimated at 97,000 litres for Casey; 95,000 litres at Davis; 296,000 litres at Mawson and 105,000 litres at Macquarie Island. Additional annual fuel savings of 15,000 litres could be obtained at Macquarie Island if limited storage is included, allowing the diesel generator to be switch off during wind production periods.

Combination of these systems with large solar arrays allows for further increased fuel savings. A 200 kW solar system, in conjunction with a 200 kW wind systems, would result in additional annual fuel savings of 60,000 litres at the continental stations.

Large storage systems, although offering methods to increase fuel savings, require large increases in generating capacity for significant improvements over mixed wind and solar systems. The large increases in production potential will result in high cost increases for small returns, potentially making such systems a non-viable option for the Antarctic stations.

Chapter 7

Conclusions

7.1 Introduction

This chapter presents a brief summary of the work completed for this thesis, together with conclusions and recommendations on the application of renewable energy systems at the Australian Antarctic stations.

7.2 Results and conclusions

As outlined in Chapter 1, research has been conducted in the following areas:

1. Identification of the renewable energy resources at the Australian Antarctic stations, focusing on wind and solar power generation;
2. Identification of the energy demands at the Australian Antarctic stations;
3. Testing of components in Antarctica at Casey Station;
4. Examination of possible renewable energy systems; and
5. Development of models to estimate the performance of different sized renewable energy system configurations.

A summary of results and conclusions drawn from this work is now presented.

7.2.1 Wind and solar energy resources

Chapter 2 presented a breakdown of the wind resources at the stations. Results show the wind resources at the ANARE stations fall into two categories, with high potential at Mawson and Macquarie Island, but only average potential at Casey and Davis. Wind capacity factors, a measure of the period during which a turbine is expected to produce at its rated power, have been estimated at 0.65 for Mawson, 0.59 for Macquarie Island, 0.23 for Casey and 0.21 for Davis (based on the Aerowatt UM-70X). This indicates that output levels for a similar type of unit will be 2 to 3 times greater at Mawson and Macquarie Island than at either Casey or Davis. Investigation of the vertical wind profile indicates that tall towers would increase the performance of wind turbines, allowing for greater capacity factors.

High frequency wind variations, recorded at Casey to vary as much as 5 m/s over a two second interval, may pose a problem unless adequately addressed in the design of systems. Wind variations could lead to large power fluctuations from wind turbine systems, necessitating the use of frequency and voltage control systems.

Chapter 3 presented an analysis of the solar radiation. Long sunshine hours combined with clear skies provide ideal conditions for power generation from solar energy over the Antarctic summer, particularly at the continental stations. Low solar radiation levels during winter, however, restrict the useful operational period of any solar based system.

Solar capacity factors, a measure of the period for which an array can be expected to produce at its rated power, have been estimated for both tracking and passive systems. For fixed systems, summer solar capacity factors have been estimated at between 0.2 and 0.3 for Casey, Davis, Mawson and just below 0.2 for Macquarie Island. By introducing single axis azimuth tracking systems, increases of as much as 30% can be achieved during the summer months at Casey, Davis and Mawson, and 10% at Macquarie Island. These advantages may be off-set by cost and reliability concerns associated with the tracking mechanisms and their ability to withstand high winds and icing. Being simpler in design and easier to maintain, fixed passive systems may prove more practical.

Production periods from wind and solar power plant differ. This has important implications for mixed wind and solar power generation systems. Out of phase wind and solar production periods would allow for extended production periods in mixed systems, minimising the use of any back-up system. At Casey and Davis, where the wind resources are low and irregular, this is the only way to achieve high fuel savings without large energy storage facilities.

Diversification of renewable power generation plant beyond wind and solar into areas such as hydro (Macquarie Island only), wave, tidal, thermal gradients and geothermal could result in additional out of phase production periods. This would further enhance renewable production coverage, allowing even greater fuel savings than those possible with wind and solar.

7.2.2 Station energy requirements

Chapter 4 presents a study of the energy usage patterns at the stations. Fuel usage and electrical energy totals indicate small diurnal and seasonal variations, superimposed onto a much larger base load. Energy consumption generally follows a summer-low / winter-high pattern, highly dependent on the content of year-to-year maintenance and science programs.

Resolution of the electrical load at Davis indicates that there is significant correlation with station population levels, inside-outside building temperature gradient and to a lesser degree, wind speed. Temperature gradient correlated loads amounted to 1.3 kW per degree, representing 15% of the total station energy consumption. Population correlated loads amounted to 1.3 kW per person, representing 20% of the total station energy consumption. Wind correlated loads amounted to 0.7 kW per m/s, representing 1% of total station energy consumption. Based on these relationships, a model was developed to generate load sequences, statistically representative of the load demand at each station. Comparison of renewable generation plant production times and station load profiles calculated using these sequences, allow the performance of different sized renewable systems to be evaluated.

Renewable energy systems would greatly benefit from reduced station energy demands and from load shifting. Reduced station energy demands are possible through the use of conservation programs. A comprehensive energy audit, extending the breakdown of station building loads at Casey (presented in Chapter 5), is the best method to identify areas where improvements could be made. An energy audit could also identify interruptable loads. Shifting these loads into periods of strong wind speeds or high solar radiation levels would increase the match between renewable energy production and station consumption, enhancing fuel savings.

Thermal energy use at the stations should also be investigated in the energy audit. Estimates of the thermal energy production based on fuel consumption levels provide an overall estimate of thermal energy use, but do not resolve when and where needs occur. Heating practices may have to be altered if a substantial reduction in fuel use results in lower thermal energy output from the diesel generator sets, the dominant heat source in the current system. A move to individual building heating systems could prove a better system.

Lowering building internal temperatures or shutting down buildings which see limited use over winter, would provide methods to reduce thermal energy in general. Well designed systems would allow for diesel fuelled heating to be minimised or eliminated through the production of thermal energy from renewable sources. These could include heat pump systems designed to exploit the natural air/ocean temperature gradient, or heating systems using wind or solar.

7.2.3 Modelling results and conclusions

Chapter 6 presents the expected performance of different renewable energy systems. Models are developed for wind/solar systems, with and without battery and hydrogen storage, using a 1-hour time step. These models are then used to calculate fuel savings, generator loading patterns and energy totals, for different mixes of wind and solar generation plant.

Estimates using the models are deliberately conservative, with possibilities for greater savings possible in many situations. Wind turbine production levels have been calculated using wind speed measurements taken at a height of 10 metres and are based on the power curve of the Aerowatt UM-70X. These production levels could be higher for a different make of turbine, especially if mounted on a tall tower. Solar energy production totals have been calculated for fixed passive systems, oriented to maximise exposure. Higher exposure levels and thus higher generating production levels could be obtained if tracking systems are used.

Even with this conservative approach, the estimated potential fuel savings are already extremely attractive. In the simplest arrangement, power production from wind or solar plant is used to displace diesel fuel that would have been used by diesel generator sets. In such systems, wind and solar power plant operate in parallel with the diesel generator with renewable power penetration limited to 40%. This allows the generator sets, kept running at all times, to maintain adequate voltage and frequency regulation. A wind/diesel system using this strategy and consisting of wind plant rated at 100 kW, could provide 10% of the energy needs at Casey, 9% at Davis, while up to 24% at Mawson. A smaller 50 kW wind system, using the same connection strategy, would be able to provide 30% of the energy needs at Macquarie Island. This amounts to annual fuel savings of 47,000 litres; 46,000 litres; 150,000 litres and 45,000 litres for Casey, Davis, Mawson and Macquarie Island respectively.

Inclusion of power conditioning equipment, necessary for renewable penetration levels above 40%, allows increased fuel savings. A 200 kW wind system would allow for 20% of the energy needs to be met at Casey, 17% at Davis and 48% at Mawson; while a 100 kW wind system would be able to provide 76% of the energy needs at Macquarie Island. This would result in annual fuel savings estimated at 97,000 litres for Casey; 95,000 litres at Davis; 296,000 litres at Mawson and 105,000 litres at Macquarie Island. If provision for intermittent diesel stopping was made in these systems, through the inclusion of a small amount of energy storage, additional fuel savings of 10% and 3% would be possible for Macquarie Island and Mawson. This is a result of better diesel loading patterns through an elimination of zero loading periods.

Combination of wind systems with large solar arrays would give further fuel savings. At the continental stations the best results are possible. A 200 kW solar system, in conjunction with a 200 kW wind systems, would be result in additional annual fuel savings of 60,000 litres at the continental stations. At Mawson and Macquarie Island the large, more regular wind resources result in higher overlap between solar and wind productions periods. This results in similar fuel savings for oversized wind only systems, and mixed wind/solar systems.

Large storage systems, while offering impressive fuel savings for the stations, come at a high price. Massive increases in the installed capacity of generation plant are needed before further substantial increases in fuel savings can be achieved. This is due to the low closed loop efficiencies associated with these systems. The rapid charge rates associated with these systems are also reason for concern, necessitating inverters and storage devices to be sized according to the installed capacity to make the best use of any excess energy. This results in high capital costs for a relatively small increase in fuel savings.

7.3 Recommendations for future work

The fuel savings estimated in this thesis have been based on a number of assumptions. Foremost amoungst these is the assumption that BoM climate records allow for adequate calculation for the avaliable wind and solar energy resources. To determine the reliablity of these estimates, the current climate monitoring program initated at the stations must be completed and data records obtained for each station, preferably over a number of years.

7.3.1 Station thermal energy needs

Station energy consumption patterns also need to quanitfied. The potential for fuel savings at the stations would be greatly enhanced if load shifting is possible and/or energy conservation programs can be extended.

One area that needs further clarification is the thermal energy needs of the stations. As indicated in Chapter 4, current estimates place thermal energy production at higher levels that electrical energy production. The difference between the thermal needs of the stations and current thermal production levels at the stations will greatly influence the net total fuel savings possible through the introduction of renewable generation plant to provide electrical energy. This in turn will have a hugh effect on the finacial viability of different systems.

Suggested systems for further investigation which should include further on site monitoring and finacial assessment, are now made for each of the stations. A phased introduction is suggested, allowing experience and expertise to be developed as systems are developed for each station. Total fuel savings are indicated for each stage, together with the amount of this fuel that would have to be off-set to enable the equivalent amount of thermal energy to produced as dislaced through lower diesel generator use. Determination of the economic viability of each stage is necessary before conclusions can be drawn as to which stage systems should be developed and at which stations.

7.3.2 Sizing of renewable energy plant for Casey and Davis

Lower wind resources reduce the fuel savings possible at Casey and Davis. In addition, estimates in this study has been based on the performance of the Aerowatt UM-70X. Wind turbine designs better suited to light winds may offer increased potential for fuel savings. Combination with other renewable generation plant, such as solar, offer another method to increase fuel savings.

Projected fuel savings for Casey and Davis are as follows:

Stage 1: Diesel displacement system involving a100 kW wind plant.

Stage 2: Extension of wind plant to 200 kW, combined with controllable dump load and power regulation equipment including limited energy storage in the order of minutes to allow diesel stopping.

Stage 3: Addition of solar plant to 200 kW to complement wind plant of 200 kW, combined with the upgrading of system controllable dump load and power regulation equipment.

Casey	Additional station fuel savings (litres)	%	Total station fuel savings (litres)	%	Thermal energy off-set (litres)	Net station fuel savings (litres)	%
Stage 1	47,000	9%	47,000	9%	20,563	26,438	5%
Stage 2	51,000	10%	98,000	19%	42,875	55,125	11%
Stage 3	61,000	12%	159,000	31%	69,563	89,438	17%

Table 7.1: Fuel savings for suggested renewable energy plant stages at Casey

Davis	Additional station fuel savings (litres)	%	Total station fuel savings (litres)	%	Thermal energy off-set (litres)	Net station fuel savings (litres)	%
Stage 1	46,000	8%	46,000	8%	20,125	25,875	5%
Stage 2	49,000	8%	95,000	16%	41,563	53,438	9%
Stage 3	64,000	10%	159,000	26%	69,563	89,438	15%

Table 7.2: Fuel savings for suggested renewable energy plant stages at Davis

The lower wind resources at Casey and Davis result in less than a third of the fuel savings obtained at Mawson with similar Stage 1 and 2 systems (see below).

7.3.3 Sizing of renewable energy plant for Mawson

At Mawson, high wind resources due to katabatic flow from the Antarctic plateau permit excellent fuel savings using wind only systems. The size of the station requires larger wind systems than for Macquarie Island.

Projected fuel savings for Mawson are as follows:

Stage 1: Diesel displacement system involving a 100 kW wind plant.

Stage 2: Extension of wind plant to 200 kW, combined with controllable dump load and power regulation equipment including limited energy storage in the order of minutes to allow diesel stopping.

Stage 3: Extension of wind plant to 400 kW, combined with the upgrading of system controllable dump load and power regulation equipment.

Mawson	Additional station fuel savings (litres)	%	Total station fuel savings (litres)	%	Thermal energy off-set (litres)	Net station fuel savings (litres)	%
Stage 1	150,000	23%	150,000	23%	65,625	84,375	13%
Stage 2	146,000	22%	296,000	45%	129,500	166,500	25%
Stage 3	157,000	23%	453,000	68%	198,188	254,813	38%

Table 7.3: Fuel savings for suggested renewable energy plant stages at Mawson

At Mawson a 100 kW wind plant will off-set a very high amount of diesel fuel. Similar fuel savings can also be obtained for Stages 2 and 3, but with the added costs associated with regulation equipment, dump load and controls.

7.3.4 Sizing of renewable energy plant for Macquarie Island

Of all the stations, Macquarie Island stands out as being the best site for renewable energy systems. The combination of strong regular winds, mild temperatures, low station population levels and small station size allow a high proportion of station energy needs to be met by wind-based systems.

Projected fuel savings for Macquarie Island are as follows:

Stage 1: Diesel displacement system involving a 50 kW wind plant.

Stage 2: Extension of wind plant to 100 kW, combined with controllable dump load and power regulation equipment including limited energy storage in the order of minutes to allow diesel stopping.

Stage 3: Extension of wind plant to 150 kW and introduction of battery storage to 400 kWh, allowing diesel generator operation periods to be minimised.

Macquarie Island	Additional station fuel savings (litres)	%	Total station fuel savings (litres)	%	Thermal energy off-set (litres)	Net station fuel savings (litres)	%
Stage 1	45,000	24%	45,000	24%	19,688	25,313	14%
Stage 2	75,000	42%	120,000	66%	52,500	67,500	34%
Stage 3	31,000	17%	151,000	83%	66,063	84,938	47%

Table 7.4: Fuel savings for suggested renewable energy plant stages at Macquarie Island

Stage 1 is the easiest to implement, requiring only wind turbines and synchronisation equipment, although Stage 2 fuel savings are greater. For stage 2 to be successful some form of short period energy storage medium and dump load system are necessary. The energy storage could be in the form of a small battery system or flywheel arrangement.

Addition fuel savings associated with Stage 3 are not as significant as for Stage 1 or Stage 2. Costs associated with battery storage may also be excessive. Upgrading of any power control and load dump system may also be necessary, further increasing capital cost requirements.

7.4 Epilogue

The inclusion of renewable energy power generation plant at the Australian Antarctic stations would result in considerable fuel savings. Implementation must be progressive and associated with a learning process, allowing experience to be gained from each stage.

Although conditions at the stations are not typical, useful information, expertise and technology can be found from the multitude of emerging organisations and companies involved in wind and solar energy systems. The use of renewable systems in remote areas, particularly far Arctic communities, is anticipated to rapidly expand. This is a natural market that will provide the designs, equipment and expertise to allow renewable energy systems to be implemented at the Australian Antarctic Stations.

By investing in renewable energy systems the energy needs of the stations can be met locally in Antarctica at the station sites. This would give the Australian Antarctic stations a level of energy self-sustainablility and reducing fuel imports, in addition to lowering atmospheric emissions and the risk for fuel spills.

References

AAD Engineering (1992-95). *Station Engineering Reports for Casey, Davis, Mawson, Macquarie Island.* (Internal reports) Hobart, Australian Antarctic Division.

Aérowatt (1983). *UM-70X wind energy systems / User's Manual / Instructions for Civil Engineering.* Reports No. T-AW 84.05.02 AW/84.09.08(A) T-AW 83.08.11 (A). Aérowatt.

Aérowatt (1984). Power Curve data for UM-70X. Aérowatt.

Aguiar, R., Collares-Pereira, M., & Conde, J. (1988). Simple Procedure for Generating Sequences of Daily Radiation Values using a Library of Markov Transition Matrices. *Solar Energy,* 40(3), 269-279.

Appleby, A. (1994). Fuel cells and Hydrogen Fuel. *Int. J. Hydrogen Energy,* 19(2), 175-180.

Archibald, J. (1992). *Engineering Services in Antarctica,* Melbourne. Australian Construction Services.

ATCPs (1991a). *Protocol on Environmental Protection to the Antarctic Treaty - Interim Report of the Second session of the Eleventh Antarctic Treaty Special Consultative Meeting,* Madrid, 17-22 June 1991, No. XI ATSCM/2. Madrid, Ministerio de Asuntos Exteriores.

ATCPs (1991b). *Report by working group II - Interim Report of the Second session of the Eleventh Antarctic Treaty Special Consultative Meeting,* Madrid, 17-22 June 1991, No. XI ATSCM/2/31. Madrid, Ministerio de Asuntos Exteriores.

Badwal, S., Foger, K., & Murray, M. (1992). Fuel Cells: Clean Alternative Energy Technology of the 21st Century. *Gippsland Basin Symposium.* Melbourne, Australia, 269-278.

Ballard, K., Haazen, H., Roura, R., & Henderson, A. (1994). *Treading Lightly: A Minimal Impact Antarctic Station,* Greenpeace International.

Bass, J. (1987). *The Potential of Combined Heat and Power Generation, Wind Power Generation and Load Management Techniques for Cost Reduction in Small Electricity Supply Systems.* PhD Thesis, University of Strathclyde.

BoM (1990-95). Climate records for Casey, Davis, Mawson and Macquarie Island. Melbourne, Australian Bureau of Meteorology.

BoM (1994). Mean Global & Diffuse Radiation Totals for Casey and Macquarie Island. Melbourne, Australian Bureau of Meteorology.

Box, G., & Jenkins, G. (1976). *Time series analysis : forecasting and control.* San Francisco: Holden-Day.

Caney, K. (1995). King Island Wind-Diesel Power System: Technical Aspects. In P. Fawcett (Ed.), *Solar '95*, Hobart, Tasmania: Australian and New Zealand Solar Energy Society, 599-606.

Castellvi, E., Meana, E., & Castejon, A. (1994). Alternative Energy at the SAB (BAE) "Juan Carlos I". In *Proceedings of the Sixth Symposium on Antarctic Logistics and Operations*. 29-31 August 1994. Rome, Italy, SCALOP, 15-121.

Chiang, E. (1994). Antarctic Alternative Energy Summary. In *Proceedings of the Sixth Symposium on Antarctic Logistics and Operations*, 29-31 August 1994. Rome, Italy, SCALOP, 123-138.

Choudhury, B. (1982). A Parameterized Model for Global Insolation Under Partially Cloudy Skies. *Solar Energy*, 29(6), 479-486.

Coleman, C. (1992). *Wind power in Antarctica: Case histories of the North Wind HR3 Wind Turbine.* Project Brief No. 9201: Northern Power Systems.

Conradsen, K., & Nielsen, L. (1984). Review of Weibull Statistics for Estimation of Wind Speed Distributions. *Journal of Climate and Applied Meteorology*, 23(August), 1173-1183.

Cramer, G., Kleinkauf, W., & Schott, T. (1993). Wind/Diesel/Battery Systems - Applications, Experience, Economy of Different System Configurations and Sizes. *Wind Engineering*, 17(5), 228-237.

Degaetano, A., Eggleston, K., & Knapp, W. (1995). A Comparison of Daily Solar Radiation Estimates for the Northeastern United States using the Northeast Regional Climate Center and National Renewable Energy Laboratory Models. *Solar Energy*, 55(3), 185-194.

Dienhart, H., & Siegel, A. (1994). Hydrogen Storage in Isolated Electrical Energy Systems with Photovoltaic and Wind Energy. *Int. J. of Hydrogen Energy*, 19(1), 61-66.

Dienhart, H., & Hille, G. (1995). *The relevance of Renewable Energies for Electricity Supplies in Isolated Grids of Developing Countries.* Report No. STB-Bericht Nr. 11). DRL-Institute for Technical Thermodynamics, Department System Analysis and Technology Assessment.

Doran, J., & Verholek, M. (1978). A Note on Vertical Extrapolation Formulas for Weibull Velocity Distribution Parameters. *Journal of Applied Meteorology*, 17(March), 410-412.

Farlin, C. (1994). *Power Surge: A guide to the coming Energy Revolution.* New York: W.W. Norton & Company Inc.

Gardner, C. L., & Nadeau, C. A. (1988). Estimating South Slope Irradiance in the Arctic - A Comparison of Experimental and Modeled Values. *Solar Energy*, 41(3), 227-240.

Gilchrist, G. (1994). *The Big Switch: Clean energy for the twenty-first century.* Sydney: Allen & Unwin.

Gordon, J., & Reddy, T. (1988). Time Series Analysis of Daily Horizontal Solar Radiation. *Solar Energy*, 41(3), 215-226.

Graham, V., Hollands, K., & Unny, T. (1988). A Time Series Model for Kt with Application to Global Sythetic Weather Generation. *Solar Energy*, 40(2), 83-92.

Guichard, A., & Steel, J. (1993). *Alternative Energy Systems for Antarctic Stations: Investing for the Future.* Second International Design for Extreme Environements Assembly (IDEEA II) 24-27 October 1993. Montreal, Canada, Centre for Northern Studies, McGill University.

Guichard, A. (1994a). Towards New Energy Systems for Antarctic Stations. In *Proceedings of the Sixth Symposium on Antarctic Logistics and Operations*, 29-31 August 1994. Rome, Italy, SCALOP, 81-96.

Guichard, A. (1994b). *Status report on the potential for the application of Alternative energy systems at Antarctic Stations.* Unpublished Report, Sandy Bay: Latitude Technologies.

Guichard, A., Magill, P., Godon, P., Lyons, D., & Brown, C. (1995). Exploiting wind power in Antarctica. In P. Fawcett (Ed.), *Solar '95*, Hobart, Tasmania: Australian and New Zealand Solar Energy Society, 69.

Hall, J. (1992). *Energy Use Study of Casey Station, Australian Antarctic Territory.* Unpublished Engineering Thesis, University of Tasmania.

Hay, J. (1979). Calculation of Monthly mean Solar Radiation for Horizontal and Inclined Surfaces. *Solar Energy*, 23, 301-307.

Hay, J. (1985). Evaluating the Solar Resource: A review of problems resulting from Temporal, Spatial and Angular Variations. *Solar Energy*, 34(2), 151-161.

Haywood, E. (1995). *Looking South: The Australian Antarctic Program in a changing world.* Hobart: Australian Antarctic Division.

He, W. (1994). A simulation Model for Wind-Diesel Systems with Multiple Units. Wind Enegineering, 18(1), 29-36.

Heidelberg, G., Kohnen, H., Kromer, I., Lehmann, D., & Zastrow, F. (1990). Vertical Axis Wind Turbine with Integrated Magnetic Generator. In *Proceedings of the Fourth Symposium on Antarctic Logistics and Operations.* San-Paulo, Brazil, 72-82.

Hennessey, J. (1977). Some Aspects of Wind Power Statistics. *Journal of Applied Meteorology*, 16(2), 119-128.

Hennessey, J. (1978). A Comparison of the Weibull and Rayleigh Distributions for Estimating Wind Power Potential. *Wind Engineering*, 2(3), 156-164.

Hoyt, D. (1978). A Model for the Calculation of Solar Global Insolation. *Solar Energy*, 21, 27-35.

Incoll, P. (1990). *An Overview of Antarctic Buildings and Services for Administrators, Scientists and Engineers* (Paper to the IASOS Polar Technology Course, University of Tasmania), Melbourne. Australian Construction Services.

Incoll, P. (1993). *Personal Communication.* Australian Construction Services.

Infield, D. (1990a). An Assessment of Flywheel Energy Storage As Applied to Wind/Diesel Systems. *Wind Engineering*, 14(2), 47-61.

Infield, D., Lundsager, P., Pierik, J., van Dijk, V., Falchetta, M., Skarstein, O., & Lund, P. (1990b). Wind/Diesel System Modelling and Design. In *Proceedings of the European Community Wind Energy Conference*. Madrid, Spain, 569-574.

Infield, D., Scotney, A., Lundsager, P., Bindner, H., Uhlen, K., Toftevaag, T., & Skarstein, Ø. (1992). Wind Diesel Systems - Design Assessment and Future Potential. *Wind Engineering*, 16(2), 84-94.

Justus, C., Hargraves, W., & Yalcin, A. (1976). Nationwide Assessment of Potential Output from Wind-Powered Generators. *Journal of Applied Meteorology*, 15(7), 673-678.

Justus, C., Hargraves, W., Mikhail, A., & Graber, D. (1978). Methods for Estimating Wind Speed Frequency Distributions. *Journal of Applied Meteorology*, 17(March), 350-353.

Kauranen, P., Lund, P., & Vanhanen, J. (1994). Development of a Self-Sufficient Solar-Hydrogen Energy System. *Int. J. Hydrogen Energy*, 19(1), 99-104.

Kimura, S., Shigeo, Ishizawa, Kenji, Susuki, & Koji (1991). Development and Low Temperature Test of the Generator of a Wind Turbine System for Antarctica. *Wind Engineering*, 15(2), 114-127.

Kimura, S., Ichikawa, Y., Ishizawa, K., Takananga, T., & Suzuki, K. (1993). Field testing of a small WECS in Antarctica. In A. Garrad (Ed.), *Proceedings of European Community Wind Energy Conference*. Lübeck-Travemünde, Germany: H.S. Stephans & Associates, 732-736.

Knudsen, T. (1990). A Stochastic Wind Model Covering Periods Ranging from a Fortnight to a Second. *Wind Engineering*, 14(6), 387-404.

Linders, J. (1989). Some Aspects of Wind Diesel Systems with Reference to Chalmers Experimental Wind Diesel System. *Wind Engineering*, 13(3), 132-142.

Little, T. (1993). Wind Induced Energy Demand in Cold Climates. *Wind Engineering*, 17(1), 9-14.

Lovatt, A. (1983). *Wind Power Generation at Mawson for Antarctic Rebuilding Programme* (Interim Progress Report No. P.G. 112). Commonwealth of Australia, Department of Housing & Construction, Central Office Power Systems Branch.

Malatestas, P., Papadopoulos, M., & Stavrakakis, G. (1993). Modelling and Identification of Diesel-Wind turbines systems for Wind Penetration Assessment. *IEEE Transactions on Power Systems*, 8(3), 1091-1097.

Olseth, J., & Skartveit, A. (1984). A Probability Density function for Daily Insolation within the Temperate Storm Belts. *Solar Energy*, 33(6), 533-542.

Paltridge, G., & Platt, C. (1976). *Radiative Processes in Meteorology and Climatology*. Amsterdam, Elsevier Scientific.

Peeran, S. (1994). Performance of PV panels for Solar Energy Conversion at the South Pole. In *Proceedings of the Sixth Symposium on Antarctic Logistics and Operations*, 29-31 August 1994. Rome, Italy, SCALOP, 139-155.

Perez, R., Ineichen, P., & Seals, R. (1990). Modeling Daylight Availability and Irradiance Components from Direct and Global Irradiance. *Solar Energy*, 44(4), 271-289.

Peterson, E., & Hennessey, J. (1978). On the Use of Power Laws for Estimates of the Wind Power Potential. *Journal of Applied Meteorology*, 17(March), 390-394.

Phillips, W. (1984). Harmonic Analysis of Climate Data. Solar Energy, 32(3), 319-328.

Sayigh, A. (1977). *Solar Energy Engineering*. New York: Academic Press.

SCALOP (1993). *Report from the sub-group on Alternative Energy*. Christchurch, New Zealand: The Standing Committee on Antarctic Logistics and Operations (SCALOP).

SCAR (1995). *SCAR Bulletin* No. 119). Scientific Committee on Antarctic Research (SCAR).

Schickedanz, P., & Bowen, E. (1977). The Computation of Climatological Power Spectra. *Journal of Applied Meteorology*, 16(April), 359-367.

Sheinstein, A. (1994). Activity of Russian Committee on Antarctic Research on Alternative Energy Sources utilization in Antarctica. In *Proceedings of the Sixth Symposium on Antarctic Logistics and Operations*, 29-31 August 1994. Rome, Italy: SCALOP, 107-114.

Skarstein, Ø., & Uhlen, K. (1989). Design Considerations with Respect to Long-Term Diesel Savings in Wind/Diesel Plants. *Wind Engineering*, 13(2), 72-89.

Snedecor, G., & Cochran, W. (1980). *Statistical Methods (7th edition ed.)*. Ames Iowa, USA: The Iowa State University Press.

Steel, J. (1993). *Alternative Energy Options for Antarctic Stations*. Unpublished Honours Thesis, Institute of Antarctic and Southern Ocean Studies, University of Tasmania.

Swan, R. (1961). *Australia in the Antarctic: interest, activity, and endeavour*. Parkville, Australia: Melbourne University Press.

Takle, E., & Brown, J. (1978). Note on the Use of Weibull Statistics to Characterize Wind-Speed Data. *Journal of Applied Meteorology*, 17(April), 556-559.

Vrana, A. (1995). *The use of wind power at Heard Island*. Hobart, Australian Antarctic Division.

Weller, G. (1968). *The heat budget and heat transfer processes in Antarctic plateau ice and sea ice*. Glaciology Series Report No 67. Melbourne, Australian Antarctic Division.